RETROFITTING DIRECT-INJECTION AND A TURBOCHARGER TO A TWO-STROKE ENGINE FOR SNOWMOBILE APPLICATIONS

A Thesis

Presented in Partial Fulfillment of the Requirements for the

Degree of Master of Science

with a

Major in Mechanical Engineering

in the

College of Graduate Studies

University of Idaho

by

Nathan E. Bradbury

May 2006

Major Professor: Karen DenBraven, Ph.D.

AUTHORIZATION TO SUBMIT THESIS

This thesis of Nathan E. Bradbury, submitted for the degree of Master of Science with a major in Mechanical Engineering and titled "Retrofitting Direct-Injection and a Turbocharger to a Two-Stroke Engine for Snowmobile Applications," has been reviewed in final form. Permission, as indicated by the signatures and dates given below, is now granted to submit final copies to the College of Graduate Studies for approval.

Major Professor   _____ Date _____
Karen DenBraven, Ph.D.

Committee
Member   _____ Date _____
Karl Rink, Ph.D.

Committee
Member   _____ Date _____
Ruprecht Machleidt, Ph.D.

Department
Administrator   _____ Date _____
Donald Blackketter, Ph.D.

Discipline's
College Dean   _____ Date _____
Charles Peterson

Final Approval and Acceptance by the College of Graduate Studies

_____ Date _____
Margrit von Braun

ABSTRACT

The University of Idaho has been working to develop internal combustion engines for snowmobiles that have reduced exhaust and noise emissions with increased fuel economy as compared to currently available technologies. The University of Idaho initially used a four-stroke engine as an alternative to the traditional carbureted two-stroke engine, which proved to be more than adequate for emissions and noise reductions. However, the performance of four-stroke powered snowmobiles only appeals to a small sector of the snowmobile industry. In order to meet both the consumer demands of snowmobiles with high-power densities and the recently imposed Environmental Protection Agency (EPA) and National Parks Service (NPS) emission regulations, the University of Idaho began developing a low-emission and fuel-efficient two-stroke engine through the use of a gasoline direct-injection engine. Two-stroke direct-injected engines show great promise to meet the proposed 2012 EPA standards and the more stringent NPS standards, while maintaining the simplicity and high power-to-weight ratio preferred for snowmobile engines.

Direct-injection also allows for further improvement of efficiency through the use of exhaust turbocharging. With the scavenging and fuel flows separated, turbocharging can efficiently increase the mass of air delivered to the engine. This increases specific power output and decreases specific fuel consumption.

This thesis is intended to provide both the history of the University of Idaho's involvement in clean snowmobile engine design and a thorough account of research conducted to this point as a reference for new students. Also included is a summary of work completed toward a naturally aspirated direct-injection engine and an investigation into the feasibility of turbocharging a direct-injected engine. The results show that direct-injection is a viable option for high performance two-stroke engines. They also show that turbocharging can successfully increase specific power while having the potential for lowered specific fuel consumption for a direct-injected two-stroke engine.

ACKNOWLEDGEMENTS

TABLE OF CONTENTS

LIST OF FIGURES

LIST OF TABLES

xi

DEFINITION OF TERMS

DEQ:	Department of Environmental Quality
NPS:	National Parks Service
BAT:	Best Available Technology
SwRI:	Southwest Research Institute
EPA:	Environmental Protection Agency
CFR	Code of Federal Regulations
FEL:	Family Emissions Level
CSC:	Clean Snowmobile Challenge
UHC:	Unburned Hydrocarbons
NO_x:	Oxides of Nitrogen
NO:	Nitric Oxide
NO_2:	Nitrous Oxide
O_2:	Oxygen
H_2:	Hydrogen
CO:	Carbon Monoxide
TDC:	Top Dead Center
BDC:	Bottom Dead Center
BTDC:	Before Top Dead Center
BBDC:	Before Bottom Dead Center
ATDC:	After Top Dead Center
GDI:	Gasoline Direct Injection
T:	Engine Torque at the output shaft
RPM:	Engine speed at the output shaft
AFR:	Air Fuel Ratio
CA:	Crank Angle
dBA:	Decibels Weighted to the A-scale
CVT:	Continuously Variable Transmission
EFI:	Electronic Fuel Injection
SDI:	Semi-Direct Injection
HPDI:	High Pressure Direct Injection
CARB:	California Air Resource Board
CFD:	Computational Fluid Dynamics
WOT:	Wide Open Throttle
PM:	Particulate Matter
EMM:	Engine Management Module
EGR:	Exhaust Gas Recirculation
HCCI:	Homogeneous Charge Compression Ignition
TC:	Throttle Counts
VNT:	Variable Nozzle Turbine
AR:	Area Ratio
CFM:	Cubic Feet per Minute
DR_{req}:	Density Ratio required
DR_{del}:	Density Ratio delivered
VOL_{eff}:	Volumetric Efficiency

DEFINITION OF TERMS CONTINUED

T_x:	Temperature at state x
PR:	Pressure Ratio
DAQ:	Data Aquisition
SPR:	Scavenging Pressure Ratio
AFR:	Air Fuel Ratio
TE_{air}:	Trapping Efficiency (air)
TE_{fuel}:	Trapping Efficiency (fuel)

1.0   INTRODUCTION AND BACKGROUND

This section describes the University of Idaho's motivation for developing clean snowmobile engines and specifically the reason for designing a direct-injected and turbocharged two-stroke engine. Also included is a discussion of the political and environmental motivation that pushed snowmobile manufacturers to begin developing clean and quiet snowmobile engines. This section explains the Clean Snowmobile Challenge (CSC) organized by the Society of Automotive Engineers (SAE), a competition that challenges university students to develop innovative snowmobile designs for use in environmentally sensitive areas. Finally, there is a detailed description of snowmobile engines, their relative emissions, and how direct-injection can alleviate many of the problems associated with two-stroke engines.

1.1   SNOWMOBILE USE

Snowmobiling is a popular method of winter recreation and transportation. Snowmobiles are used for several different purposes including utility, leisure, touring, and performance riding. Each type of riding may be conducted on groomed trails, deep snow, or mountainous conditions.   The many possible combinations of snowmobile use and riding conditions have resulted in several different designs of snowmobile chasses and power plants. Touring snowmobiles are the most widely used and are especially popular for visitors to national parks such as Yellowstone, Grand Teton National Park, and John D. Rockefeller Jr. Memorial Parkway.

Snowmobiling is the primary activity of many guests while visiting the Yellowstone during the winter.   People are drawn to the parks for wildlife watching and to use the numerous snowmobile trails during the winter. In the past, the snowmobiles allowed into Yellowstone and other environmentally sensitive areas have had a large negative impact on the environment. Snowmobile impact studies can be found on the Montana Department of Environmental Quality (DEQ) webpage [1]. That page provides links to several government agencies that are trying to further understand vehicle impact in the National Parks. Snowmobile impact has led to controversy and new regulations regarding snowmobile usage and emissions standards for National Parks.

1.2   LEGISLATION AND STANDARDS

Concerns over snowmobile impact in our national parks—specifically Yellowstone, Grand Teton, and John D. Rockefeller Jr. Memorial Parkway—led the National Park Service (NPS) to issue a Proposed Rule in December of 2000 concerning snowmobiles and their use in U.S. National Parks. The proposed rule capped the snowmobile use in the winters of 2002 and 2003 and completely eliminated the use of snowmobiles by the 2004 season.[*] On January 22, 2001, the NPS implemented the proposed rule as the Final Rule, dubbed the "Snowcoach Rule" [2]. Specifically, this rule allowed snowmobile use to continue through the 2002 season, while mandating significant reductions in snowmobile use in 2003 and eliminating snowmobiles in National Parks in favor of snowcoaches in 2004 [2]. The NPS published a revised alternative to the Snowcoach Rule in 2003, allowing for a set maximum number of snowmobiles to enter the National Parks each day [3]. However, the snowmobiles allowed to enter the Parks would be required to conform to "best available technology" (BAT) standards, an adaptive management program, and 80percent of the snowmobiles would have to be guided through the Parks by trained park rangers [3].

On December 16, 2003, the U.S. District Court for the District of Columbia vacated the 2003 Final Rule and remanded the case for further investigation by the NPS [4], finding that there was not enough scientific and environmental impact data to support the 2003 rule. The court's ruling left the January 22, 2001 Snowcoach Rule in effect, which would have limited the number of snowmobiles allowed into the park for the 2004 season and phased out snowmobiles in favor of snowcoaches. This ruling did not permanently close the door on snowmobiles entering Yellowstone. Rather, it required the NPS to scientifically determine the full environmental impact of allowing snowmobiles in the park before imposing new regulations. This decision placed more pressure on the NPS to continue research on environmentally-friendly ways to include snowmobiles in Yellowstone and other National Parks.

On February 10, 2004 (after the D.C. court issued its decision) the U.S. District Court for the District of Wyoming enjoined the NPS from implementing the 2001 Snowcoach Rule,

---

[*]Winters, snowmobile seasons, and Clean Snowmobile Challenges are referred to by their ending year.

which would have banned all snowmobiles from entering Yellowstone for the 2004 season. [5]. Later that year, the Wyoming court held that the January 2001 Rule was arbitrary, and required the NPS to provide temporary rules for the 2004 snowmobile season that were "fair and equitable" to all parties [6]. In response to this ruling, the NPS produced a compendium amendment setting out temporary rules [7]. The Temporary Rules allowed 720 snowmobiles, rather than the 493 allowed under the 2001 Snowcoach rule, to enter Yellowstone per day [7]. According to the Temporary Rule, the additional snowmobiles allowed into the park had to meet BAT standards and all snowmobiles had to be commercially guided [7]. The 2003-2004 BAT standards required that all snowmobiles achieve a 90 percent reduction in hydrocarbons and oxides of nitrogen (UHC+NO$_x$) and a 70 percent reduction in carbon monoxide (CO) relative to the NPS baseline emissions testing for conventional two-stroke snowmobiles, which was 150 g/kW-hr UHC and 400 g/kW-hr of CO [34]. The 2004 Temporary Rule has been upheld by at least one court [9]

Beginning with 2005 model year, all snowmobiles entering Yellowstone, Grand Teton, or the Rockefeller Memorial Parks had to be certified with emissions no greater than 15 g/kW-hr for UHC+NO$_x$ and 120 g/kW-hr for CO [7]. Emissions measurements were based on the five-mode and weighted testing procedure developed by Southwest Research Institute (SwRI), Table 1. The five-mode test represents the typical duty cycle for snowmobile engines while in operation [15]. The procedures for the emissions tests are outlined in the Code of Federal Regulations [8]. In addition to the exhaust emissions standard, snowmobiles entering the Parks must also produce less than 73 decibels weighted on the A-scale (dBA) sound pressure measured at full throttle. This is tested according to the SAE J192 (1985, NPS modified) test procedure [7].

Table 1: *Five-Mode Weighted Testing Points for Snowmobile Engines [8].*

Mode Point	Speed [percent of Rated]	Torque [percent of Rated]	Weighting [percent]
1	100	100	12
2	85	51	27
3	75	33	25
4	65	19	31
5	Idle	N/A	5

Next, in 2005, the EPA released a family emissions limit (FEL) standard for snowmobile manufacturers [8]. The FEL is a "café standard" and mandates that the average snowmobile emissions for any given production year meet the EPA's minimum emissions requirements. This allows snowmobile manufacturers to continue producing snowmobiles that do not meet the contemporary emissions standards as long as those "dirty" engines are offset by "clean" engines. Engine family's emissions are rated based on their emissions score, E. The emissions score is calculated using equation 1.2.1, shown below. The SwRI five-mode weighted emissions test is used to determine the weighted UHC+NO$_x$ and CO emission values for the scoring function.

$$E = \left[1 - \frac{(UHC + NO_x) - 15}{150} \right] * 100 + \left[1 - \frac{CO}{400} \right] * 100 \qquad \textbf{Equation 1.2.1}$$

For a snowmobile manufacturer to sell snowmobiles in the United States in 2012, their corporate average snowmobile emissions number must be *greater* than 100 points. Along with the minimum E score, the EPA also created a maximum level for the corporate average UHC+NO$_X$ and CO emissions: they may not be higher than 90 g/kW-hr and 275 gm/kW-hr, respectively. Manufacturers are given additional credits for producing snowmobile engine families with an E score above the minimum. The credits can be used to further offset engine families that do not meet the minimum standard or they can be sold to other engine manufacturers. Purchased credits can be applied to that manufacturer's corporate average to increase their E number so a manufacturer can produce more dirty engines. The NPS has also adopted the "E score" system for its requirements; each snowmobile allowed into Yellowstone must have an EPA certified E score of at least 170 [13].

Like the NPS, the EPA also set noise limits for snowmobiles. The test is based on the SAE J192 pass by sound pressure testing procedure and is slightly different than the 1985 modified SAE J192 test used by the NPS. The NPS testing procedure is based on the altitudes encountered in Yellowstone and uses faster responding equipment than the EPA. The EPA and NPS procedures both measure sound pressure from snowmobile engines at

WOT (wide-open-throttle); however, the different testing altitudes and testing equipment result in different sound pressure levels from the two tests. As of yet, no study has correlated data from the two testing procedures. The EPA pass-by noise standards states that snowmobiles cannot produce more than 78 dBA, which is the standard set by the International Snowmobile Manufacturers' Association.

1.3   SAE CLEAN SNOWMOBILE CHALLENGE

The Society of Automotive Engineers, along with others concerned about snowmobile impact, began the SAE Clean Snowmobile Challenge (CSC) student design competition in 2000. The competition encourages the development of touring snowmobiles for use in environmentally sensitive areas [14].   In the past, the student-designed snowmobiles were expected to produce less UHC and CO without significantly increasing the levels of NO_x when compared to a representative production touring snowmobile. The snowmobiles were also expected to be quieter than the conventional technology. The Final Rule released by the NPS prompted the CSC organization to slightly alter the emission and noise design goals for the 2006 competition, where teams were awarded points for emissions and noise testing based on how much they lowered emissions and noise levels below the 2012 EPA standards [15].

There are several other design goals for the student teams. There is a 100 mi (161 km) endurance/fuel economy competition. Each snowmobile must complete the endurance event while following a trail judge pacing them at a speed of no more than 45 mph (72 km/h). This allows all of the competition snowmobiles fuel consumption to be based on the same duty cycle. The students also compete in a 500 ft (152 m) acceleration event which must be completed in less than 12 seconds. There are also other events for handling, cold start, oral presentation, technical paper, and static display [15].

1.4   UNIVERSITY OF IDAHO'S CLEAN SNOWMOBILE HISTORY

The University of Idaho (UI) first attended the CSC solely as an observer in 2000. Since then, the team has been returning to compete every year. The first year the team competed they received fifth place using an open-loop fuel-injected four-stroke engine with

exhaust after-treatment [25]. Over the next two years the team continued development of the four-stroke engine [19, 29]. Several modifications were made to increase the engine power while further reducing the noise and emissions output. The team returned to the competitions with more refined engine and chassis combinations. The UICSC team won first place overall for the 2002 and 2003 competitions with the four-stroke design. The team also received awards in several other areas; 2002—Best Performance, Best Design, Best Fuel Economy, and Hill Climb Champion; 2003—Best Performance, Best Emissions, Best Fuel Economy, Quietest Snowmobile, and Best Value.

After the success with the four-stroke engine, the team decided to look for other power plants for snowmobiles. Although the four-stroke engine proved to be an excellent choice for a clean and quiet snowmobile, it was heavy, mechanically complex, and had a lower power-to-weight ratio compared to a two-stroke engine. During the 2003 CSC design year the team weighed the pros and cons of using a two-stroke engine versus a four-stroke engine. After considering the types of engines that were allowed at the competition and the large potential for improvement of two-stroke engines, the team decided to begin researching technologies to develop a clean two-stroke engine [19]. The team found that gasoline-direct-injection (GDI) could be used to make a clean two-stroke engine.

During the summer of 2003 a research project was conducted to determine if high-pressure gasoline injectors borrowed from a three-cylinder, two-stroke personal-watercraft engine could be used for the project. The injectors operated with a non-traditional 55 volt power source and the principles and current signal requirements for the injectors were unknown at the time. Through patent research and with the aid of a UI mechanical engineering faculty member, an injector-driver circuit and power source was developed. The injectors were tested to determine their maximum fuel delivery and time constraints. At the conclusion of the project it was decided that the injectors could be used for the CSC team. A UI mechanical engineering senior design team began the process of developing a clean and quiet two-stroke powered snowmobile during the 2003 school year [30, 31]. The GDI two-stroke was used for the 2004 CSC competition. The snowmobile did not finish the competition due to piston seizure and an incomplete fuel map. It was later concluded that the injectors were not being operated as they were intended, causing erratic fuel delivery.

During the summer of 2004, another UI mechanical engineering senior design team

began further development of the GDI two-stroke engine. This team focused on a more refined combustion chamber shape while implementing the second-generation of the high-pressure fuel-injectors. They also focused on adapting a 55 volt permanent-magnet alternator to the snowmobile engine that would allow battery-less operation. The combustion chamber design and overall system architecture was much better than the first-generation DI engine developed. The engine was used at the 2005 CSC competition. A lack of oil control and problems with fuel mapping lead to a disappointing emissions and fuel economy performance at the competition [20. However, the team was at the top of several events focused on engineering design. The snowmobile also performed well in the acceleration event. This thesis continued research and development of the 2005 CSC engine.

1.5   SNOWMOBILE ENGINES AND THEIR EMISSIONS

Traditionally, touring snowmobiles were powered by mid-sized (440 cc-700 cc) two or three cylinder two-stroke engines. Snowmobile two-stroke engines are low-maintenance engines with unsurpassed power-to-weight ratios. Their low weight and high power make them well suited for over-the-snow travel. Furthermore, two-stroke engines have excellent cold start abilities down to temperatures as low as -40°C [11]. Finally, two-strokes have a torque curve that is well suited for the belt-type continuously variable transmission (CVT) used in snowmobiles [11].

Typically, snowmobile two-stroke engines are crankcase charged and loop-scavenged with exhaust-pipe tuning. The induction system is usually piston-port with rotary-valve or reed-valve induction and the fuel metering is by carburetion, electronic fuel-injection (EFI), or semi-direct fuel-injection (SDI). The literature is full of alternative designs for charging, scavenging, fuel delivery, and ignition control, but none provide the lightweight and high-power combination like the simple two-stroke described in this thesis [16,18,20]. Figure 1 is schematic of a carbureted, reed-valve, crankcase charged, loop-scavenged, and piston-controlled two-stroke with a tuned exhaust, typical of traditional touring snowmobiles (hereafter referred to as a two-stroke). These engines use a total-loss oiling system. The oil is either premixed with the fuel or the oil is pumped into the inlet-air stream where it mixes with the incoming fuel. As the fresh air/fuel/oil mixture travels through the crankcase, an oil film is deposited on the cylinder walls and bearings. Oil that does not attach to a surface is

scavenged into the combustion chamber where it lubricates the walls above the piston rings or is lost to the exhaust. This system does not require oil filters or oil changes.
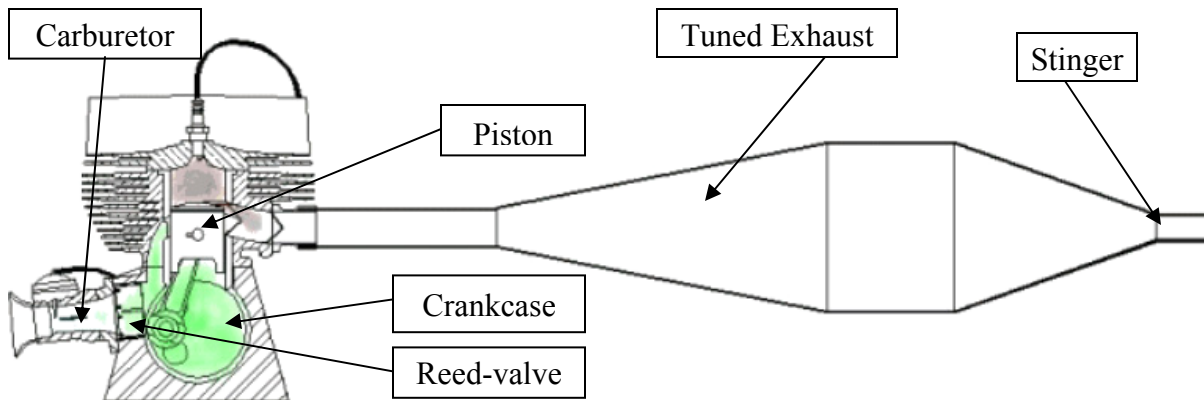
Figure 1: *Traditional snowmobile two-stroke engine.*

Because two-strokes do not have separate intake and exhaust strokes, a scavenging pump must be used to introduce the fresh charge into the cylinder to push the exhaust gasses out during the scavenging process [17]. Two-strokes use one of the simplest forms of scavenging pumps. It is referred to as crankcase scavenging. The bottom of the piston in conjunction with the portion of the crankcase below each cylinder is used for scavenging. The movement of the piston up and down produces the pumping action required to push the air/fuel mixture into the combustion chamber through the intake ports cut into the side of the cylinder. The geometry of the intake and exhaust ports determine the action of the scavenging flows used to displace the combustion products and provide a new intake charge.

The most widely used port layout is an adaptation of the Schnurle loop-scavenging system called the Curtis-Type loop-scavenging system, shown in Figure 2. It is used because the main scavenging ports are directed away from the exhaust ports and a piston with a flat top can be used [17]. It is an improvement over the cross-scavenged design, shown in Figure 3, that directs the scavenging air towards the exhaust port and deflects it upwards by a piston crown. The crown on the piston is susceptible to hot spots that can lead to pre-ignition and premature engine failure. The loop design also allows for a more compact combustion chamber that leads to a more rapid and efficient combustion process.
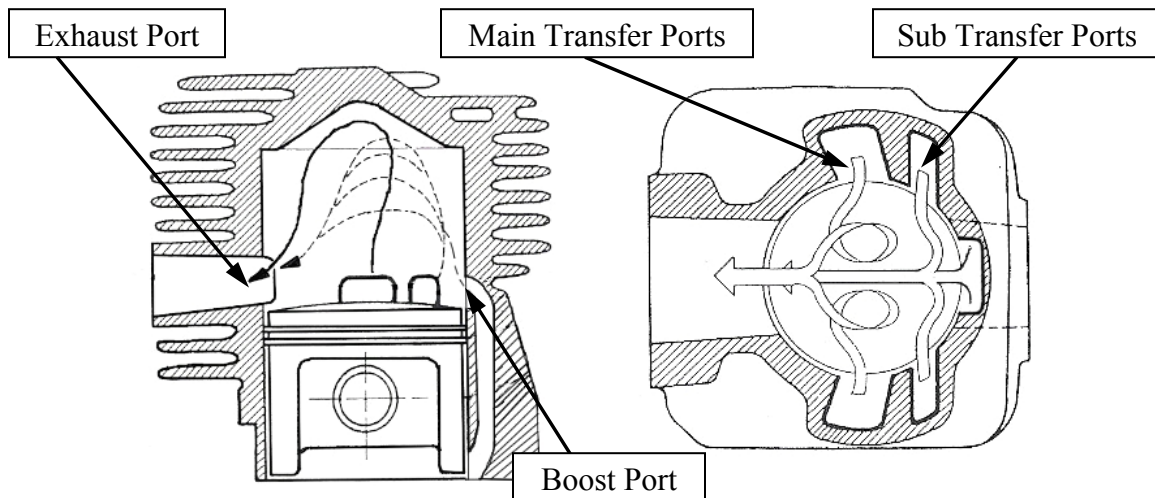
Figure 2: *Schematic of in-cylinder flows for a Curtis-Type loop-scavenged engine [18].*
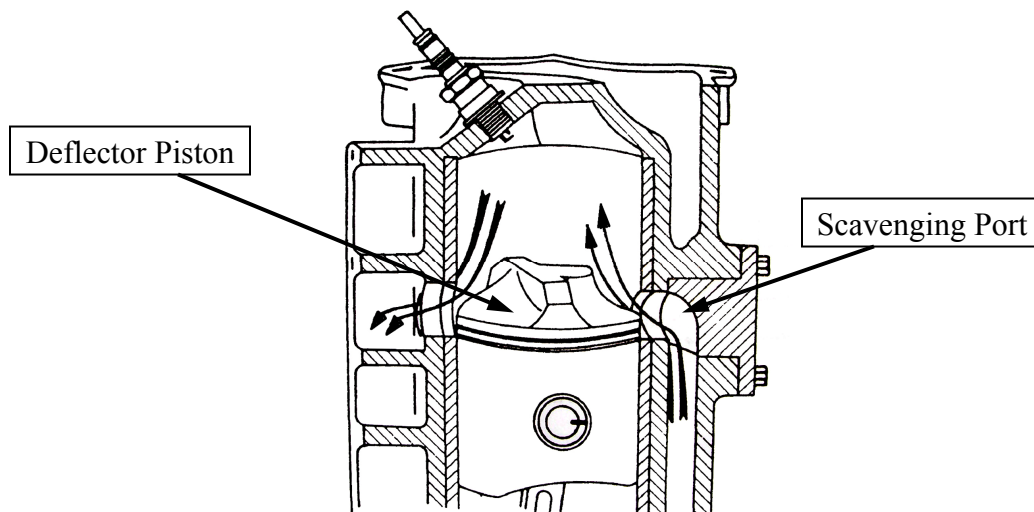
Figure 3: *Schematic of in-cylinder flows for a cross-scavenged engine [18].*

While the two-stroke engine is mechanically simple, the scavenging process is very complex. Because the intake and exhaust ports are open at the same time some unique problems arise related to intake and exhaust gas mixing.   More discussion on the problems associated with the scavenging process will be presented later in this section. The following description of the two-stroke cycle highlights some of the most important concepts of the gas-exchange process, a more detailed description can be found from Blair and Heywood.

1. After ignition, there is about 70° crank angle (CA) of useful expansion and work. At about 80° before bottom dead center (BBDC), the piston uncovers the exhaust port and the combustion gasses begin to evacuate the cylinder. The cylinder pressure drops drastically and a negative pressure wave in the pipe aids with pulling exhaust gasses out. This is the end of the power portion of the cycle (Figure 4).
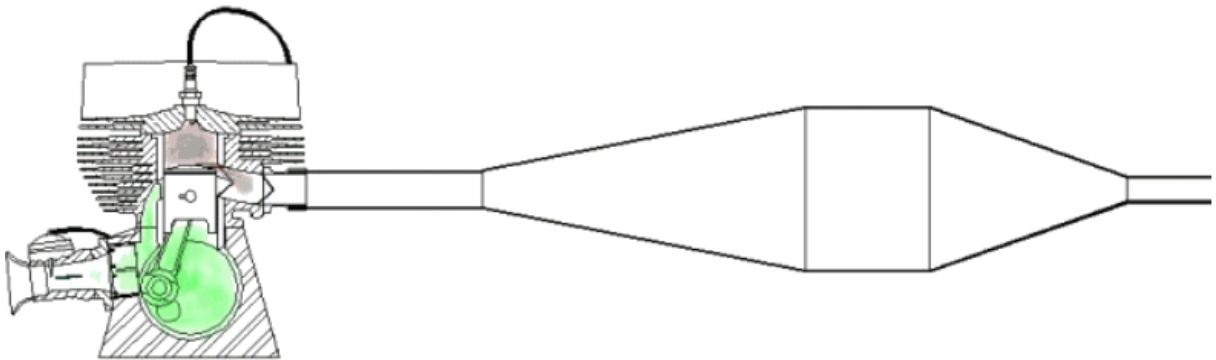
Figure 4: *The end of the power stroke and the beginning of blow-down.*

2. Some 10-20° later the intake ports open and a fresh air/fuel charge, compressed in the crankcase by the underside of the piston, begins to enter the combustion chamber. The incoming charge displaces and mixes with the exhaust-gas residuals. The tuned pipe continues to aid in pulling the cylinder contents out and some of the charge will be short-circuited (Figure 5).
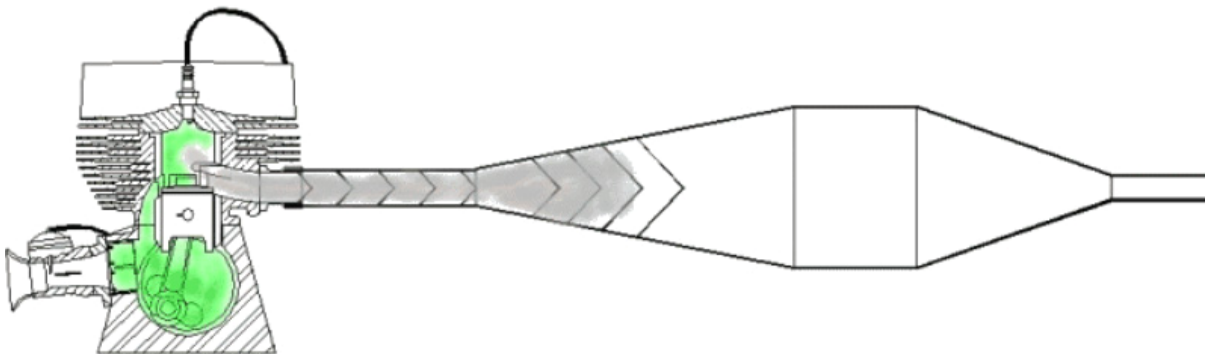
Figure 5: *Intake ports begin to open; scavenging begins.*

3. The scavenging process ends with both the crankcase and cylinder pressure close to the ambient pressure level just as the inlet port closes (about 60° after bottom dead center [ABDC]). Towards the end of the scavenge process, there can be a back flow of charge and exhaust gas residuals into the combustion chamber from the plugging pulse of the tuned pipe. The continued upward movement of the piston reduces the pressure in the crankcase and the reed valves begin to open (Figure 6).
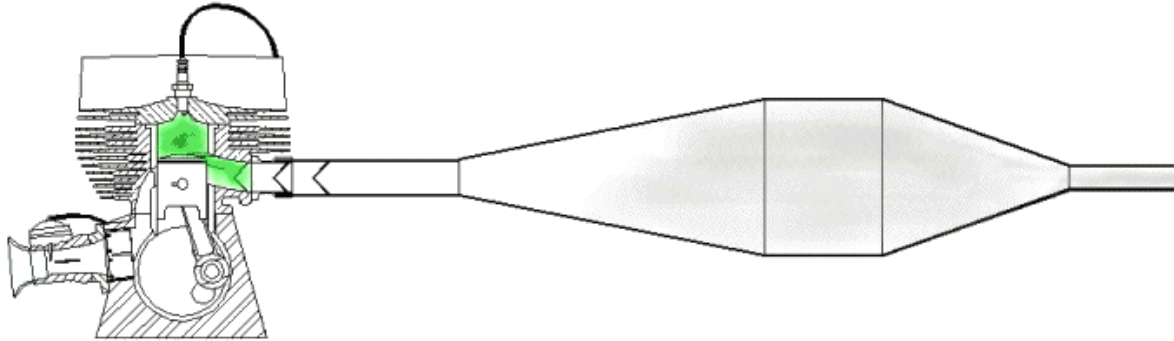
Figure 6: End of scavenging and the plugging pulse.

4. At about 80° ABDC, the exhaust port is closed, and the upward movement of the piston begins to compresses the freshly scavenged charge. The pressure in the crankcase continues to drop until the pressure is low enough to draw the next cycle's fresh charge in through the reed valves (Figure 7). A ram tuning effect similar to the one in the exhaust system can be designed into the intake system in order to trap more mass in the crankcase [17].
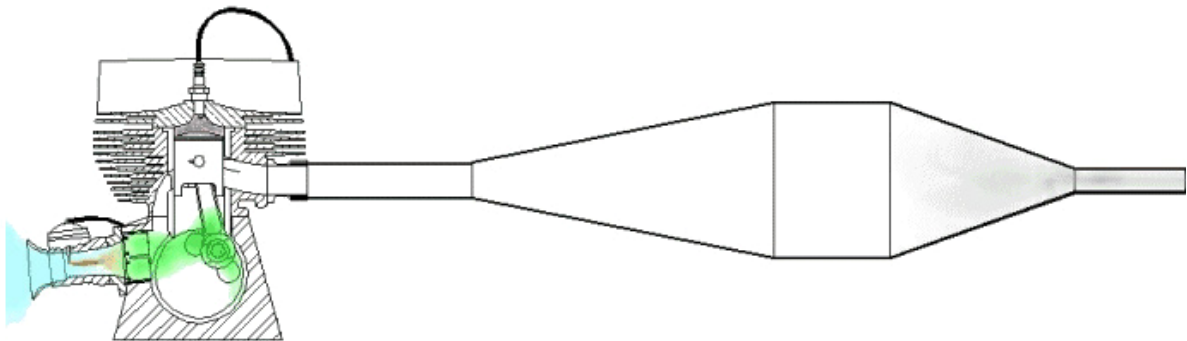
Figure 7: Compression and induction of a fresh charge into the crankcase.

5. Ignition typically occurs within the range of 10-40° BTDC. The burning fuel creates a pressure rise in the cylinder that is timed to peak around 10° ATDC for maximum torque output. Work is done by the expanding gasses on the piston until the exhaust port opens and the cycle repeats (Figure 8).
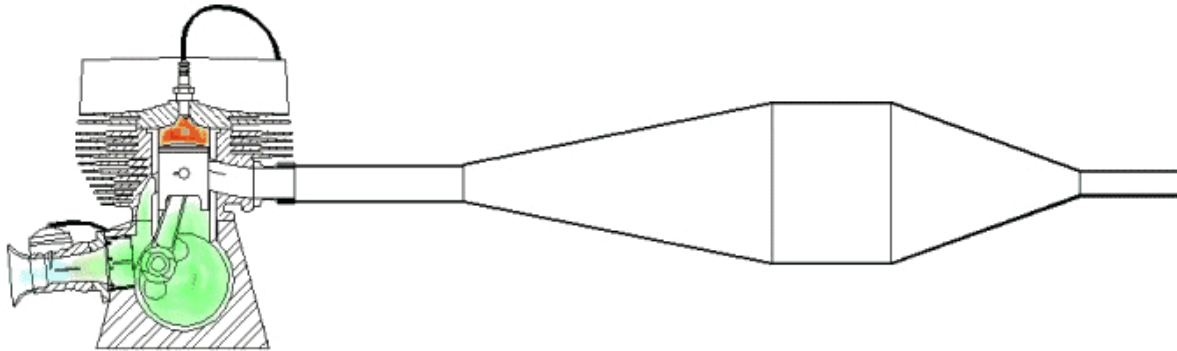
Figure 8: *Ignition occurs and the power stroke begins.*

A tuned pipe is an acoustic supercharger that it utilizes traveling waves in the exhaust system to increase the trapped mass in the cylinder and is critical to a high-performance two-stoke engine's performance. A well-tuned exhaust system aids in scavenging and reduces short-circuited fuel. Tuned exhaust systems are highly dependent on engine speed and load and typically are more efficient over a narrow rpm range. Tuned exhaust systems can be made from one common pipe or individual pipes for each cylinder. Multiple pipes can increase power output, but they are costly and require a significant amount of under-hood space. Tuned exhaust pipes consist of a header pipe that is connected to the exhaust outlet of the cylinders by a branch-pipe. Following the header pipe is a diverging cone, center section, and a converging cone. Just after the converging cone there is section of straight pipe called the stinger (Figure 1).

The pipe works by reflecting waves in the exhaust system [17]. When the exhaust port opens, a pressure wave created by combustion enters the divergent cone and a negative pressure wave is reflected back into the cylinder. This pressure wave aids in removing exhaust gasses from the cylinder while also pulling fresh air/fuel mixture in. When the original pressure wave reaches the converging cone a positive pressure wave is reflected back towards the cylinder. The positive pressure wave often referred to as the plugging-

pulse, forces some of the exhaust contents just outside of the exhaust port back into the cylinder. Tuned exhausts maximize charging efficiency at particular engine speeds and loads, which lowers brake-specific emissions and fuel-consumption [17]. When the engine is operated at off-design engine speeds and loads the plugging-pulse is not optimal and there is a significant loss in torque and an increase in emissions and fuel consumption.

It is evident that the two-stroke gas-exchange process is complex due to the in-cylinder flows as the fresh charge mixes and displaces the combustion products. During the scavenging process when the piston is near BDC the intake and exhaust ports are both open. This results in some fresh charge flowing directly into the exhaust system. The loss of the incoming fuel directly to the exhaust is called short-circuiting. Short-circuited fuel is the single largest contributor to the poor thermal efficiency, excessive UHC emissions, and particulate matter. Short-circuited fuel can account for losses of as much as 50 percent of the supplied fuel, especially during off-design speeds and loads. However, the CVT used for snowmobiles keeps the engine operating conditions close to the designed engine speeds and loads, limiting the short-circuited fuel to around 10-30 percent. This is shown in Figure 9 which shows calculated short-circuited fuel from measured data of a 2003 Arctic Cat Mountain Cat 600 cc EFI two-stroke [19]. These data correspond well to similar data in the literature [20].
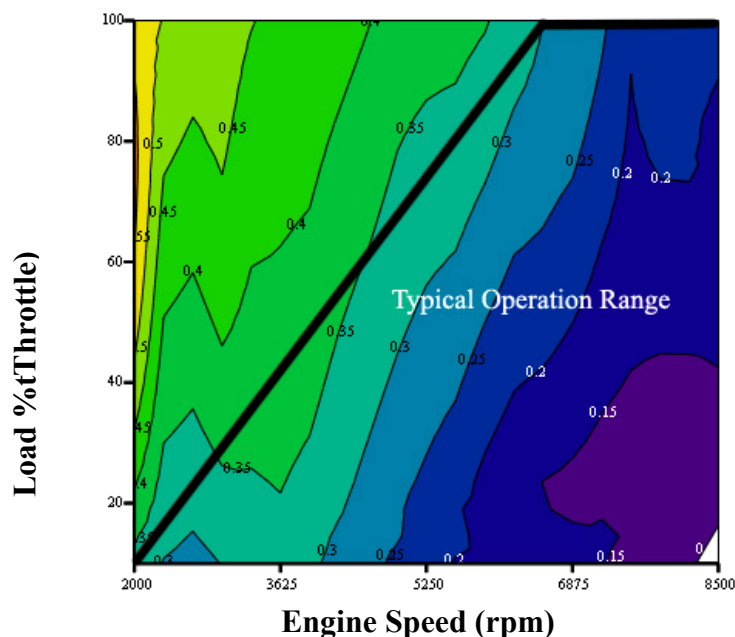
Figure 9: *Fraction short-circuited fuel of a two-stroke snowmobile engine [19].*

Although the largest portions of UHCs are from short-circuited fuel, the combustion process also produces unburned hydrocarbon emissions. Specifically, flame quenching, crevice-volume filling, and incomplete combustion are mechanisms for combustion related UHC formation [20]. Flame quenching occurs when fuel adheres to cylinder walls and combustion can only happen through surface evaporation and subsequent oxidation. Hydrocarbon emissions from flame quenching are many orders of magnitude less than short-circuited UHC [20]. As technologies advance and short-circuited emissions are reduced, reducing flame-quenching emissions will become important [21].

The crevice-volume filling UHC mechanism occurs during compression and combustion.   During these parts of the cycle a mass flow of fuel is directed into the crevices inside the combustion chamber where oxidation cannot occur. As the pressure drops during expansion a small portion of the trapped fuel can be drawn out of the crevices to participate in late combustion. The fuel that does not oxidize is scavenged into the exhaust system. Hydrocarbon emissions from crevice-volumes account for approximately 2.5 to 4 percent of total UHC emissions [20].

Incomplete combustion and/or misfire can be a major source of UHC emissions, especially during low loads and engine speeds. At off design speeds and loads the engine can have a low delivery ratio, which is the ratio of the actual mass of air delivered to the mass of air required to fill the swept volume at the prevailing atmospheric conditions [17]. The low delivery ratio leads to large amounts of exhaust gas residuals retained in the cylinder [20]. With the excessive trapped exhaust residuals, the combustion process becomes unstable to the point where several cycles can occur with partial or no heat release [17]. The partially combusted charge is then lost to the exhaust system.

Two-stroke engines are also known to have high CO emissions. The formation process for carbon-monoxide in two-stroke engines is exactly the same as that for other engines. Extensive discussions on CO formation can be found from Blair and Stone [16,17]. Simply stated, CO formation results from operating an engine fuel-rich. The lack of oxygen in the prevents the carbon from fully oxidizing to carbon dioxide resulting in CO formation. Two-stroke engines are operated fuel-rich for three reasons: (1) excess fuel cools the piston crown and prevents seizure; (2) it increases power output due to a maximum heat release occurring just rich of stoichiometric air/fuel ratios, and (3) for rapid transient response [20].

Nitrogen oxide emissions, NO_x, are a combination of NO and NO_2 that are formed from the high temperatures and pressures that occur during combustion. Nitric oxide represents more than 95 percent of the total NO_x emissions and it is a key player in the formation of smog [15]. The formation process of NO_x is called the Zeldovich mechanism. It is based on the dissociation of N_2 and O_2 molecules following the flame boundary and a lack of time available for chemical equilibrium to be reached [20]. Nitrogen oxide formation depends on two basic things; (1) peak temperatures reached during combustion, and (2) oxygen content in the trapped mixture [20]. Typical two-strokes have inherently low NO_x emissions because they have low effective compression ratios, they are operated fuel-rich, and have high residual exhaust gasses, all of which contribute to lower peak cylinder temperatures and less NO_x formation [11].

Understanding the emissions formation mechanisms is important for designing and tuning an internal combustion engine. Figure 10 describes emissions formation trends based on equivalence ratio, ϕ. Fuel/Air equivalence ratio and the relative air/fuel ratio, λ (= $1/\phi$), are two often used normalized mixture composition parameters [32], where:

$$\phi = (F/A)_{actual} / (F/A)_s$$

Equation 1.4.1

and

$$\lambda = (A/F)_{actual} / (A/F)_s$$

Equation 1.4.2
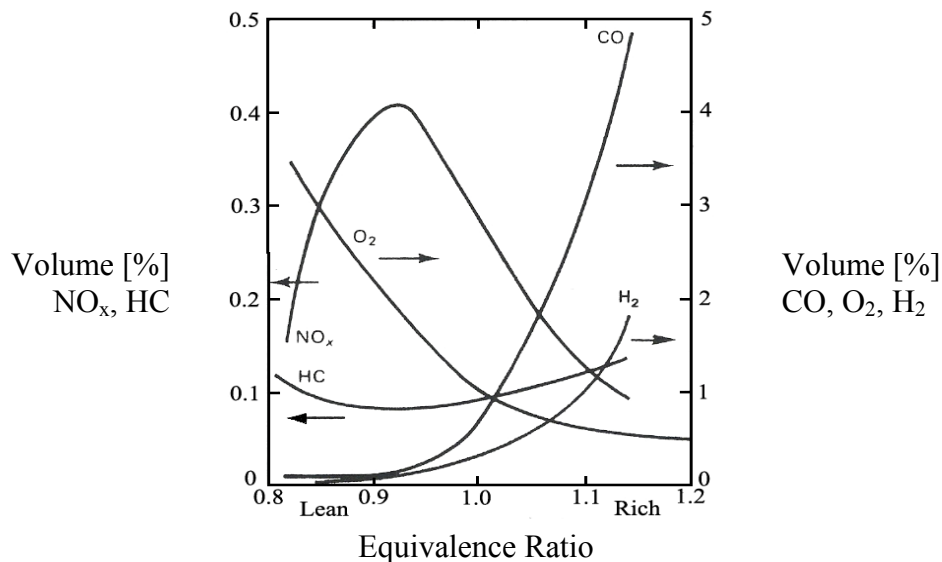
Figure 10: *Emission trends for spark-ignition engines at different equivalence ratios [16].*

Contrary to common belief, two-stroke lubricating oil is not a significant source of UHC [17,20,22]. Two-stroke engines do have excessive particulate matter (PM) emissions due to the total-loss lubrication system. Improved oil refining and changes in the type of oils used have resulted in less PM emissions. Recently, technologies have been able to lower PM emissions to levels below the EPA 2004-2012 off-road tier 3 regulations of 0.4g/kW-hr [22].

In order to meet the EPA exhaust emission regulations, manufacturers have been developing new technologies for two-stroke engines. The latest development for snowmobile two-strokes has been semi-direct injection (SDI), or boost-port injection. Bombardier introduced a SDI system, 2-TEC®, for the 2004 snowmobile season and Polaris introduced their SDI system, Cleanfire®, for the 2006 snowmobile season. These engines use low-pressure fuel-injectors, similar to those used in automobiles, to inject fuel into the boost-port. Figure 11 shows one possible location for an SDI injector.
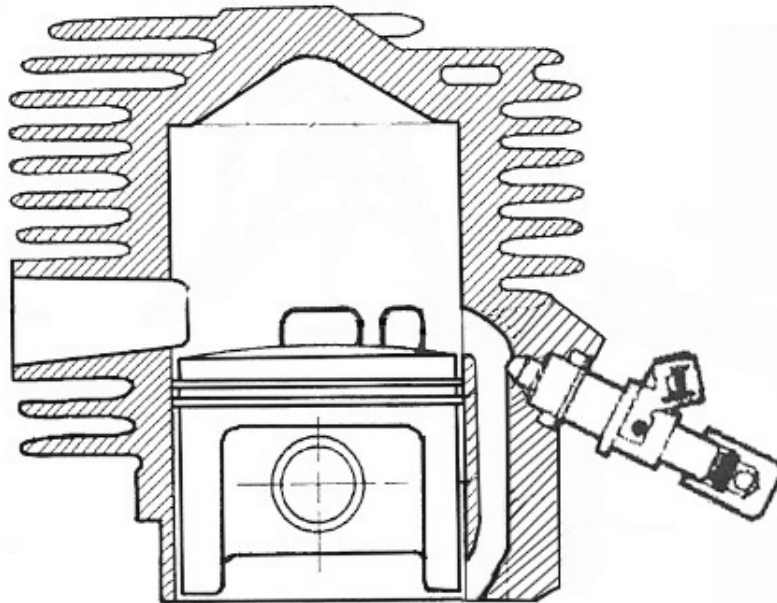
Figure 11: Schematic of a possible arrangement of an injector for a SDI cylinder.

Semi-direct fuel-injection has significantly reduced short-circuiting and UHC emissions, decreasing the five-mode weighted UHC emissions by about 50 percent. The SDI engines are still operated under slightly fuel-rich conditions and the reduction in CO emissions is not as dramatic, with approximately 30 percent less CO production. There is an increase in NO_x, due to higher in-cylinder temperatures, although it is still lower than four-

stroke NO_x production. Table 2 shows a comparison of five-mode weighted emissions and the EPA E scores for a carbureted and SDI two-stroke [23,25]. Both of the engines were from commercially available 600 cc two-stroke touring snowmobiles that represented the industry standard during the CSC competition for the particular design year.

Table 2: *Comparisons between carbureted and SDI two-stroke emissions [23,25].*

	CO [g/kW-hr]	UHC [g/kW-hr]	NOx [g/kW-hr]	EPA CFR 40	MPG
2003 CSC Control (Carbureted 2-Stroke)	319.94	125.50	0.73	46	6.9
2005 CSC Control (SDI 2-Stroke)	215.38	63.53	2.39	112	19.1

It is evident that SDI technology reduced the UHC and CO emissions enough to meet the 2012 EPA regulations, but the SDI engine does not meet the NPS standards and these engines will not be allowed into Yellowstone. The SDI engine saw a dramatic improvement in fuel economy, which is directly related to the reduction of short-circuited fuel. Although comparing in-field fuel economy is difficult with snowmobiles, these snowmobiles were operated under similar conditions. It is evident that two-stroke engines need further reductions of UHC and CO emissions if they are going to be allowed into Yellowstone.

Four-stroke engines are an alternative power plant for snowmobile engines. They are inherently cleaner and quieter than two-stroke engines. This is because each phase of the gas-exchange process, intake, compression, expansion, and exhaust, are separated from each other by the action of poppet valves. Figure 12 shows the four phases of the four-stroke cycle. By separating the phases of the cycle, the short-circuited fuel and high residual exhaust gasses associated with two-stroke engines are eliminated. This has two main effects: (1) lower UHC and CO and (2) higher NO_x emissions [16].
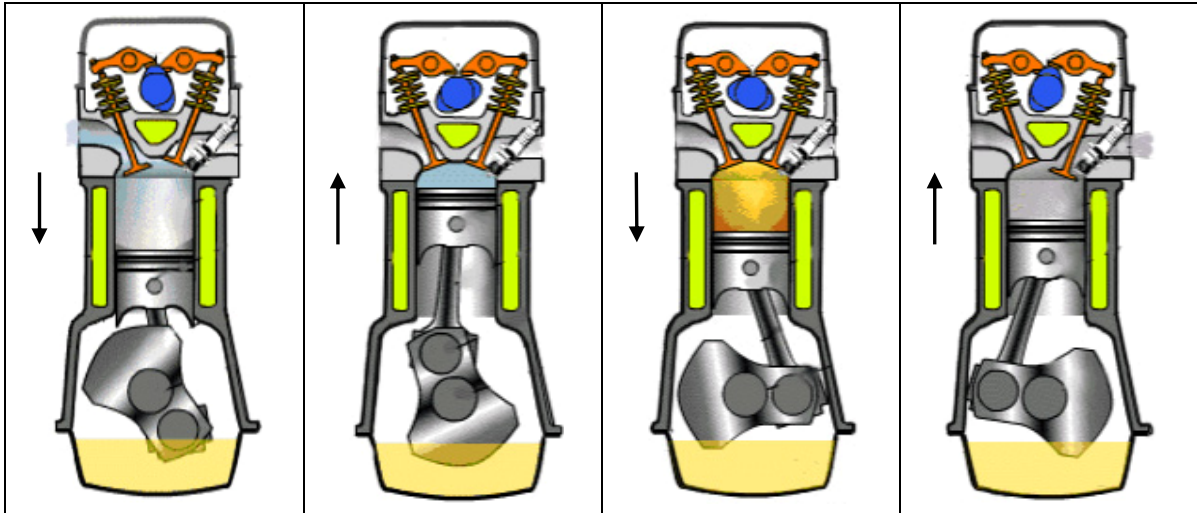
Figure 12*: Four-stroke cycle [27].*

When the CSC first started in 2000, four-stroke powered snowmobiles were virtually non-existent. Consumers wanted light-weight and powerful snowmobiles and outfitters wanted easy and low cost maintenance for their fleets. Four-stroke engines don't meet these requirements. They use poppet valves and a gear-train driven by the crankshaft to separate the phases of the cycle. They also use dedicated and pressurized oiling systems. In addition, a heavy flywheel is needed to aid in engine rotation during the additional two strokes of the piston [18]. All of these characteristics increase weight, mechanical complexity, and required maintenance. Finally, there is only one power-stroke every other revolution, half as often as a two-stroke, reducing relative power output.   But with NPS and EPA regulations on the horizon, engine manufacturers began producing four-stroke powered snowmobiles.

Four-stroke touring snowmobile engines have one to three cylinders and are either naturally aspirated or turbocharged with displacements ranging between 600 and 800 cc. They are almost always fuel-injected with an oxygen sensor for closed-loop operation. Because the EPA and NPS regulations focus on lowering UHC and CO emissions, these engines are often operated fuel-lean. This strategy is effective at reducing UHC and CO but dramatically increases NO_x emissions. Four-strokes easily meet the EPA standards, but they are significantly heavier than the two-stroke SDI engines currently on the market. This has a direct effect on fuel economy. Although SDI two-strokes waste fuel through short-circuiting, they have similar fuel economy because they are lighter. Table 3 compares some two and four-stroke snowmobile engines whose performance were scientifically measured at a CSC

competition [23, 24, 25]. Note that the two best four-stroke engines in the group also had catalytic converters that further reduced emissions. A comparison between two and four-stroke snowmobile engines that meet the 2012 EPA emission regulations is given in Table 4. It shows the differences in engine size, power output, and vehicle weight. It is clear that two-stroke powered snowmobiles offer better power-to-weight ratios.

Table 3: Emissions of CSC two and four-stroke snowmobile engines [23, 24, 25].

	CO [g/kW-hr]	UHC [g/kW-hr]	NO_x [g/kW-hr]	$UHC+NO_x$ [g/kW-hr]	MPG	EPA Score (40 CFR)
2003 CSC Champion (EFI 4-stroke **w/cat**)	23.75	2.09	5.47	7.56	20.1	199
2003 CSC Control (2-stroke)	319.94	125.50	0.73	126.23	8.7	46
2004 CSC Team #8 (2-stroke **w/cat**)	333.62	7.08	0.26	7.34	11.7	121*
2004 CSC Control (EFI 4-stoke)	99.84	11.48	23.33	34.81	15.3	162
2005 CSC Champion (EFI 4-stroke **w/cat**)	57.100	1.800	0.400	2.20	18.2	194
2005 CSC Control (SDI 2-stroke)	215.38	63.53	2.39	65.92	19.1	112

Exceeded EPA maximum CO $_{limit}$ and would not pass.

Table 4: Comparison between two and four-stroke snowmobile engines [26].

	Engine Type	Engine size [cc]	Engine Power [hp]	Dry Weight [lb.]	Power to Weight [lb./hp]
2006 Polaris 700 touring	2-Stroke SDI	755	130*	598	4.6
2006 Ski-Doo GTX Limited	2-Stroke SDI	600	120	533	4.4
2006 Arctic Cat T660 Turbo Touring	4-Stroke EFI Turbo	660	110	640	5.8
2006 Arctic Cat T660 Touring	4-Stroke EFI	660	55	620	11.3
2006 Polaris FS Touring	4-Stroke EFI	750	63*	628	9.9
2006 Polaris FST Touring	4-Stroke EFI Turbo	750	125*	643	5.1
2006 Yamaha RS Venture GT	4-Stroke Carbureted	937	120	625	5.2
2007 Yamaha Venture Lite	4-Stroke EFI	500	80	582	7.3

* Engine power is estimated based on [hp/cc] of similar engines.

**2.0	GASOLINE DIRECT-INJECTION**

This section describes current gasoline direct-injection technologies and how they can be utilized to significantly improve two-stroke emission and efficiency. The different types of GDI injectors and systems are given classifications and the basic operating principles of each system are discussed. Several descriptions of existing GDI two-stroke engines are used to highlight the fact that high-performance GDI engines have not yet been achieved. Finally, there is a discussion of the special considerations that need to be taken into account while designing a high performance GDI engine.

**2.1	DIRECT-INJECTION INTRODUCTION**

The two-stroke engine remains the engine of choice for snowmobile riders, outfitters, and manufacturers due to its simple construction, high power-to-weight ratio, and low cost. It is also used in many other arenas where a high power-to-weight ratio is required, such as motorcycles, handheld power equipment, and marine power generation. As discussed earlier, the two main undesirable side effects of the two-stroke cycle are: (1) mixing of the fresh air/fuel charge with the exhaust gas residuals and (2) the short-circuiting of the fresh charge during the scavenging process. It is imperative that these problems be overcome if the two-stroke engine is to meet the new recreational vehicle emissions standards. Unfortunately, any method used to increase fuel economy and reduce emissions cannot significantly increase engine complexity or weight in order to maintain the low cost and high power-to-weight advantage over four-stroke engines [55].

A significant amount of work has been performed attempting to overcome the two-stroke problems outlined above over the past two decades [17, 18, 20]. Of the concepts researched, gasoline direct-injection has had the largest impact on two-stroke engines. In a GDI engine, gasoline is injected directly into the combustion chamber at an optimal time to promote efficient combustion. An engine scavenged with only air would not lose any fuel during scavenging because most of the scavenging takes place when the piston is near BDC. The obvious advantage of GDI is the separation of scavenging air and the fuel; GDI also lessens the effects of fresh-charge and exhaust-gas mixing and is known to improve cold start reliability [36]. Furthermore, the combustion chamber can be designed to produce a non-uniform fuel distribution inside the chamber. This non-uniform fuel distribution can be used

to operate the engine in two different charging modes—stratified and homogeneous.

Initially, GDI developments were focused on four-stroke engines in the automotive sector. There are currently many GDI systems that are being used for automobiles [36]. GDI system classifications arose from the specific emissions and fuel delivery requirements of four-stroke engines because research and development started with these applications. The classifications help define the fuel delivery and combustion strategies. Logically, in order to classify two-stroke GDI systems, the four-stroke classifications defined by Zhao were modified for two-stroke applications, Table 5 below. The major differences in the classifications between two and four-stroke systems are the definitions of air/fuel ratio, injection timing, and charge motion.

The ability to use two different types of charging strategies makes GDI especially attractive to two-stroke designers. A stratified-charged engine promises to significantly reduce fuel consumption, CO, and UHC emissions [16]. Also, stratified-charged combustion can eliminate poor idle quality and poor low-load operation [21]. Stratified-charged combustion requires a readily ignitable mixture near the spark plug with a weaker, often non-ignitable, mixture in the rest of the combustion chamber [16]. This way, the power output of the engine can be controlled by varying the fuel supply rather than throttling the engine, which eliminates throttling pressure losses. The classic example of a stratified engine is the diesel cycle.

Stratified-charged combustion in a two-stroke GDI engine occurs when fuel-injection is timed late in the cycle and ignition is delayed until there is a fuel rich mixture surrounding the spark plug. The rich condition occurring at the onset of combustion results in a reaction rate high enough to initiate combustion [36]. The flame front, occurring at the interface between the fuel and oxidant, propagates from the spark plug gap burning continuously leaner until combustion can no longer be sustained [16]. One possible disadvantage of stratified charging is the potential for an increased production of NO_x from the excess oxygen in the cylinder, slower flame speeds, and the just lean of stoichiometric combustion occurring at the outer edges of the flame front [16]. This can be combated with the use of a catalyst specifically designed for a GDI two-stroke and the use of exhaust gas recirculation (EGR). Stratified combustion can be difficult to orchestrate, especially at high engine speeds.

Table 5: *GDI classifications modified from those used with four-stroke engines [36].*

Category	Classification	Description
Distance between spark plug gap and injector tip	Narrow-Spacing	The spark plug gap is close to the injector tip in order to ignite the spray periphery directly. Also called spray-guided.
	Wide-Spacing	A relatively large distance between the spark plug and injector tip. Stratification is a result of air-flow or spray/wall impingement. Also called air-guided or wall-guided.
Approach to creating a stratified charge	Spray-Guided	Stratification results from spray penetration and mixing. Spark plug gap is close to the injector tip and is a narrow spacing concept.
	Wall-Guided	Fuel spray is directed towards a shaped cavity in the piston crown with stratification resulting from this interaction.
	Air-Guided	Stratification is achieved through the use of air-assisted injectors and/or the interaction between the fuel spray and in-cylinder air flows and is usually a wide spacing concept.
Charge Motion	Tumble-Based	Tumble is used to create or assist in charge stratification.
	Swirl-Based	Swirl is used to create or assist in charge stratification.
	Squish-Based	Squish is used to localize stratified fuel distribution near the spark plug (not typically used in four-stroke applications).
Injector Location	Centrally-Mounted	Injector is located near the center of the combustion chamber
	Side-Mounted	Injector is located in the periphery with the spark plug neat the center.
Injector Type	Single-Fluid	Single-liquid fuel is injected at high pressure
	Air-Assisted	A mixture of air and fuel is injected using moderate to low pressures
Fuel Distribution	Homogeneous	Maximum air utilization and a homogeneous or nearly homogeneous air/fuel mixture exist throughout the cylinder.
	Stratified	Highly stratified charge is used with varying degrees of AFR throughout the cylinder, locally rich near the spark plug gap.
Injection Timing	Early Injection	Fuel is injected late in the expansion stroke or early in the compression stroke (avoiding scavenging flows), some stratification may still result.
	Late Injection	Fuel is injected just before or after the exhaust ports are closed to form a highly stratified air/fuel mixture.
Air/Fuel Ratio	Rich	The trapped air/fuel ratio is rich of stoichiometric, regardless charge stratification.
	Stoichiometric	The trapped air/fuel ratio is stoichiometric, regardless of charge stratification
	Lean	The trapped air/fuel is lean of stoichiometric. This can be a result of a homogeneous-lean mixture or a stratified (locally rich) mixture.

A GDI system can also create a homogeneously charged combustion chamber. For the GDI engine, homogeneous operation is accomplished when fuel is injected early in the cycle, allowing time for the fuel to completely atomize and mix with the freshly scavenged air. Homogeneous combustion is used for medium to high loads and is accomplished in one

of two ways. During medium loads, an overall trapped lean air/fuel ratio with some exhaust gas residuals are desired to limit heat release [36]. During high loads, the goal is to maximize air utilization and to operate the engine with a stoichiometric or slightly rich condition to maximize power [36]. The timing of the fuel injection for homogeneous charging—while much earlier than stratified injection—must be late enough to avoid any fuel from becoming involved with the scavenging flows to avoid short-circuiting fuel [18]. Figure 13 shows the difference between in-cylinder equivalence ratios for a stratified and homogeneously charged engine.
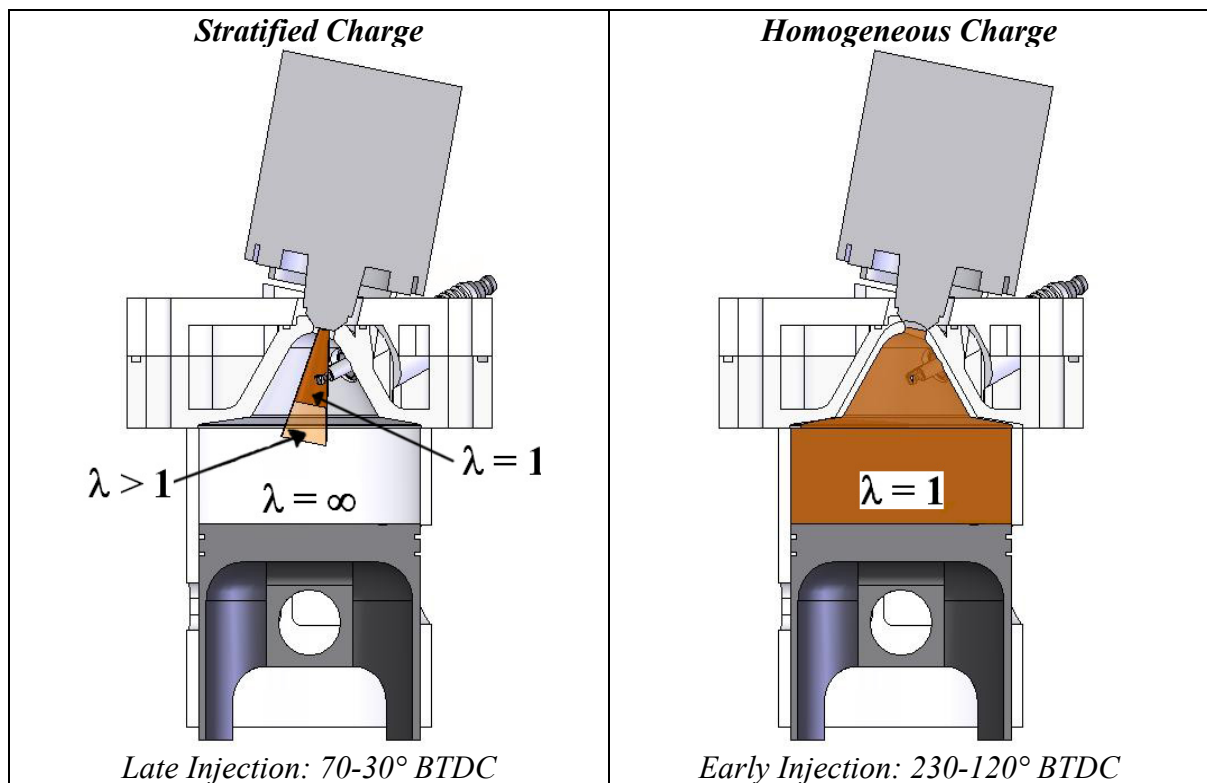
Figure 13: *Difference between stratified and homogeneous equivalence ratios.*

As shown in Table 5, there are two types of fuel-injectors used for GDI engines: air-assist and single-fluid. Air-assisted systems rely on injectors that utilize pressurized air to assist in injecting medium-pressure fuel [37]. The distinct feature of this type of system is the "good vaporization of the injection spray due to the aerosol generated by adding air to the gasoline [55 page 2]." Air-assisted injection can be accomplished several ways, though one of the best known air-assist systems for two-stroke engines was developed by the Orbital

Engine Company, illustrated in Figure 14. This is a crank-case scavenged engine that utilizes an air pump driven by a belt or gear connected to the crankshaft in order to supply pressurized air at 70 psig to the main injector, which is located in the cylinder head [20]. Fuel is also supplied at 90 psig to the main injector where the fluids meet before blasting the mixture into the cylinder. This system produces fuel droplets smaller than 10 mm [16]. The fluids are metered separately allowing very precise control of the injected fuel and air [17]. Orbital has developed GDI two-stroke engines for prototype automobiles and motor scooters. Both have been shown to have low emissions and fuel consumption better than many four-stroke engines [17].
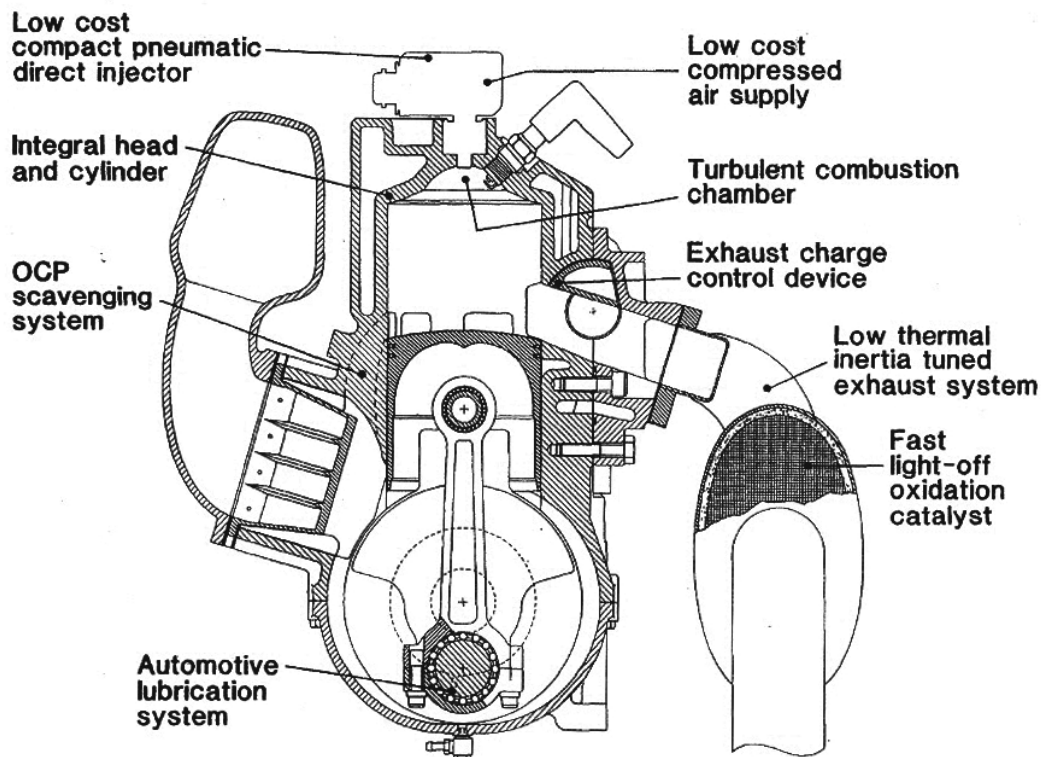
Figure 14: *Orbital Engine Company crankcase scavenged GDI air-assist engine [32].*

Another air-assist system, considered by Blair to be the most "significant yet proposed," was developed by the Institute Français du Pétrole, named the IAPAC (Iniection Assistée Par Air Comprimé) system [17 page 504]. This engine has been shown to have emissions, specific fuel consumption, and a power-to-displacement ratio similar to some of the most advanced four-stroke engines. However, the IAPAC system is significantly lighter

than many other systems, which allows a vehicle to have excellent fuel economy [17]. A small car operating on the European driving cycle at 56 and 75 miles/hr had an average fuel consumption of 73.2 miles/gallon [17]. The system uses compressed air in a storage tank, supplied by the crankcase, to blow air into the top of the combustion chamber through a poppet valve. The fuel is supplied by a low-pressure injector located behind the poppet valve in the cylinder head, see Figure 15. Fuel injection is timed to allow some residence time on the back side of the valve to allow for evaporation before the poppet valve is opened [17]. Obvious added engine complexity exists, although the engine still remains less complex and lighter than a four-stroke engine. There are many other designs for air-assist GDI [36]. However, the Orbital and the IAPAC are the most attractive air-assist systems for two-stroke applications.
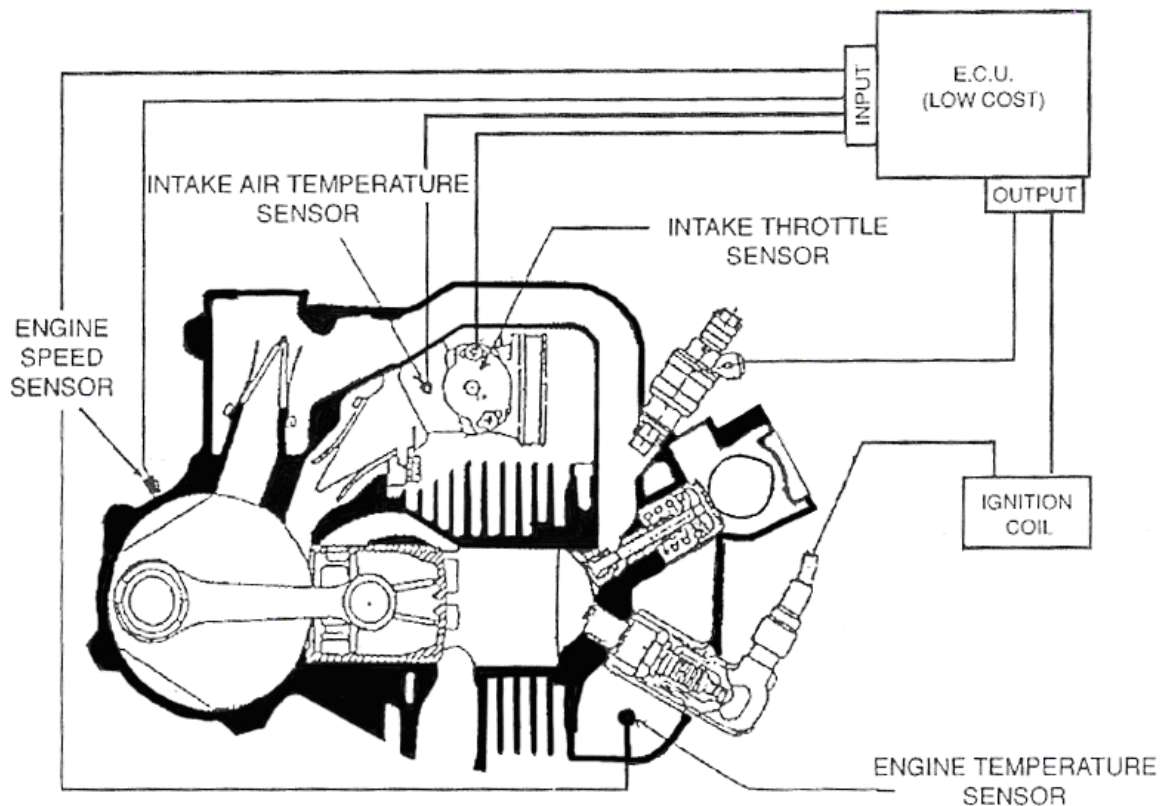
***Figure 15**: Cross section of an IAPAC crankcase scavenged GDI engine [20].*

Single-fluid GDI systems operate with much higher fuel injection pressures (300-2000 psig) and they are referred to as High-Pressure Direct-Injection (HPDI). There are two

methods used to generate the high fuel pressures, constant high pressure and modulated high pressure [55].   In the first type of HPDI, the high injection pressure (800-2000 psig) is constantly provided by a high-pressure fuel pump driven by a belt or gear powered by the crankshaft. The high pressure fuel is supplied to a common rail that feeds the electronically, or mechanically operated fuel injectors [37]. Because of the extremely high injection pressures, constant pressure HPDI systems can inject fuel much more quickly than air-assist DI systems. The injector nozzles are normally outwardly opening swirl type [36]. This type HPDI is often chosen because of the consistency of injection rate and easily tailored fuel droplet size, and is readily available on the market [37].   Figure 16 shows a constant pressure HPDI system on a two-stroke engine similar to a snowmobile engine [37].
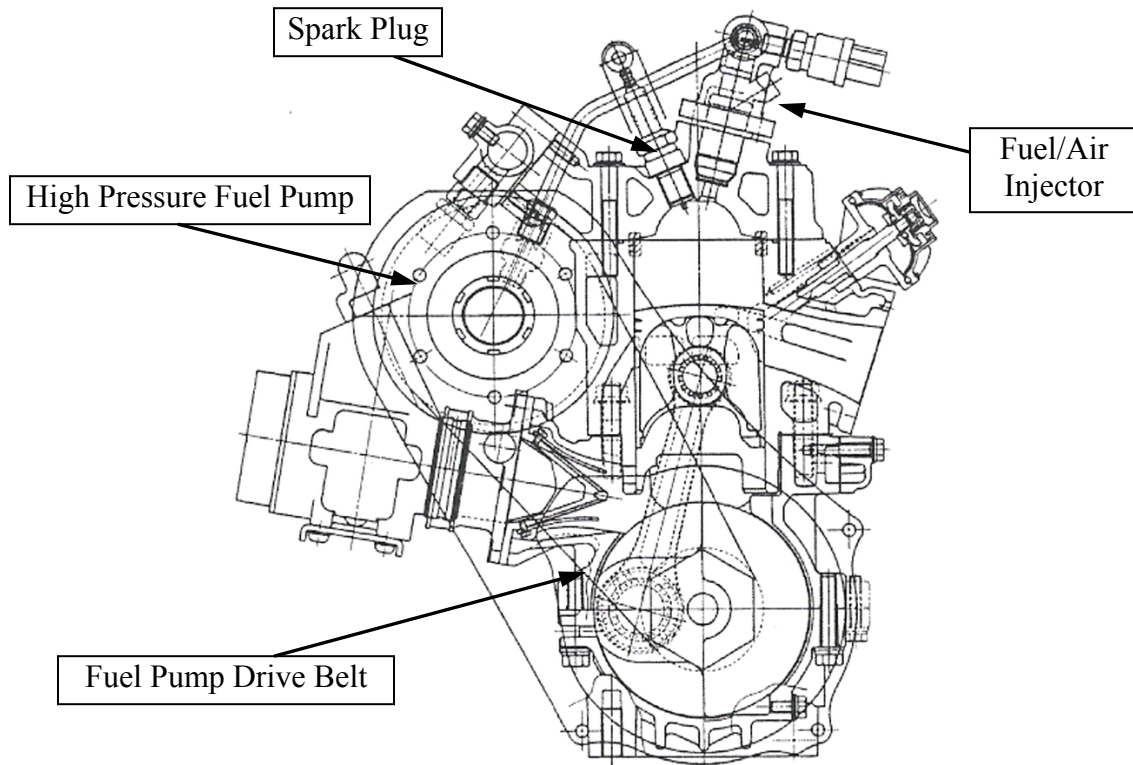
Figure 16: Schematic of a crank-case scavenged HPDI GDI engine [37].

The second type of HPDI uses modulated fuel pressure. These systems produce fuel pressures in the range of 300-800 psig [55]. One of these systems is referred to as the "Ram-tuned liquid fuel injection system [17 page 514]." The Ram-tuned system uses the principal of water hammer. When a moving column of liquid is quickly decelerated a high-pressure

wave can be created [17]. Using several valves, regulators, and pipes, a pressure rise of 400 psig can be developed and used to inject the fuel. It is a complicated system and requires a significant amount of development time. Another system that utilized the water hammer effect with fewer moving parts, less system complexity, and more precise fuel metering was the FICHT system. It was used on the first successful production modulated HPDI engines [17]. FICHT injectors were developed by the Outboard Marine Corporation (OMC) and were used with Evinrude outboard engines as well as Polaris and Kawasaki personal watercraft [21]. The second-generation modulated injection system, E-TEC, is now being used by BRP, formerly OMC, on the new Evinrude engines. The unit injectors are supplied with fuel at 35 psig and increase it to nearly 800 psig [21]. Figure 17 is the UICSC experimental engine that utilizes the E-TEC modulated injection system.
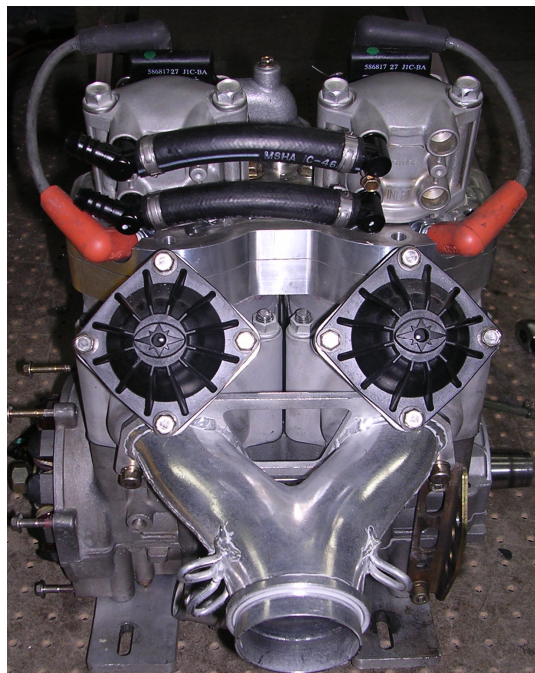
Figure 17: *Modulated HPDI two-stroke engine using E-TEC injectors [21].*

The above examples of GDI two-stroke engines represent simple crankcase scavenged GDI engines that attempt to retain the low engine bulk volume, low weight, and mechanical simplicity that leads to high power density and low cost. These engines would typically be used for off-road transportation or motor scooter applications. There have been

recent developments in two-stroke GDI engines for use in automotive applications. Figure 18 shows layout drawings of two such engines [32]. The first engine pictured is a crankcase scavenged Orbital engine that uses air-assist injection. The second engine is the externally scavenged Toyota S-2 HPDI that used a roots-type blower with poppet valves. Poppet-valve and externally scavenged engines are superior in oil consumption, durability, and scavenging efficiency [32]. However, they are inferior to crankcase scavenged engines in terms of maximum engine speed, engine size, and cost [32]. As of yet, two-stroke GDI engines have not been used successfully in production automotive vehicles.
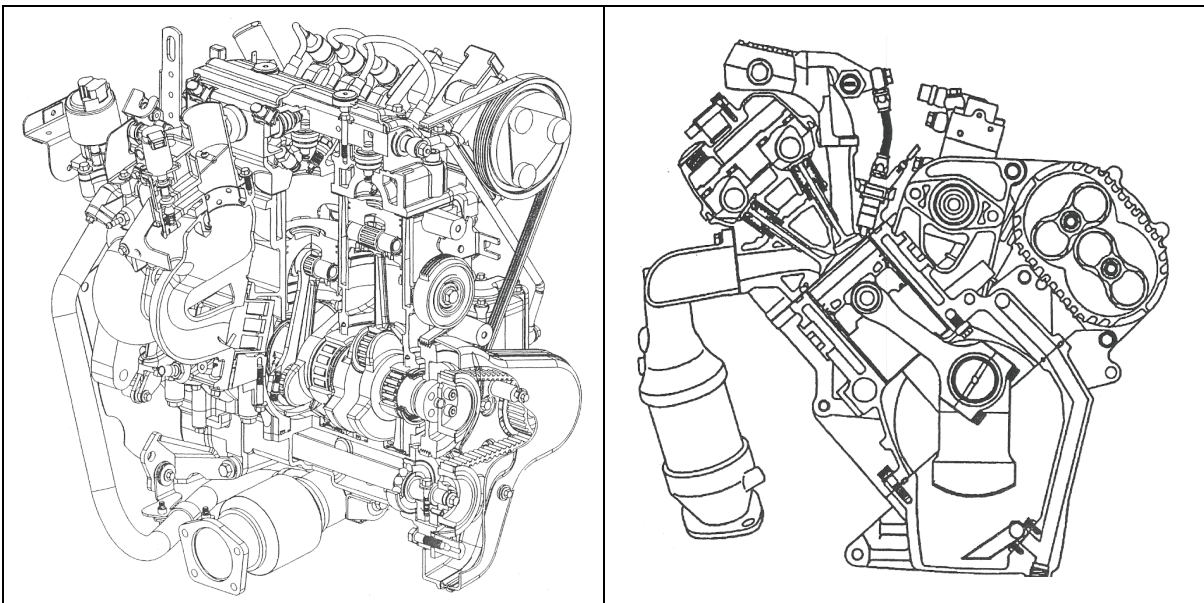
Figure 18: Orbital and Toyota two-stroke automobile GDI engines [32].

Currently, the only transportation industry producing GDI two-strokes for consumers is the outboard marine industry. Successful marine two-stroke GDI systems, such as the Orbital air-assist system used by Mercury Marine and the E-TEC HPDI system from BRP, meet the stringent California Air Resource Board's (CARB) "Ultra-low" 3-Star emissions for outboard marine engines [21]. In the marine industry, two-stoke GDI engines have been shown to have better fuel economy, less oil consumption, similar $UHC+NO_x$, and significantly less CO than their four-stroke counterparts [12, 22]. Figure 19 shows the total reportable ICOMIA emissions and the 3-Star levels for outboard engines [Courtesy of BRP]. Most of the research and component selection for the UI GDI engine was found from

outboard GDI literature because of the success the industry has had. However, there are significant challenges that need to be overcome before a snowmobile GDI two-stroke engine can meet the NPS emission requirements.
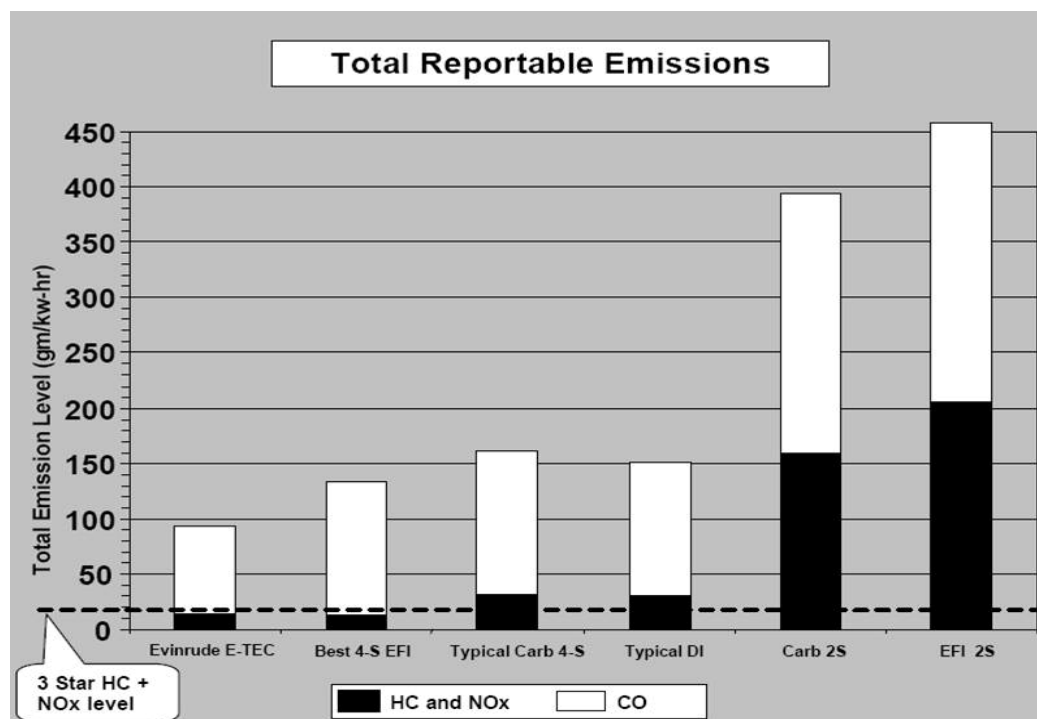
Figure 19: *Total reportable ICOMIA emissions for marine engines [Courtesy of BRP].*

2.2   SPECIAL CONSIDERATIONS FOR SNOWMOBILE GDI ENGINES

Marine GDI systems were developed specifically for outboard engines and their performance requirements. Those requirements are significantly different than those for snowmobile engines. This is highlighted by the differences in the modal weighting for the five-mode testing procedures used by both industries. Outboard emission measurements use a five-mode testing procedure called the ICOMIA cycle. Table 6 compares the differences between the ICOMIA and the SwRI five-mode testing procedures. It is clear that the outboard emission cycle focuses on part load and idle conditions while the snowmobile cycle weights medium and high loads more. The SwRI five-mode focus on high engine speeds and loads makes developing a GDI system for a high-performance two-stroke engine difficult.

Table 6: *ICOMIA and SwRI Engine cycles for exhaust emissions [8].*

ICOMIA Mode Points					SwRI Mode Points			
Mode Point	Speed [percent of Rated]	Torque [percent of Rated]	Weighting [percent]		Mode Point	Speed [percent of Rated]	Torque [percent of Rated]	Weighting [percent]
1	100	100	6		1	100	100	12
2	80	71.6	14		2	85	51	27
3	60	50	15		3	75	33	25
4	40	25	25		4	65	19	31
5	Idle	N/A	40		5	Idle	N/A	5

The main reason why GDI systems for a high-performance two-strokes are difficult to design is because snowmobile two-stroke engines operate at significantly higher engine speeds with greater fuel demands in order to produce high power output. Snowmobile engines operate at speeds in excess of 8000 rpm with specific power outputs of nearly 150 kW/liter. This is compared to outboard and automobile engines that have rated engine speeds around 6000 rpm and specific power outputs of just 70 kW/liter. At peak loads a short period of time, 1.2-3.5 ms, exists where a large amounts of fuel must be injected, and fully atomized, while avoiding short-circuiting.

The large peak load fuel requirements pose a challenge for low load and idle fuel requirements. An injector nozzle designed to deliver high quantities of fuel quickly, usually has poor light-load and idle fuel-spray qualities [36]. A two-stroke GDI at full power can use in excess of 40 kg/hr of fuel while at idle only needing 0.5 kg/hr, leading to the difficult task of designing a precision nozzle capable delivering high flow rates and precise fuel metering.

Beyond performance requirements, another obstacle is the economic impact associated with producing a high-performance GDI two-stroke. Industries where two-stroke engines are attractive require low production costs. Even small increases in costs associated with parts or research and development may impact overall production costs significantly, eliminating the low-cost production advantage that the traditional two-stroke has over four-stroke engines [55]. Any increases in cost passed on to the consumer will be expected to be partnered with an increase in performance through increased fuel economy and/or power output without increasing maintenance costs.

3.0   UNIVERSITY OF IDAHO SINGLE-FLUID SPRAY-GUIDED GDI SYSTEM

This section describes the baseline engine, the components that were adapted, modified, or designed to allow for GDI operation, and the fuel control strategies used. There is a description of the operating principles of the E-TEC injectors, their fuel-spray pattern, and how the injected fuel spray characteristics affected the combustion chamber design. Additional supporting hardware, such as electrical power generation, are described in detail. Finally, there is a discussion of the different types of combustion strategies that can be used as well as guidelines that describe when certain types of combustion should be used and how to transition between them.

3.1   BASELINE ENGINE

The baseline engine was a 2005 Polaris Liberty 600 cc two-stroke with variable exhaust valves and a tuned exhaust. This engine was chosen for two reasons: First, it represented a standard engine size for two-stroke touring snowmobile engines; second, it was the maximum allowable two-stroke displacement for engines competing in the SAE CSC competition [14, 15]. Table 7 shows the specifications of the engine and Figure 20 shows a cross section of an engine similar to the one used for research.

Table 7: *Polaris Liberty 600 cc Baseline Engine Specifications*

Engine Type	Two-Stroke, Carbureted, Liquid Cooled
Number of Cylinders	2
Bore	77.24 [mm]
Stroke	64 [mm]
Displacement	600 [cm^3]
Compression Ratio	6.5 (Trapped)
Intake Type	Crankcase Reed Valve
Scavenging Type	Loop (Curtis-type)
Rated Power	86 [kW]
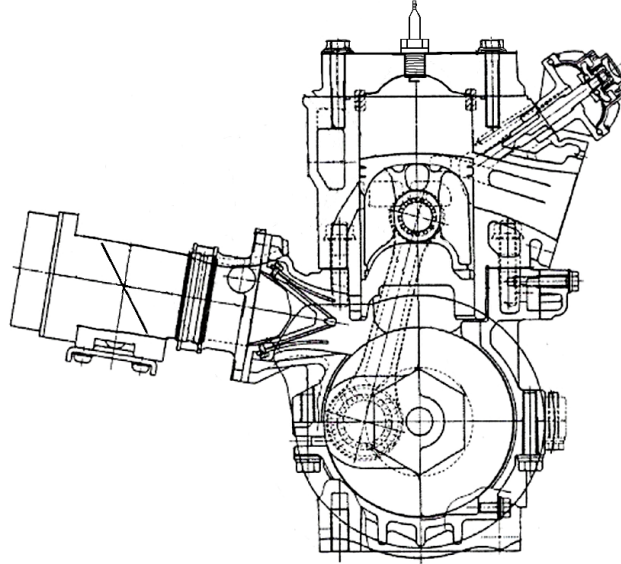
Figure 20: *Engine cross-section similar to the UI CSC test engine, adapted from [37].*

3.2   E-TEC HPDI SYSTEM

After researching many GDI systems, the University of Idaho chose to adapt the E-TEC single-fluid and modulated HPDI system. This system was chosen after considering availability, system complexity, and the aforementioned special requirements for snowmobiles. Modulated systems have the fewest components, good fuel atomization, low-pressure fuel supply, and can adapt to any number of cylinders or engine sizes [21]. Also, as will be discussed later, these systems offer the greatest potential for high-performance GDI engines because of their fuel-spray characteristics and minimal weight increase. The E-TEC system was chosen because it was the only modulated system available that, through research and extensive testing, had been proven to offer the performance desired for the UI CSC test engine. The most appealing features of the E-TEC system were:

- The system was designed with two-stroke engines in mind;

- It is easily adapted to any number of cylinders or displacements;

- The injectors have high fuel flow and speed potential;

- Very precise fuel metering is possible;

- Few components are required to make the system work;

- A significant amount of information about the system was available.

The E-TEC engines use second generation electromechanical injectors developed by BRP. These injectors are 25 percent lighter and have 50 percent fewer moving parts than the previous FICHT injectors [Courtesy of BRP]. The E-TEC injectors are vastly superior to the FICHT injectors because they have faster operation, higher fuel flow rates, higher fuel pressures, and better fuel atomization. Table 8 compares the FICHT and the E-TEC injectors.

Table 8: *A comparison between the FICHT and E-TEC direct injectors [Courtesy of BRP].*

	FICHT	E-TEC
Maximum Power [hp/cylinder]	45	80
Maximum RPM [min^{-1}]	7500	10,000
Injection Time [ms]	5	2.5
Maximum Injection Pressure [psig]	450	>700*

* Maximum E-TEC Fuel pressure is from [16].

The E-TEC injectors are able to perform better than the previous FICHT injectors because of new internal parts, improved nozzle design, and an improved electronic control strategy [55]. The cross-section view shown in Figure 21 highlights the different designs and internal parts between the E-TEC and FICHT injectors. The following description outlines the E-TEC injector operating principles and how they are able to perform better than the FICHT injectors:

> Similar to the FICHT injectors, fuel is re-circulated through the injector bodies to continuously cool them and to ensure all vapor is removed. Vapor removal is important to ensure accurate and consistent fuel metering. Also like the FICHT injectors, the E-TEC injectors use an electromagnet.   But rather than a fixed coil, a moving steel armature, and one-way current polarity, they use a lightweight moving coil, lightweight plunger, and dual polarity current.

> Inside the lightweight coil there are three fixed and powerful rare-earth magnets. When current is supplied to the coil, an electromagnetic field is produce which interacts with the permanent magnetic field of the magnets causing coil bobbin to move with great force. The coil bobbin pushes the plunger, initially through a free stroke, through the fuel until it contacts the poppet valve. Together, the poppet valve and the plunger act as a piston pressurizing the fuel behind the nozzle. The pressure rise forces open the nozzle where the fuel travels through an outwardly opening swirl type nozzle.

After the fuel has been ejected, the current is turned off and a brief reverse
polarity current is supplied to the coil. The reverse current stops the movement
of the bobbin and plunger, and starts its return to begin the next injection event.
As the coil approaches its initial position a second forward current pulse is used
to slow it down to prevent bounce, which leads to instability. Finally, a second
reverse current is sent to stabilize the coil bobbin before the next injection event
occurs. The lightweight materials, moving coil, and use of dual polarity electric
pulses allow the E-TEC injectors to be more powerful, faster, and more precise

[Courtesy of BRP].
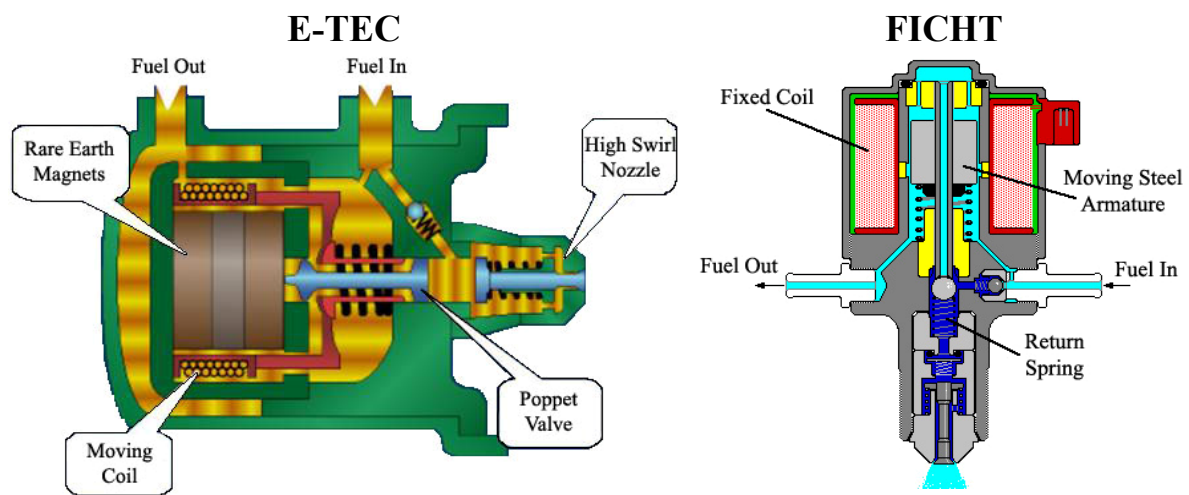
Figure 21: *Cross-section of the E-TEC and FICHT injectors [Courtesy of BRP].*

Another unique feature of the E-TEC injector is the swirl nozzle that is shown in
Figure 22. The tangential swirl channels, a lower needle lift (100-160 mm), and the resulting
higher fuel pressures reduce the average droplets size from 40 to 25 mm [21]. The new
nozzle also improved the spray homogeneity, which was reflected by the reduction of droplet
size and increase in penetration velocity. Currently, injector nozzles are available with
needle strokes of 100, 130, and 160 mm and the injectors are capable of delivering between 0
and 65 mm^3 of fuel per stroke.
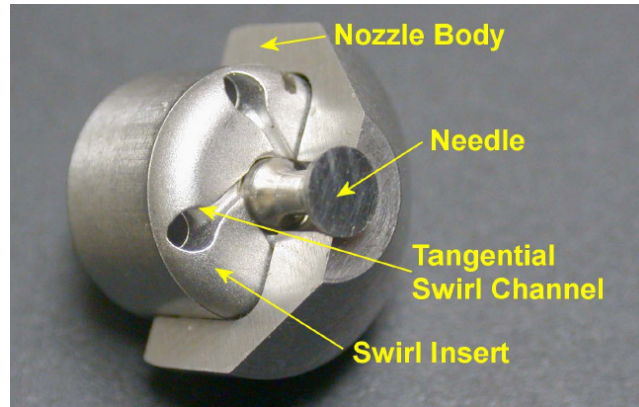
Figure 22: *Outwardly opening swirl nozzle used in the E-TEC injectors [21].*

For fully functional GDI engines the purpose of the injector is to provide fuel that leads to the desired in-cylinder mixture distribution for the various modes of combustion. These goals are extremely important for GDI engines where low emissions, high performance, and good run-quality are desired [55]. Much of the research on GDI engines has been focused on developing injectors capable of providing very small droplet sizes, less than 10 mm [21]. Smaller droplet sizes were thought to be essential for GDI engines because [36]:

- Fuel vaporization times are largely driven by droplet size. With the already short mixture preparation times available for two-strokes, small droplets were thought to be necessary.

- To avoid wall-wetting, which leads to UHC and PM emissions, a fuel spray with low penetration and fast fuel vaporization is required. This can usually be accomplished with small droplets.

- Wall-guided systems use small droplets with low momentum so fuel can follow the bulk flow of air to be distributed.

- During stratified operation, a compact fuel spray is necessary to reduce over-mixing.

This ideology was passed on from both four-stroke GDI development and two-stroke "thought" experiments to current two-stroke GDI development. Thought experiments were designed to limit short-circuited fuel by utilizing late injection timing, which requires very rapid fuel vaporization and, therefore, small droplet sizes. Previous experiments have shown

strong correlations between lowered emissions due to smaller droplet size coupled with late injection [17, 20, 32].

However, those experiments were conducted on low-speed engines with low specific power when compared to the goals of this research. Recently, there have been studies showing that smaller droplets are not necessarily better for all engine designs [21]. The main conclusion from the recent studies was that different engines respond differently to similar fuel spray characteristics. Strauss's tests showed that smaller droplet sizes can actually lead to more UHC emissions for some two-stroke engines, especially at high engine speeds. This can be explained by differences of in-cylinder flows and the momentum exchange between the fuel spray and the scavenging flows.

With four-stroke GDI engines, fuel is normally injected in the same direction as the bulk flow [36]. The injected fuel in two-stroke GDI engines is usually injected *against* the bulk flow [21]. At very late injection timing, typical of stratified combustion, this is not critical. However, when high speed and high specific power are desired, it is important to fully understand how the fuel-spray interacts with the counter-flow of scavenging air and how this impacts engine design. Strauss conducted several experiments to analyze the impact droplet size has on emissions and mixture preparation for two-stroke GDI engines using the E-TEC system [55]. First, he compared the emissions of two different engines; each engine was tested with two different nozzle sizes. Strauss found that nozzle size, and therefore droplet size, played an important role in the engine-out emissions. From the nozzle comparison, he was able to conclude that "fuel behavior in one engine is not necessarily indicative of its behavior in another engine. Despite the geometric similarities, the engines differ in the in-cylinder flow structures and it is suspected that it is these differences and the consequent interaction with the fuel spray that cause the observed behavior [55 page 5]."

To further understand the interaction between the E-TEC fuel spray and the scavenging flows, Strauss evaluated E-TEC injector spray interactions with varying speeds of counter flow. He compared injector strokes of 100 and 130 mm with a delivered fuel quantity of 30 mm^3 [55]. Figure 23 is a series of spray images for the 100 mm stroke nozzle at 1 and 2 ms after the injection event into various counter-flow velocities. Clearly, the counter-flow has a significant impact on the fuel spray—the penetration distance is reduced, Figure 24, and the cone angle increases with increasing air velocity. Also, secondary

breakup length, which describes where the injected fuel begins vaporize more quickly, decreases with increasing air velocity, highlighted by the step change in spray dispersion [55]. Further insight into the fuel spray interaction with counter-flow is seen in Figure 25, which shows the maximum fuel penetration for 100 and 130 micron stroke nozzles.
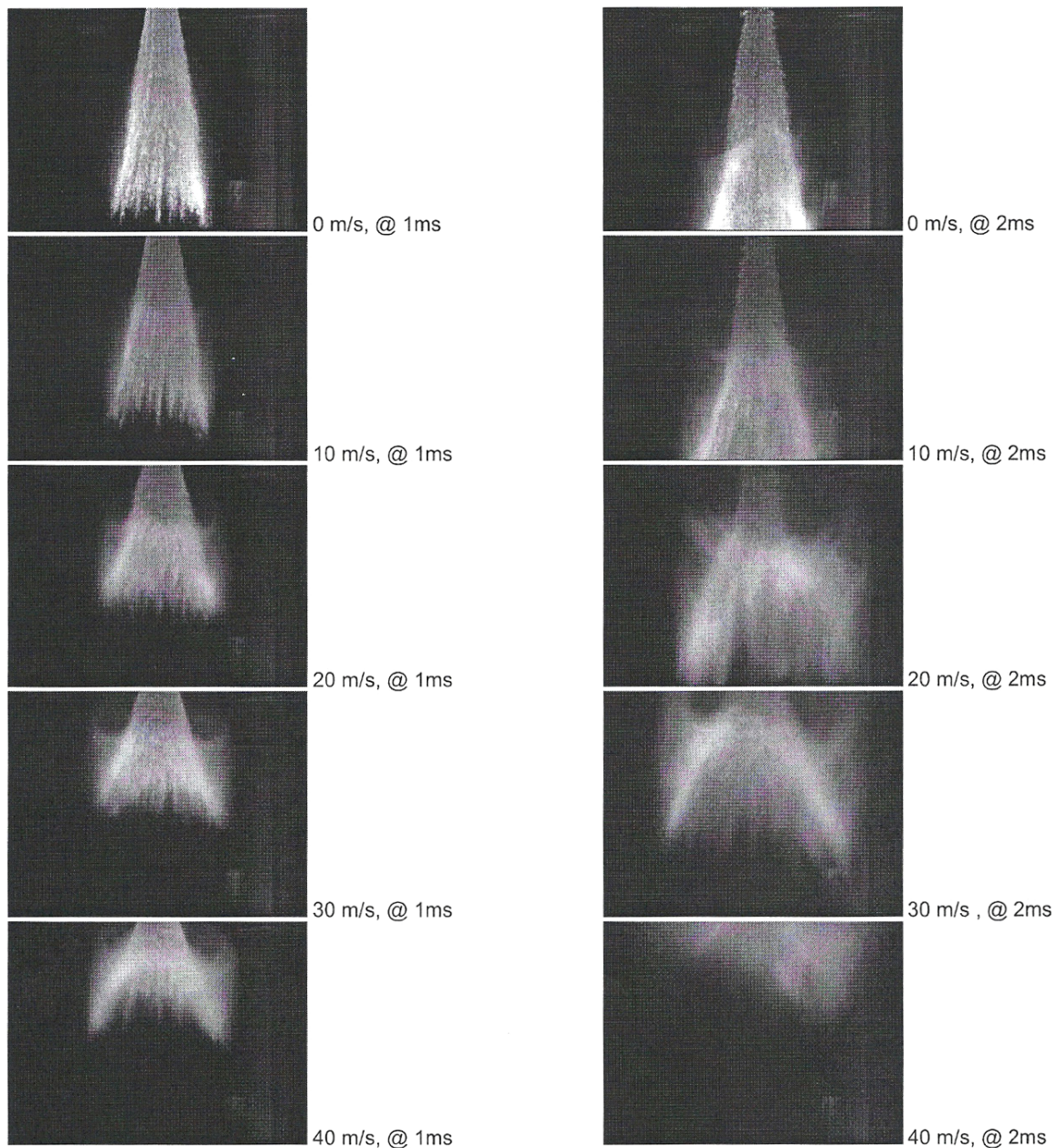
Figure 23: *E-TEC fuel spray images into varying speeds of counter-flow [55].*

It can be concluded from these studies that two-stroke scavenging flows have a

significant effect of fuel dispersion and emissions, especially for high speed engines with high specific power. For engines with aggressive port geometry and scavenging flows—as in a snowmobile engine—a fuel spray with larger droplets may actually be more desirable. When early injection times are required, larger droplets should resist the initial scavenging flows, which will reduce UHC emissions and the amount of short-circuited fuel.
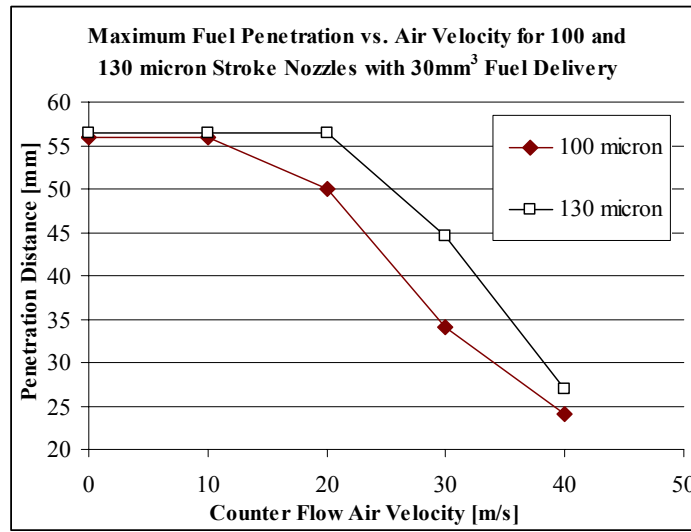
Figure 24: Maximum fuel penetration from E-TEC fuel spray [adapted from 55].

3.3   COMBUSTION CHAMBER DESIGN

Combustion chamber design is of paramount importance for GDI engines, especially when applied to two-stroke engines. While the two-stroke GDI combustion chamber is less complex than that of a four-stroke engine, designing around the in-cylinder flows and fuel spray characteristics can be more difficult because of the counter-flows of air inside the two-stroke cylinder during scavenging. The in-cylinder air motion, fuel spray characteristics, and interaction between the two require careful consideration of the following when designing the combustion chamber:

1) Compression ratio,
2) Combustion chamber shape and location of fuel spray,
3) Location of injector nozzle and targeting of the fuel spray, and
4) Sparkplug location.

Two-stroke engine compression ratios are defined in two ways, geometric or trapped.

The geometric compression ratio is calculated the same way as with four-stroke engines, using the ratio of the cylinder volume at BDC and TDC. The geometric compression ratio does not represent the actual two-stroke compression ratio—and is therefore rarely used to define two-stroke engines—because the actual compression process in two-stroke engines does not begin until around exhaust port closure, well beyond BDC. The trapped (CR_t) compression ratio, often referred to as the effective compression ratio, is more representative of the actual compression process. It is defined by the ratio of the volume of the cylinder at exhaust port closing and TDC. The equations used to determine both geometric and trapped compression ratios can be found in Appendix A. It is well know that higher compression ratios lead to higher thermal efficiencies and lowered brake-specific fuel consumption. However, increasing the compression ratio too much leads to detonation and engine failure.

At higher compression ratios, peak cylinder pressures increase in magnitude and occur earlier. Also, the burned and unburned zones in the cylinder see a rise in temperature [17]. Detonation can occur by auto-ignition in gasoline-vapor mixtures if the temperature is above 880°C [17]. If the temperature in the end zones, or other localized pockets of end zone gasses, reach the auto-ignition temperature then detonation can occur. Knowing if a particular compression ratio will lead to excessive end-zone temperatures is difficult without experimental data. Furthermore, as stated by Blair, "the subject [compression ratio selection] is not one which is amenable to empiricism, other than the (ridiculously) simplistic statement that trapped compression ratios, CR_t, of less than 7, operating on gasoline of better than 90 octane, rarely give rise to detonation. [17 page 490]" According to Blair, the proper approach is one that utilizes computer simulation.

Because computer simulation was not available to determine the best compression ratio for the UI GDI engine, estimation was made using the base-line engine. The stock carbureted engine used for the UI GDI project had an effective compression ratio of 6.52, which is in the middle of typical values of 5.9—7.0 [32]. Initially, it was thought that the compression ratio of the UI GDI engine could be increased due to the latent heat of vaporization of the fuel being injected into the combustion chamber [37]. Vaporizing fuel pulls heat out of the air in the cylinder, which raises the knock limit and allows for a higher compression ratio [37]. From this assessment, the first compression ratio used was increased to 7.06. However, during initial testing of the engine, excessive detonations in the

combustion chamber lead to piston failure. It was determined that because the fuel was no longer going through the crankcase and cooling it, the crankcase maintained a higher temperature. The benefit of injecting the fuel into the combustion chamber was offset by the hotter air entering the combustion chamber from the crankcase. Therefore, without crankcase temperature management, compression ratio should not be increased.

The volume of the combustion chamber is defined by the compression ratio. The next step is to determine the shape of the combustion chamber when the piston is at TDC— the clearance volume. An understanding of the fuel-spray characteristics and its interaction with in-cylinder airflow aids in chamber design. As discussed earlier, the injected fuel spray varies significantly depending on the airflow it encounters. During stratified operation, fuel spray and scavenging air flow interaction is expected to be minimal and fuel spray penetration is expected to be significant and the fuel spray from the E-TEC injectors will have deep penetration, see Figure 23. This deep penetration would cause fuel impingement on the piston surface in a standard hemispherical combustion chamber and wall impingement of the fuel spray has been shown to be a major source of UHC [21]. Therefore, a tall combustion chamber was required for this engine. Two other factors that are critical for optimal fuel spray development and mixture preparation are the near nozzle geometry and the distance between the fuel cone and the cylinder walls [21]. Figure 25 illustrates a combustion chamber that incorporates these factors. The near nozzle geometry allows spray development, the height of the chamber limits fuel impingement, and the fuel cone is equidistant from the chamber walls.
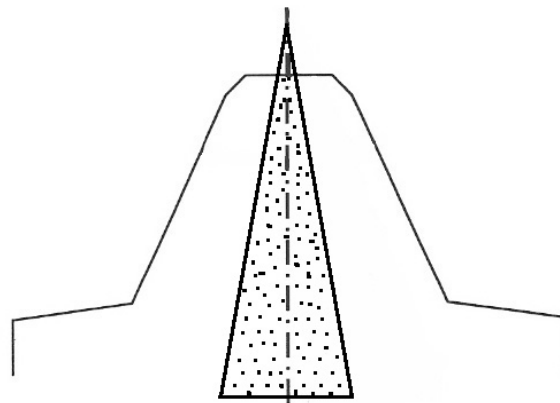
Figure 25: *Schematic of a tall combustion chamber with a centrally located injector [21].*
Studies have shown that fuel-spray targeting towards the boost port can have a

positive effect on emissions and power output [21,37]. These benefits are attributed to improved fuel trapping and atomization. One study of an experimental constant-pressure HPDI crankcase and Schnurle loop scavenged engine for snowmobile applications compared CO emissions for two different injectors and fuel-spray targets [37] Figure 26 shows the two targeting schemes considered in that study. The injector used for targeting labeled "A" had a 60 degree cone angle, 15 mm droplets, and a penetration distance of 30 mm; the injector used for targeting labeled "B" had a 20 degree cone angle, 20 mm droplets, and a penetration distance of 60 mm. The authors found that targeting B was able to utilize earlier injection timings and had reduced CO emissions.
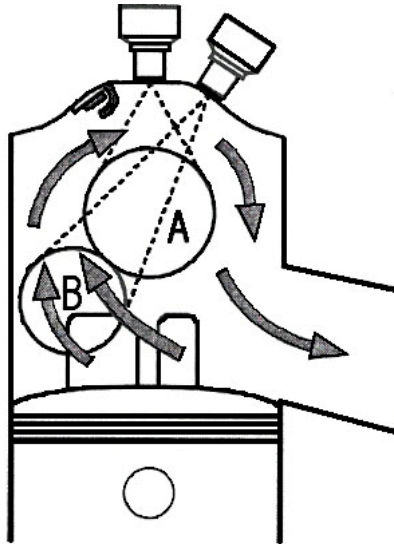
Figure 26: *Different fuel-spray targeting strategies for a HPDI engine [37].*

The fuel spray characteristics of the E-TEC injectors used in the UI engine are similar to the injectors used in targeting B. Given the results of the study, injector targeting in the UI GDI engine was modeled after targeting B. Another study, conducted on E-TEC injector targeting, suggests the injectors should be angled between 7 and 20 degrees [21]. A 20 degree targeting angle provided fewer UHC+NO_x emissions at early injection angles while the 7 degree targeting angle provided slightly more power at early injection angles. Based on this information the fuel injectors for the UI GDI engine were angled 11 degrees towards the boost port.

However, targeting the fuel spray towards the boost port created a problem. As the

injector was angled, the fuel spray necessarily became further from one wall and closer to the other, as shown in Figure 27a. This condition would have had a negative impact on fuel-spray development, proper air/fuel distribution, and wall impingement [21]. In order to alleviate this problem, the combustion chamber dome was offset toward the intake ports to center the fuel spray in the combustion chamber, similar to Figure 27b.
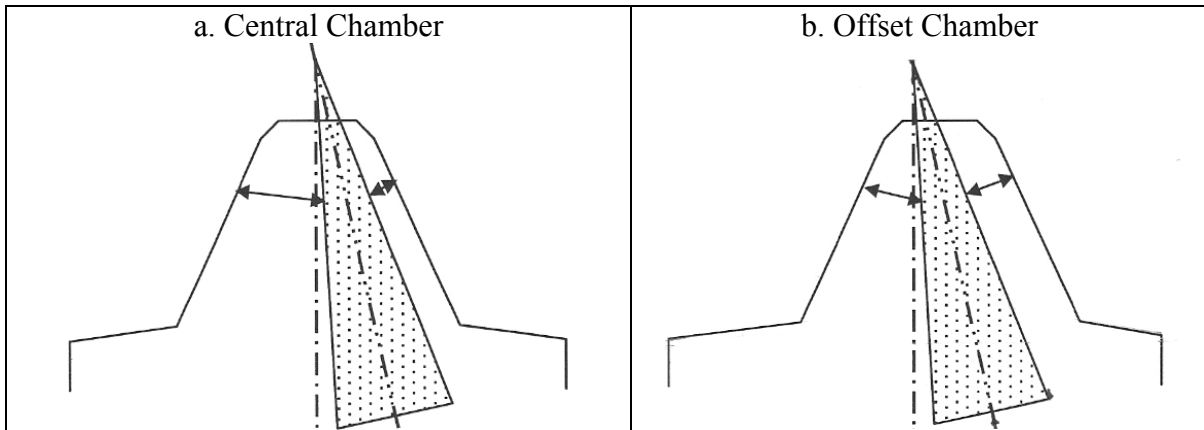
Figure 27: *Schematics comparing central and offset chambers [21].*

The first UI GDI combustion chamber was designed for a naturally aspirated engine using the FICHT injectors, shown in Figure 28. The chamber was very similar to the offset chamber shown in Figure 27b above. With the combustion chamber offset towards the intake ports, the length of the squish band on the exhaust side lengthened significantly. This had a negative effect. As the plugging pulse returned from the tuned exhaust system, a backflow of hot gasses entered the chamber. The gasses were directed up and toward the centerline of the chamber. Presumably, the hot gasses were impacting the large squish band, creating odd in-cylinder flows and hot spots on the squish band edge; the hot spots led to excessive detonation and piston failure. Also, with the near nozzle geometry, there was not enough space at the injector tip for the fuel spray to develop properly.
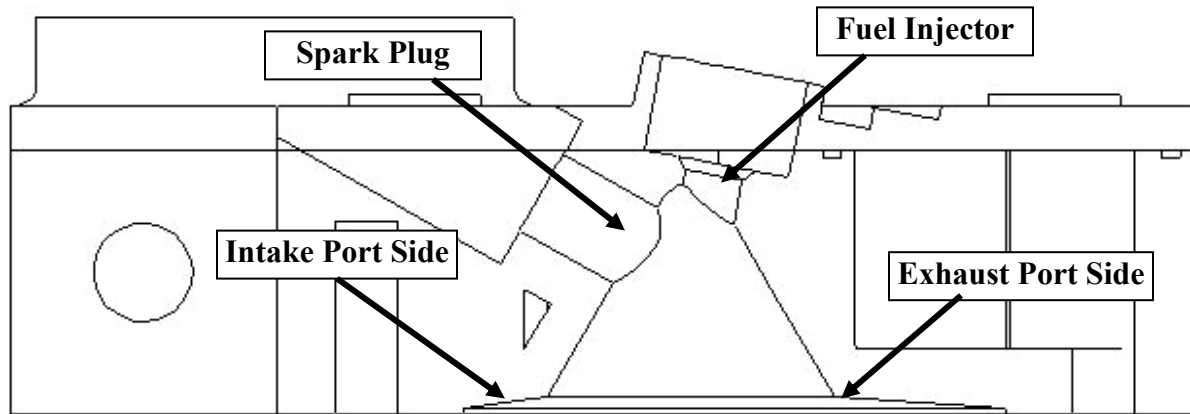
Figure 28: *Cross-section of the UI FICHT GDI combustion chamber.*

The second naturally aspirated UI GDI combustion chamber developed for the E-TEC injectors, and shown in Figure 29, addressed the downfalls of the first chamber. The top of the chamber utilized a larger radius for better near-nozzle geometry and the height of the chamber was modeled after the dimensions from a in-line two-cylinder E-TEC engine combustion chamber. In an attempt to eliminate the detonation problems of the first GDI head and to centralize the fuel spray, the combustion chamber was offset to the exhaust side rather than the intake side. As stated earlier, this combustion chamber was designed with a trapped compression ratio of 7.02. Unfortunately, the higher-than-stock compression ratio paired with high intake charge temperatures led to excessive detonation. To alleviate the detonation problem, this head should be modified so it has a 6.5 compression ratio, similar to the stock engine.
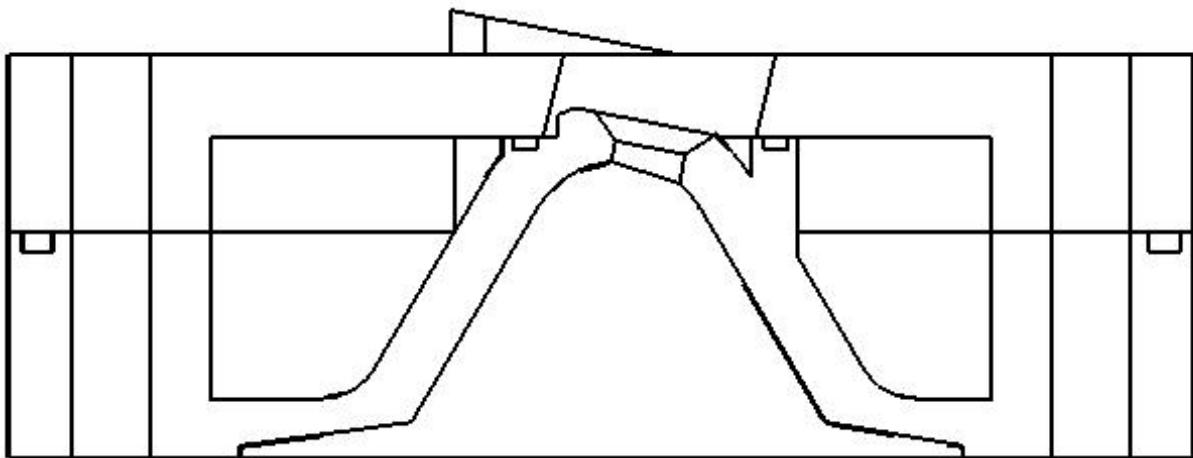
Figure 29: *Cross-section of the UI E-TEC GDI combustion chamber.*

After deciding on the chamber geometry, the sparkplug location needed to be determined. A fuel rich condition needs to occur near the spark plug for combustion to initiate during stratified operation. To accomplish this, Strauss suggests that the sparkplug electrode just barely extend into the injected fuel spray [21]. The distance between the sparkplug electrode and the tip of the injector was determined by measuring a combustion chamber from an E-TEC engine, which is based on the distance the injected fuel can travel into the combustion chamber during stratified operating conditions.

During homogeneous operation, the geometry of the combustion chamber, piston, and scavenging flows should provide for complete mixing of the fuel and air and produce an ignitable mixture near the spark plug. Research and CFD modeling of an E-TEC combustion chamber (similar to the UI GDI chamber) found that during homogeneous operation at WOT; a slightly richer condition exists on the exhaust-port side of the chamber [54]. Figure 30 shows the simulated equivalence ratios in an E-TEC chamber. Based on both the CFD modeling and measurements of the E-TEC engine, the spark plug electrode was located 0.67 inches from the injector tip near the exhaust side of the chamber. Figure 31 shows a cross section of the naturally aspirated UI GDI combustion chamber.
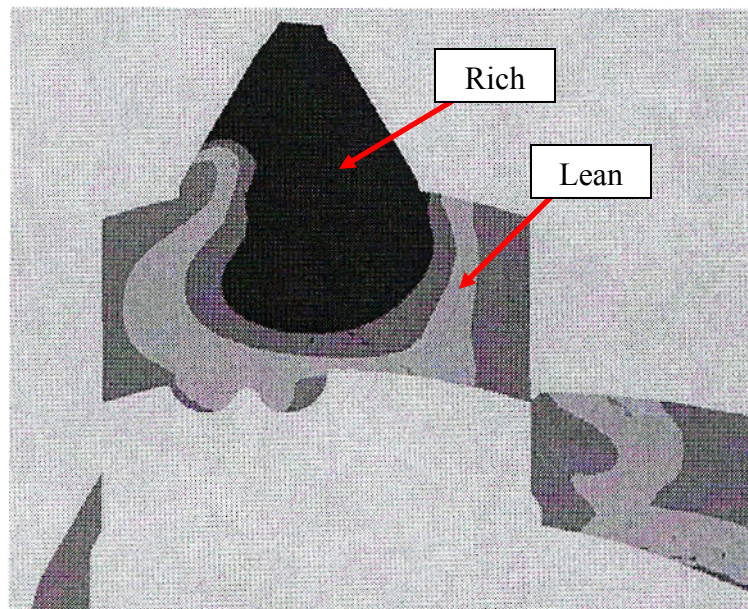
Figure 30: Simulated equivalence ratio distribution for an E-TEC engine [54].
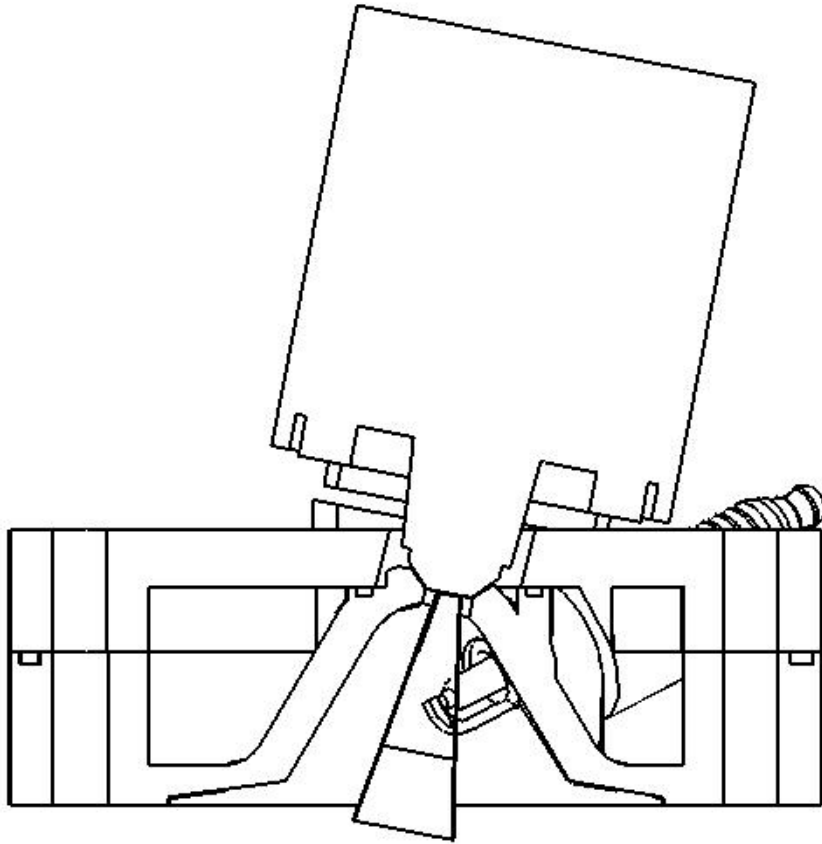
Figure 31: *Fuel spray and the spark plug relationship in the UI GDI engine.*

Using the classification table presented earlier (Table 5) the combustion chamber can be described by [36]:

1) Narrow Spacing: Spark plug gap is located close to the injector tip.
2) Spray-Guided: A narrow spacing concept where the stratification results from fuel spray penetration and mixing.
3) Squish Based: The squish area and motion induced by the intake ports are used to assist in charge stratification.
4) Centrally-Mounted: The injector is located near the center of the combustion chamber.

The GDI head was designed as two pieces and later bolted together. Each half was machined from billet 7076 T6 aluminum. The head manufacturing was performed in the University of Idaho Mechanical Engineering machine shop. Students, aided by the mechanical engineering department's machinist, conducted all of the machining procedures.

The machined head with the injector and coil assemblies is shown below in Figure 32. Engine parameters for the stock, naturally aspirated, and turbocharged engines are located in Appendix A.
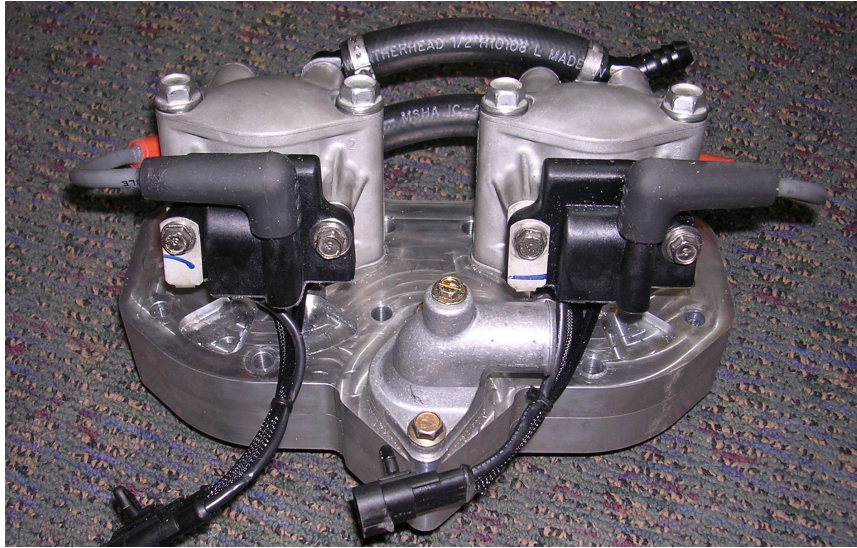
Figure 32: *The completed assembly of the GDI head with injectors and coils.*

3.4   SUPPORTING SYSTEM COMPONENTS FOR THE GDI ENGINE

Along with the injectors, several other components needed to be designed or modified for the E-TEC system to work with the snowmobile engine. The most important support system for the engine was the electrical system. The E-TEC direct-injection system was designed to operate with 55 volts, rather than a standard 14 volts, to make the electrical system more efficient [53]. However, some components on the snowmobile still required 14 volts, including head lights, tail lights, hand warmers, and other accessories.   Not only did the electrical system need to provide two different voltages, it would also need to be able to provide in excess of 1000 watts [53]. Compared to a carbureted two cylinder two-stroke engine that requires less than 200 watts, 1000 watts is a significant demand on this system. Most of the additional power requirement arises from the injectors (275W), high-energy ignition (55W), and the fuel pump (45W) [53]. Figure 33 compares electrical power consumption for an E-TEC engine with two carbureted engines. It is clear that the GDI engine requires significantly more electrical power.
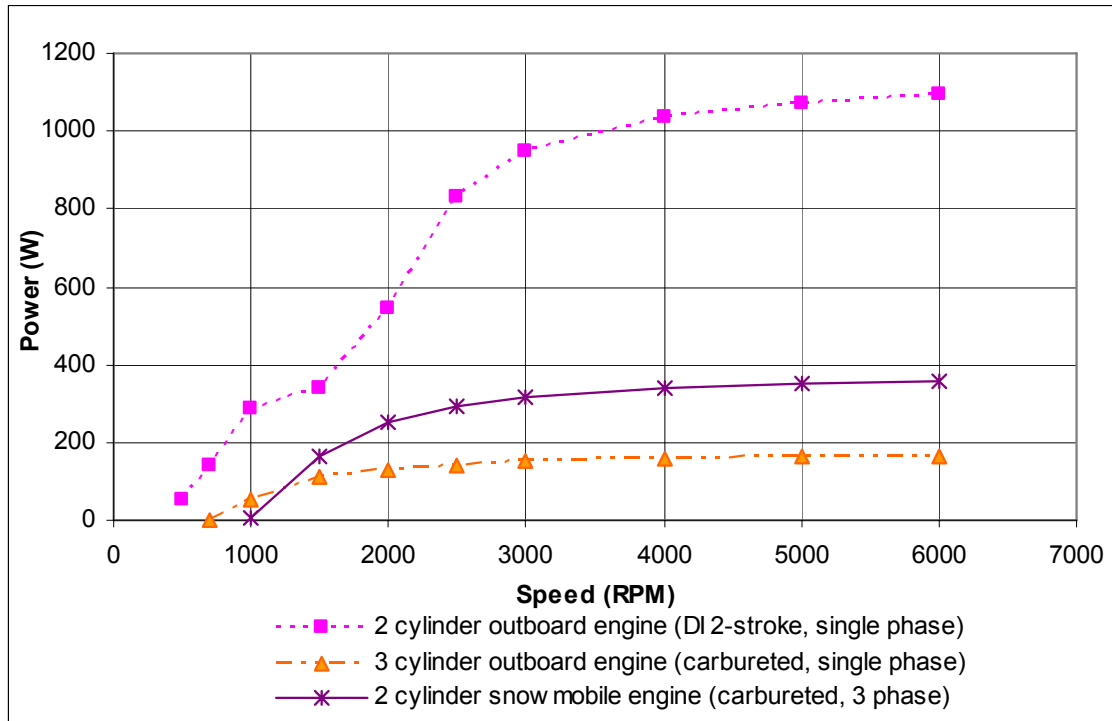
Figure 33: *Required electrical power for various two-stroke engines [53].*

In order to supply both voltages at the high-power demands, two solutions were considered. The first design employed the stock 14V permanent magnet (PM) alternator in combination with a 14V high-output automotive style alternator driven by the crankshaft to provide the necessary electrical power. A DC-DC converter could be used to step the 14 volts up to the 55 volts necessary for the E-TEC system. The FICHT GDI engine used this set up with a DC-DC converter designed by modifying a Coleman® 1200 watt power inverter [30]. While this system worked, it was heavy, inefficient, and required too much under-hood and under-seat space for the alternator, battery, and DC-DC converter. Additionally, it does not look attractive to consumers. Figure 34 shows the alternator, bracket, and drive belt used to produce the electrical power for the UI FICHT engine.
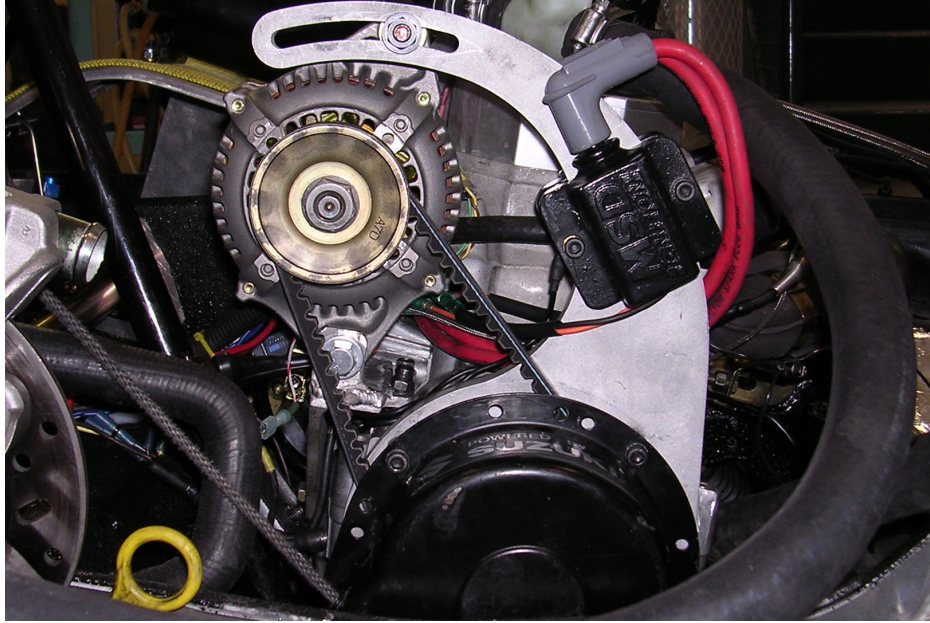
Figure 34: *External 12V alternator used to supply electrical power to a DC-DC converter.*

A more efficient and lightweight electrical system was desired for the E-TEC engine, as well as one that could be located in the pull-rope housing at the end of the engine. The E-TEC outboard engines offered a solution, as they use a PM alternator that has a unique control strategy that generates 55V and more than 1000 watts [53]. The PM alternator control strategy also allows for battery-less operation and easy pull-rope starting. To supply power to the 14V components, the EMM uses a DC-DC buck converter to step the 55V power down to 14V. However, several changes had to be made to the components to adapt the PM alternator to the snowmobile engine.

The outboard flywheel, which was 14 inches in diameter, housed the magnets for the PM alternator, served as the starter ring gear, and held the reference pattern for the crankshaft position sensor. The flywheel was too large to fit within the snowmobile engine pull-rope housing. Additionally, the shaft taper of the flywheel was different than the taper of the crankshaft of the snowmobile engine. In order to utilize the outboard flywheel it would have to be machined to a diameter of less 5.75 inches and a taper adapter would have to be made.

The outboard engine's PM alternator used a twelve pole stator that had windings of laminated copper wire and had a diameter of 5 inches. The stator was small enough to fit in the pull rope housing. However, the bolt pattern of the outboard stator was different than the bolt pattern of the snowmobile stator. To use the outboard stator, an adapter would need to

be made to accommodate the bolt pattern of the engine as well as the stator.

To determine if the outboard PM components could be used, the stator, flywheel, and engine crankshaft were solid modeled and modified. The solid modeling proved that the components could be modified to work together and fit inside the pull-rope housing. During the machining process the reference teeth for the crankshaft position sensor were also cut into the flywheel. Along with the machined flywheel, a stator adaptor and a crankshaft-taper adaptor were designed and manufactured. Figure 35, below shows the solid model assembly of the modified PM alternator parts and the designed components for the snowmobile engine electrical power source. The following figure, figure 36, shows the UI GDI engine with the stator assembly installed and the modified flywheel lying next to the engine.
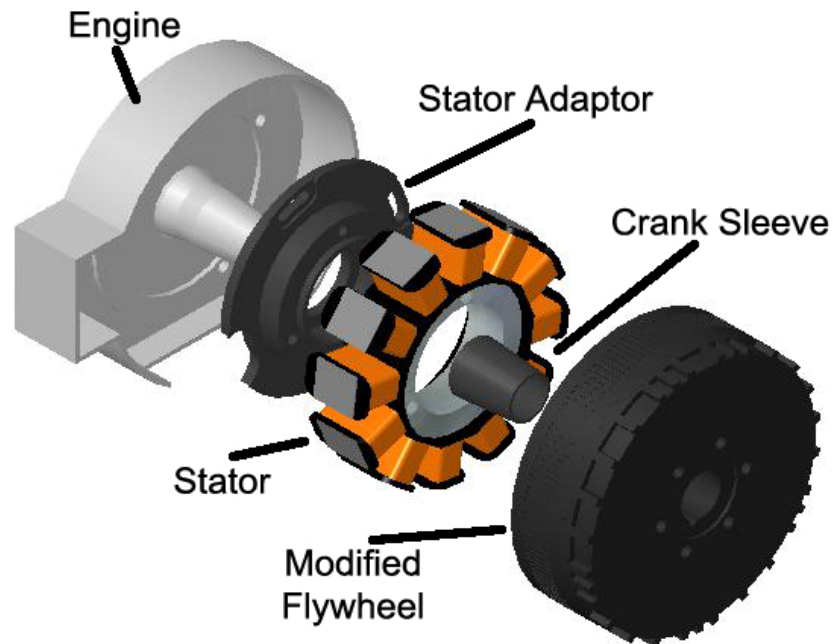
Figure 35: *UI GDI modified 55V permanent magnet alternator assembly.*
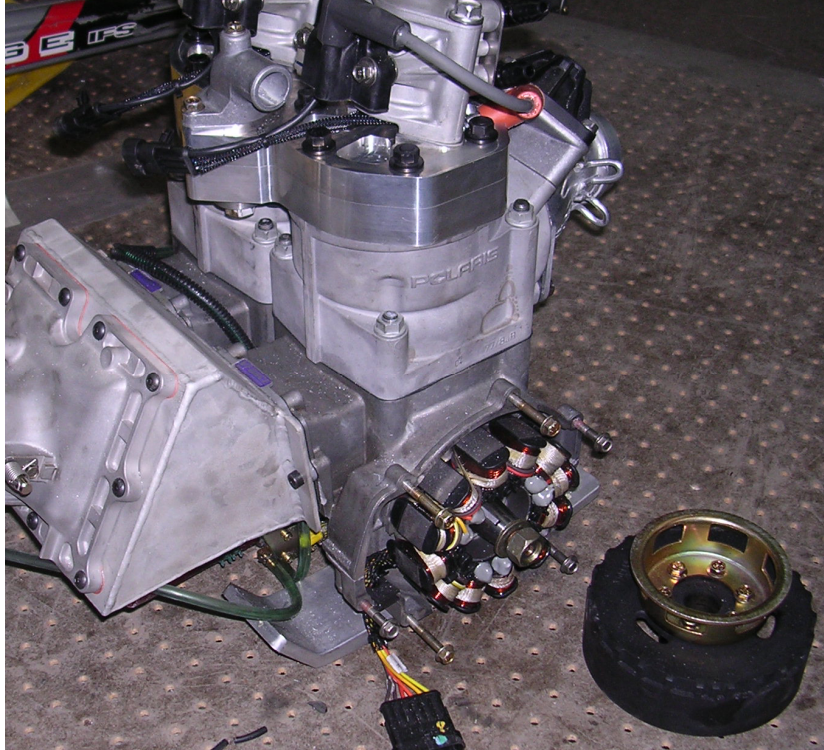
Figure 36: *Installed 55V alternator and the flywheel.*

Another important system that needed to be modified for direct-injection was the oiling system. As stated earlier, two-stoke engines use a total-loss oiling system. Traditional two-stroke engines use a mechanical oil pump driven by the crankshaft. The pump is also connected to the throttle through linkage. Oil delivery rate depends on engine speed and throttle position. The oil is usually pumped to four locations. Two oil lines go to the engine block where the oil is directed to the crankshaft bearings. The other two oil lines go the carburetors or throttle bodies where the injected oil mixes with the air/fuel mixture before it enters the crankcase. As the fresh air/fuel/oil mixture travels through the crankcase, an oil film is deposited on the surfaces. Any oil that does not attach to a wall is scavenged into the combustion chamber where it either combusts or is scavenged into the exhaust stream. A highlight of this system is that that it does not require oil filters or oil changes.

Initially the standard oiling system was used with the UI GDI engine. Two problems arose when using the mechanical system. First, there was not enough control of the oil flow for precise oiling. Second, with no fuel in the inlet air stream, which normally reduces the viscosity of the oil making it easier to disperse within the crankcase, oil would pool in the

bottom of the crankcase. Rapid increases of engine rpm or throttle position would force air at high speed through the crankcase that would pick the pooled oil up and send it through the combustion chamber. The result was a large amount of raw oil in the exhaust stream.

Two changes were made to the total-loss oiling system to reduce oil consumption, provide more precise oil control, and to reduce oil pooling. First, an electronic oil pump from the E-TEC motor was adapted. The oil-pump assembly consists of a pickup line with a filter, low-oil sensor, pump, oil-pressure sensor, and distribution manifold. The oil pump delivers 0.65 cc of oil for each pulse command from the EMM. Depending on the fuel/oil ratio desired, an oil map in the EMM—rpm and load dependant—sets the time between oil-pump pulses. The oil is pumped through the pressure sensor to the oil distribution manifold where it is directed to specific oiling points on the engine. The pressure sensor is used to ensure oil is being supplied to the engine. If a pressure rise is not detected in the manifold, a no-oil fault will be recorded in the EMM and the pump will operate continuously until pressure is restored. Figure 37 is the oil-pump assembly and Figure 38 is the oil assembly as installed in the oil reservoir on the vehicle. The oil was delivered to the same locations as with the stock system with one additional line supplying a small amount of oil into the inlet fuel for the injectors to reduce carbon buildup on the injector nozzles.
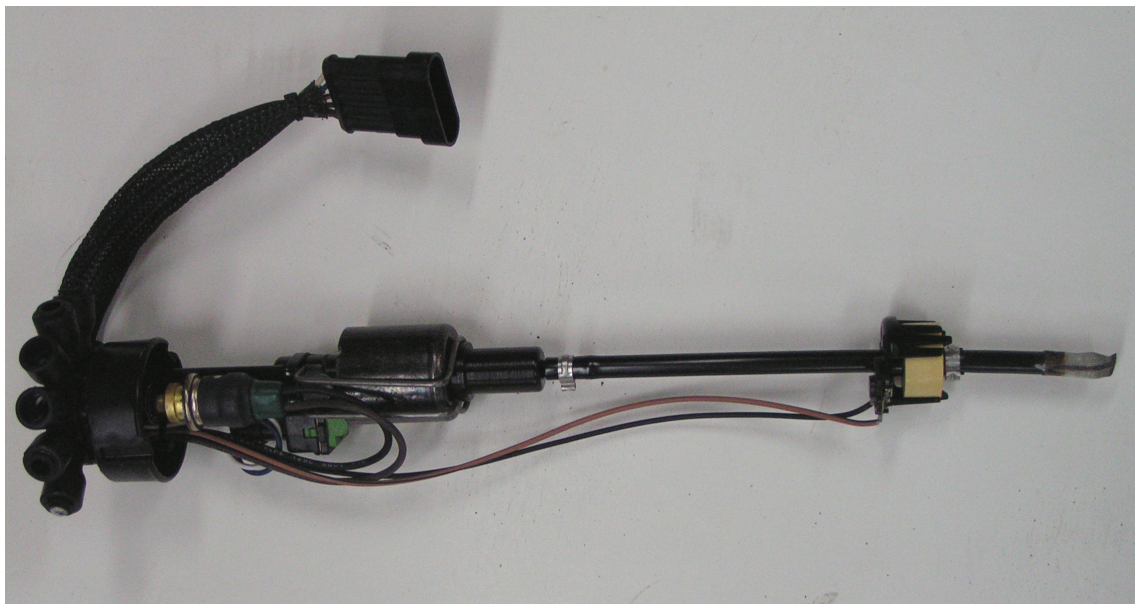
Figure 37: Oil-pump assembly that was adapted to the UI GDI engine.
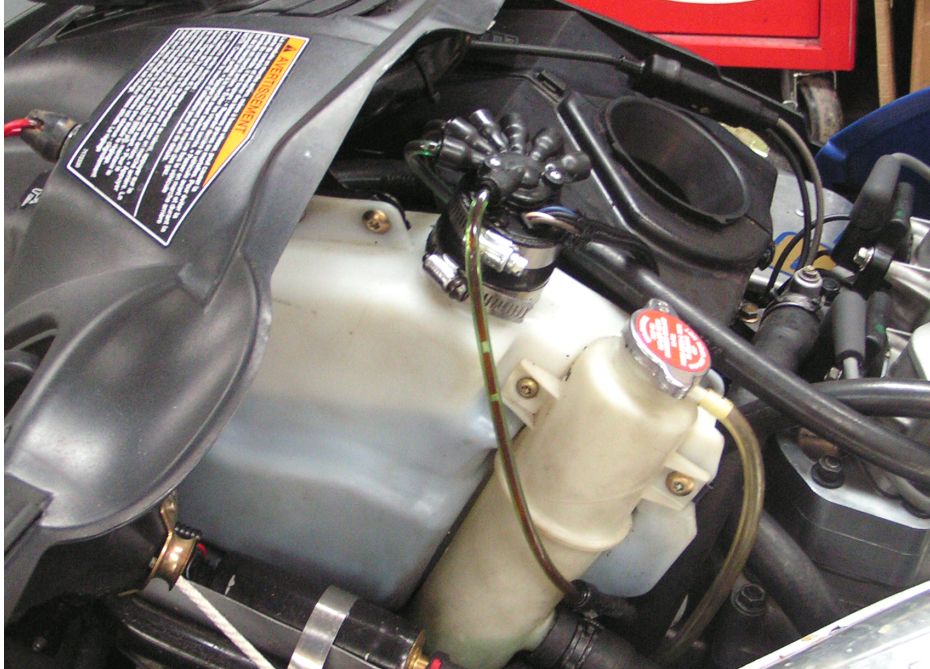
Figure 38: *Oil-pump assembly as installed in the oil reservoir and in the vehicle.*

In addition to the electronic oiling system, an oil recirculation system was added to the crankcase to alleviate the oil pooling problem. It consisted of a hole drilled into the bottom of each half of the crankcase with a hollow brass fitting pressed into each hole. The fittings were connected to a one-way check valve with plastic tubing. The check-valves were connected to the opposite cylinder with tubing, where another brass fitting was pressed into a hole that was drilled into the side of each cylinder at the height of the lower piston ring when the piston was at BDC. The system worked by using the pressure rise in the crankcase to push the oil to the opposite cylinder lining. As the piston traveled down in its stroke, the crankcase was pressurized. The high pressure forced the pooled oil through the check valve to the opposite cylinder where a low pressure had been created by the upward movement of that piston. The oil recirculation system was effective at reducing wasted oil and it decreased piston skirt wear.

3.5   FUEL CONTROL STRATEGIES

No matter the GDI system used, the objective is to confine the bulk of the fuel/air mixture in a region around the spark plug during light loads (so the engine can operate with

high residual exhaust gas or excessive air), and to fill the cylinder as completely as possible with a stoichiometric or slightly rich mixture to produce the maximum power at high loads [32]. Accomplishing these goals can be difficult across the entire speed and load range of the engine, especially with an engine that is designed to operate in a narrow rpm range, such as a high-performance snowmobile engine. Stratified and homogeneous-charged combustion require very different control strategies. Operation of GDI engines that are to include stratified operation are classified into four operating modes, shown in Table 9 [36]. Although the classifications originated with four-stroke engine development, they are transferable to two-stroke engines with modifications made to injection timing and engine speed.

Table 9: *Operating mode classifications for GDI engines utilizing stratified charging [36].*

GDI Operating Classification	Engine Load and Speed	Injection Timing	Description
1	Very light load, low rpm and idle	Very late injection (20-0° BTDC)	Stratified, overall lean
2	Light to medium load, medium rpm	Late injection (100-20° BTDC)	Stratified, overall lean, no throttling
3	Medium load, medium to high rpm	Early injection (210-140° BTDC)	Homogeneous, stoichiometric with EGR or lean
4	Full load, maximum engine speed	Early injection (240-210° BTDC)	Homogeneous, stoichiometric or rich

The least complicated of the operating modes is the homogeneous-rich with maximum air utilization required for high specific-power output. During medium load operation a lean-homogeneous (with EGR to control heat release) should be optimized for fuel economy and stable combustion. The lean-stratified operation is the most difficult to orchestrate. It is used during light-load and idle conditions to achieve maximum fuel economy [36]. From a drivability standpoint, the most difficult mode to achieve is that of load transition, where the combustion modes are transitioning between each other.

Stratified-charged combustion, touched on earlier, is achieved when the injection event is timed late in the cycle to obtain a stratified charge in the cylinder. Depending on the trapped air/fuel ratio the mixture could be lean-stratified or stoichiometric-stratified. The term "stratified combustion" is generally taken to mean lean-stratified operation [36]. The term "stoichiometric-stratified" refers to a special strategy that is used to reduce catalyst light-off time through the use of late combustion and after-burn [36]. Stoichiometric-stratified combustion was not considered during this research due to the added complexities associated with sizing a catalyst and the addition of yet another fuel control strategy. The main objective of charge-stratification in a GDI engine with a lean trapped air/fuel ratio should be to operate the engine unthrottled at part load with and overall air/fuel ratio that is leaner than is combustible with a conventional lean-homogeneous mixture [36]. This is accomplished by creating and maintaining charge stratification that results in a combustible mixture at the spark plug gap at the time of ignition that leads to stable flame propagation while the rest of the cylinder is very lean or absent of fuel. The use of stratified combustion has been shown to provide a significant reduction in brake-specific fuel consumption (BSFC) [17, 20, 36]. In two-stroke engines, this is considered to be due to a higher content of trapped air from the throttle-less operation. However, the literature agrees that achieving stable stratified combustion while achieving very low levels of UHC emissions is a difficult task. The engine out UHC levels are typically low enough for the 2012 EPA snowmobile regulations, but not for automotive applications.

Efficient stratified combustion is highly dependant on the complex interrelationships between injector location, fuel-spray characteristics, combustion chamber geometry, trapped exhaust residuals, injection timing, and spark timing. For two-stroke engines, fuel penetration and stratification is also highly dependant on time due to the counter-flow the fuel-spray encounters. To effectively utilize the available thermodynamic benefits of stratified combustion, the engine operating range for stratified combustion should be wide enough to encompass the most frequent engine operating points [36]. Also, the transitions between combustion modes should be located as to avoid frequent transitions that lead to poor run quality and high BSFC. Stratified combustion can be difficult to achieve due to its dependence on engine design. Optimization therefore, should be specific to individual systems.

Homogeneous combustion is used to meet the power demands of medium to high-load operating conditions. Depending on the trapped air/fuel ratio, the mixture can be considered homogeneous-stoichiometric or homogeneous-lean. For both types of homogeneous operation, early injection timing is used to provide sufficient time for the fuel to completely atomize and mix with the freshly scavenged air. When the engine is operating at design speeds and peak power is required, homogeneous-stoichiometric or slightly rich combustion should be used. The engine will be operating near peak scavenging efficiency and the cylinders will have a high trapping efficiency. Peak power and acceptable emissions can be attained with precise injection timing and maximum air utilization. This requires carefully timed injection to allow for a complete homogeneity, while avoiding fuel-spray interaction with the main scavenging flows that occur around BDC to limit short-circuited fuel.

When medium loads and load control are required, homogeneous-lean combustion should be used. Homogeneous-lean can refer to both an over-all lean trapped air/fuel ratio with very little exhaust gas residuals, and an over-all lean air/fuel mixture with high rates of residual exhaust gas. The second definition will be used in this work. Traditionally, two-stroke load control is accomplished through controlling the quantity of trapped exhaust gas and delivered fresh charge. Typically, this is accomplished with a throttle. The throttle acts as a restriction on the intake side, limiting the amount of fresh charge that can be delivered to the crankcase. The resulting low delivery ratio reduces the amount of fresh charge that can displace the exhaust gasses during scavenging. The limited delivered fresh charge to the combustion space coupled with high amounts of exhaust gas limits heat release.

As stated earlier, the most efficient GDI engine will be operated absent of a throttle. Theoretically, it is more efficient to operate an internal combustion engine without a throttle. Pumping losses are reduced in four-stroke engines and increased delivery ratios and trapped purity occurs in two-stroke engines. However, without a throttle, there is no convenient method for controlling heat release in a homogeneously charged engine. For a throttle-less homogeneously charged two-stroke GDI engine, load control can be found through the use of exhaust gas recirculation (EGR) or exhaust throttling. EGR is accomplished by directing inert exhaust gas taken from the exhaust stream into the intake air stream. The EGR acts exactly like trapped exhaust gas residuals in a throttled engine. Throttling the exhaust is

another method that can be employed to control trapped exhaust gas residuals. These two methods are preferred because they do not restrict inlet air.

Regardless of throttling technique, all three modes of combustion, homogeneous-rich, homogeneous-lean, and stratified-charge, should be exploited for increased fuel economy while providing acceptable power output. A comparison of engine fuel consumption and power output trends for the three modes of combustion is given in Figure 39 [36]. It clear that stratified-charge operation is only advantageous for low engine loads. When the brake mean effective pressure (BMEP) approaches 5 bar, a more efficient combustion can be accomplished using homogeneous-lean operation. It is also clear that peak power can only be developed with a homogeneous-stoichiometric or rich mixture. It should be noted that Figure 39 was developed from four-stroke GDI data. Likely, the BMEP limit where stratified combustion becomes less efficient for two-stroke engines will be at a lower BMEP due to the reduced amount of crank-angle available during the power-stroke for complete combustion of a highly stratified charge.
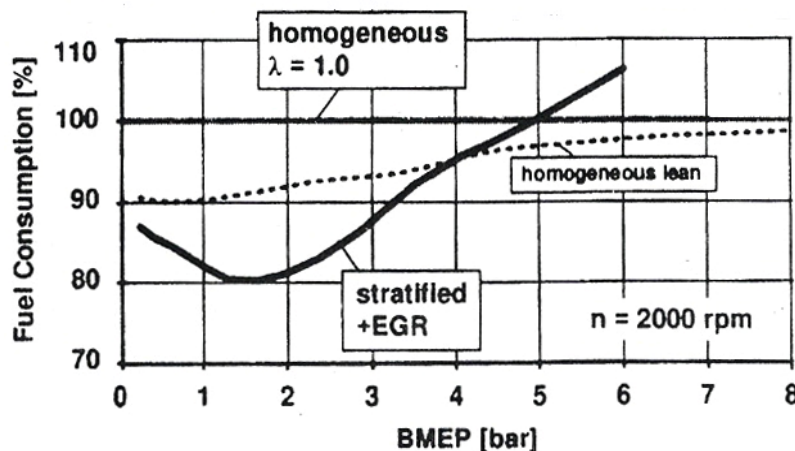
Figure 39: *Four-stroke GDI engine fuel consumption vs. engine load [36].*

Another combustion mode that can be employed with GDI two-stroke engines is homogeneous-charge-compression-ignition (HCCI). HCCI combustion is a process whereby a homogeneous mixture is auto-ignited through compression. This type of combustion has the potential to significantly reduce NO_x and PM emissions, while achieving higher thermal efficiencies [36]. It combines the combustion characteristics of both gasoline fueled and diesel engines. Similar to standard SI engines, a homogeneous mixture is used, which can

eliminate the fuel-rich diffusion combustion associated with stratified combustion, drastically reducing particulate emissions [36]. With an ignition process that is similar to diesel engines and an extremely lean mixture that supports flame propagation, an auto-ignition process can occur that eliminates the bulk flame propagation of a conventional SI engine. Result from experiments have shown that HCCI combustion is possible with a equivalence ratio of just 0.3 and an EGR rate of 45 percent without misfire, leading to very high thermal efficiencies and very low NO_x emissions that is normally associated with lean combustion [36].

HCCI combustion is possible by controlling the in-cylinder temperature, pressure, composition of the air/fuel mixture at the time of ignition so that the charge spontaneously ignites throughout the entire cylinder. This type of combustion process has proven to be difficult to control and it was not considered for the combustion strategy for this thesis. However, based on its potential for increased fuel economy it deserves further attention.

As stated earlier, a strategy needs to be developed to efficiently use the three modes of combustion. Particularly, stratified-charge combustion should be used during light-load operation to reduce fuel consumption. However, efficient stratified operation is dependant on required power output. The power-transfer systems used on snowmobiles is not very efficient, with losses of power up to 50 percent from the engine to the track. With such large power losses, efficient stratified combustion may not be able to produce enough power to propel the snowmobile at cruising speeds. This concern was investigated in order to determine if stratified operation was a viable option for cruising.

Snowmobiles relay on continuously variable transmissions (CVT) to transfer power from the engine to the track. The CVT is made up of two variable diameter pulleys that are connected by a cogged belt. The primary clutch is sensitive to engine rpm, the diameter of the pulley changes based on engine speed. The secondary clutch is sensitive to track torque. The secondary clutch diameter changes as the torque required to rotate the track changes. The two clutches work together to change the effective gear ratio between the engine and track. Power delivered to the secondary clutch is transferred to a fixed gear reduction by the jackshaft. From the output of the gear reduction, the power is transferred to the driven shaft that is connected to the track by cogged drivers. Friction, belt slippage, rotating mass, and tack slippage on the snow all contribute to the loss of power during transmission from the engine to the track. A schematic of the power transfer system is shown in Figure 40.
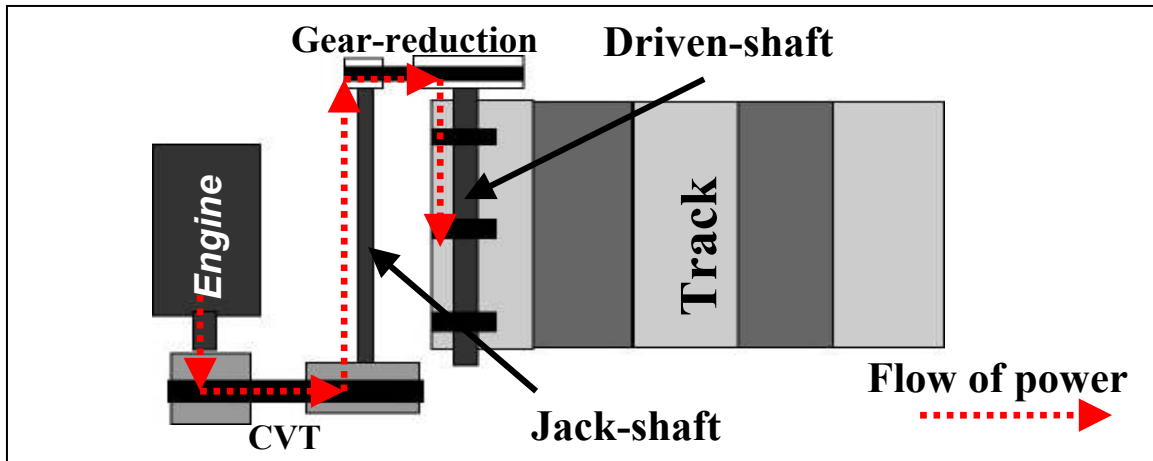
Figure 40: *Schematic describing the path of power transfers for snowmobile engines.*

A study was conducted to determine if stratified combustion could be used for cruising operation using research for developing a hybrid gasoline/electric snowmobile [40]. Auth developed a modified road-load equation that estimated the power required (P_{rl}) to propel a snowmobile at various vehicle speeds and incline angles, equation 3.5.1. The coefficients C_{v3} and C_f were derived from coast down data of a snowmobile traveling at an initial speed of 55 m/hr on a flat and groomed trail. The snowmobile chassis used in Auth's research was similar to the one used for the UI GDI project. Therefore, the coefficients calculated in Auth's research were used to calculate road load for the UI GDI chassis.

$$P_{rl} = \left(\frac{1}{2} \cdot C_{v3} \cdot A_p \cdot \rho \cdot V^2 + C_f \cdot M_v \cdot g \cdot \cos(\theta) + M_v \cdot g \cdot \sin(\theta) \right) \cdot V \qquad \textbf{Equation 3.5.1}$$

Topographical data of Yellowstone were used to determine the magnitude of expected incline angles for trail riding. Estimations for the required power were made using the road-load equation and the weight of the UICSC snowmobile, 700 lb including the rider, traveling at 45 m/hr. The results of the calculations are shown in Table 10. Dynamometer testing was used to determine if the engine could produce the estimated required power during stratified operation. As shown in Table 11, the engine was able to produce enough power for all but the steepest incline angles during stratified operation. Based on the ability of the engine to produce enough power during stratified operation, a fuel delivery strategy similar to the one shown in Figure 41 was used for the UI GDI engine.

Table 10: *Predicted power requirements for the snowmobile to travel 45 m/hr.*

Incline [deg]	θ	2	3	4	5	6	7
Req. Power [hp]	P_{rl}	18	19	21	22	23	25

Table 11: *Measured stratified power at various engine speeds.*

Engine Speed [rpm]	4000	4500	5000	5500
Power [hp]	13	15	18	23
BMEP [bar]	2.42	2.49	2.69	3.12

Fuel delivery and ignition is controlled by user programmed maps in the EMM similar to the one shown in Table 12. The maps consist of three main "look-up" tables maps to control fuel-injection timing, spark timing, and delivered fuel quantity. The EMM real time engine speed and throttle counts (TC) to determine what cell in the look-up table for fuel and spark timing. Stratified maps use degrees BTDC for injection timing, ms of delay after injection timing for spark timing, and mm^3 for fuel quantity. Homogeneous maps used degrees BTDC for both fuel and spark timing and mm^3 for fuel quantity. The transition between stratified to homogeneous strategies occurs between 300 and 301 TC. The grayed portion in Table 12 describes the locations where the engine operates most often. Other look-up tables compensate for engine and air temperature as well as barometric pressure.
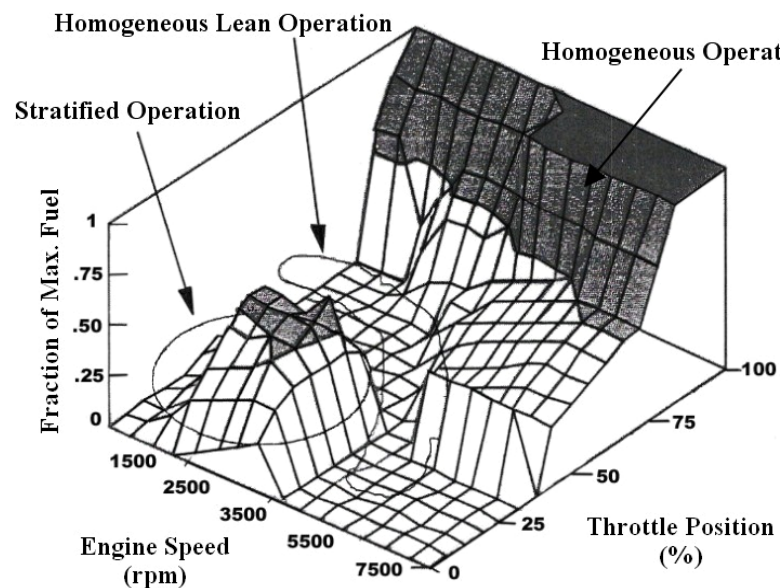
Figure 41: *Fuel delivery and combustion control strategy adapted from Zhao [36].*

Table 12: *EMM "look-up" table for fuel delivery, injection timing, and ignition timing.*

	500	1000	1500	2000	3000	4000	5000	5500	6000	7000	8000
10											
50											
80				**Stratified**							
100											
150											
200											
250											
300						**Transition**					
301											
400											
500											
600						**Homogeneous**					
700											
800											
1000											

The final assembly of the naturally aspirated GDI engine in the 2006 Polaris IQ chassis is shown in Figure 42. The limited number of additional components required for GDI operation compared to a carbureted or throttle-body fuel injected engine allowed for a clean installation with negligible weight increase.

Figure 42: *The final design of the naturally aspirated UI GDI engine [33].*

4.0   TURBOCHARGING A TWO-STROKE ENGINE

This section describes turbochargers and how they are used to improve the performance of internal combustion engines. Specific design considerations that can significantly affect over-all system operation for two-stroke engines are discussed. There is a description of how to select the proper turbocharger based on the desired performance. Finally, there is a description of the turbocharger and system layout for the UI GDI engine.

4.1   TURBOCHARGING INTRODUCTION

The fundamental purpose of turbocharging is to increase available engine power while reducing specific fuel consumption. Power developed by an engine is determined by the amount of fuel that can be efficiently combusted in the cylinder. The amount of trapped air in the cylinders determines the amount of fuel that can be used. It follows that the power output of an engine can be increased by increasing the density of the delivered air. Turbocharging is one method often employed to achieve the desired increase in air density. Turbochargers are most often used on four-stroke diesel engines in order to increase efficiency and fuel economy. They are also used in high performance applications with four-stroke gasoline engines. There are almost no applications of original equipment manufacturers (OEM) producing turbocharged two-stroke gasoline engines.

Turbochargers utilize a turbine that uses the energy in the exhaust gas to drive a compressor, via a common shaft, to raise the inlet air pressure. The pressure rise of the intake air increases the density, and therefore the mass, of air delivered to the engine. A typical turbocharger is shown in Figure 43. Turbochargers usually feature a radial flow turbine connected to a centrifugal compressor. The turbine side consists of an inlet volute or scroll, nozzle vanes (may not be present), a turbine housing, and the turbine wheel. As exhaust gasses enter the volute it accelerates radially inwards towards the turbine. The nozzle vanes, if present, further accelerate the flow. As the exhaust gasses flow towards the turbine they accumulate more kinetic energy. The high velocity and high temperature exhaust gasses then enter the turbine wheel. The gasses expand through the turbine wheel where energy is extracted and transferred to the turbocharger shaft. The gasses exit the turbine housing axially, having been turned 90° as they traveled through the turbine housing [42].
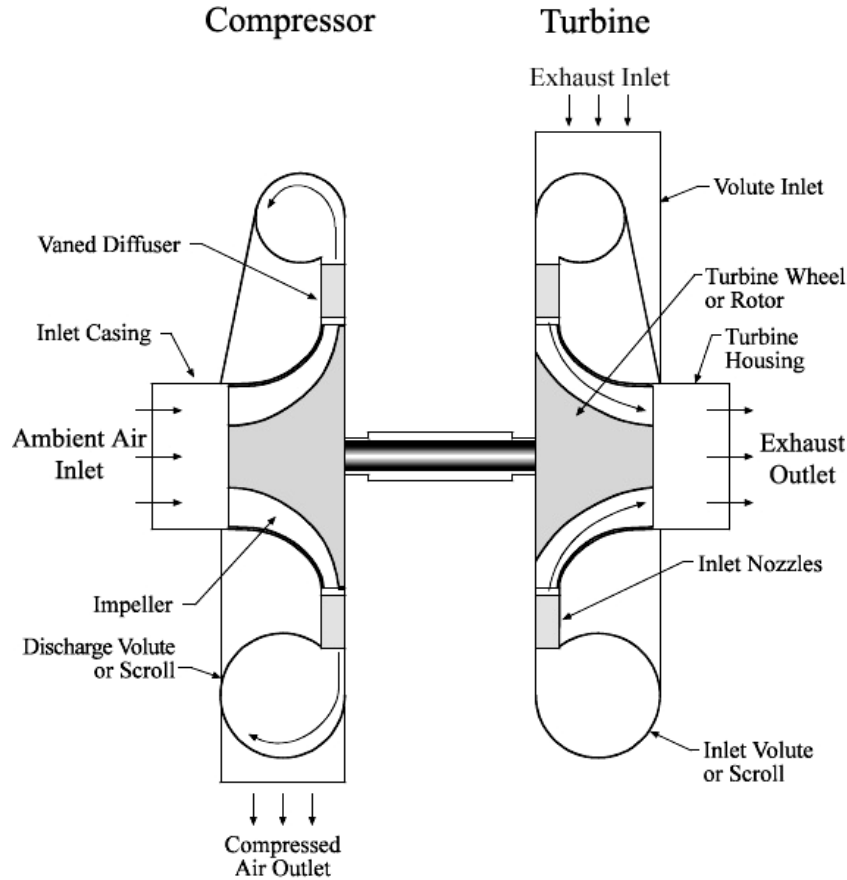
Figure 43: *Cross section of a typical turbocharger [43].*

Turbines are steady flow devices designed to operate at specific conditions. Turbines with fixed geometry cannot efficiently support an engine over a wide range of speeds [44]. Comparing turbines of different sizes highlights this problem. A large turbine will supply high pressures to the intake manifold during high speed operation, providing good fuel economy. However, at low engine speeds the mass flow through the engine will not provide sufficient energy to the turbine, resulting in low boost pressures and poor throttle response. With a small turbine the inlet pressure can be boosted significantly providing good low-end torque and transient response. Again there is a drawback, at high engine speeds there will be too much energy in the exhaust, resulting in too high intake pressures or turbine over-speeding. To alleviate these problems a waste-gate can be used to bypass some of the exhaust gasses past the turbine or a blow-off valve can be used in the intake side to release intake pressure if it is too high. Either method wastes useable energy, reducing fuel economy and thermal efficiency [44].

One proposed solution is to use a variable geometry turbocharger that allows the turbine nozzle area to be varied with engine speed and load. Variable nozzle turbines (VNT) offer many benefits, including improved fuel economy and throttle response [44]. The nozzle area of the turbine can be controlled by a single vane or by multiple vanes [45]. A schematic of a multiple vane VNT is shown in Figure 44. The vanes close when the exhaust flow is low in order to provide a small nozzle area. As exhaust gasses speed up the vanes progressively open to create a larger nozzle area. The movable vanes allow the turbocharger to provide the best characteristics of both small and large turbines; better throttle response and low-end performance coupled with high power output and improved fuel economy [45]. A downfall of the multi-vane turbine is the added complexity that leads to higher manufacturing costs and an increased risk of component failure [45].
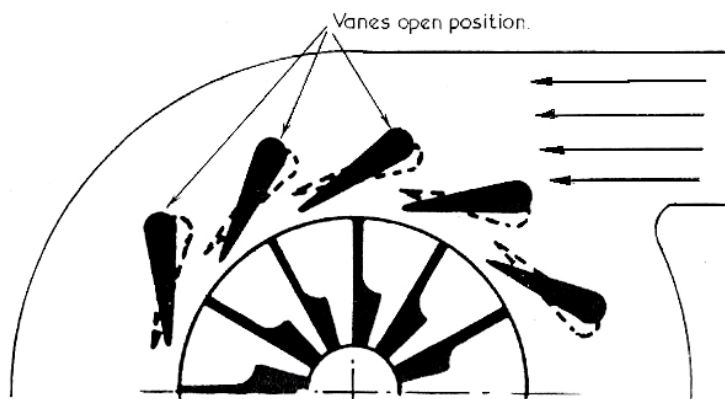
Figure 44: Schematic of a multiple vane VNT turbine [45].

The compressor side of a turbocharger consists of a inlet casing, compressor wheel, a diffuser with vanes (or vane-less), and a discharge volute or scroll. The shaft work created by the turbine is used to turn the compressor wheel at very high speeds, 120,000 rpm or greater. As the intake air enters the compressor housing axially through the inlet casing it is accelerated by centrifugal force [46]. The air then travels through the diffuser where it is slowed down and the kinetic energy of the air is converted to a static pressure rise. Finally, the compressed air flows through the volute to a pipe connected to inlet of the engine. Unfortunately, the compression process causes an increase in temperature of the air. The amount of temperature increase depends on the efficiency of the compressor at the operating conditions. An intercooler can be used to reduce the temperature of the inlet air.

Today, there are two popular methods used for turbocharging, pulse turbocharging and constant-pressure turbocharging [42]. Four-stroke engines most often employ pulse turbocharging. It uses a compact exhaust manifold with short runners with a small cross-sectional area to reduce losses of the kinetic energy as the exhaust gas travels to the turbine inlet. This type of turbocharging allows for a large fraction of the available exhaust energy to be delivered to the turbine. A negative effect of pulse turbocharging is that the turbine is subjected to inlet mass flow, pressure, and temperature pulsations. Although a significant amount of energy is available to do work, the pulse system can have a detrimental effect on the engine gas exchange process and turbine efficiency. The small volume and short runner exhaust give rise to pressure propagation and reflection similar to the tuned exhaust of a two-stroke engine. In a four-stroke engine, this can be acceptable because the pulsations of the combustion events can be, for the most part, separated from the other cylinders scavenging events [42]. Another problem arises from attempting to select a turbocharger for a pulse system. Turbochargers are characterized by steady-flow conditions which are not valid in the highly turbulent pulse turbocharging system. More information can be found from Watson and Janota, who provide an in-depth description of pulse turbocharging [47].

The second type of turbocharging is termed constant-pressure turbocharging. This type of turbocharging addresses the issue of unsteady turbine performance. A large volume exhaust manifold is used to damp out the mass flow and pressure pulsations resulting from exhaust port opening. This essentially provides a steady flow at the turbine inlet. However, there is a loss of exhaust gas energy as the high-velocity gasses exiting the cylinders mix with the low velocity gasses in the exhaust manifold. Although this type of system operates more predictably, and more efficiently, the maximum amount of work available in the exhaust is not utilized [42].

4.2   TWO-STROKE TURBOCHARGING

In two-stroke engines where the opening and closing of the ports are controlled by the piston, the exhaust ports close after the intake ports. Therefore, the trapped pressure is determined by the pressure of the exhaust system. Even if a large amount of air with a significant pressure rise is supplied to the engine, the trapped pressure will not increase without a similar rise in back-pressure. The degree of supercharging is therefore limited by

exhaust back-pressure. Fortunately for simple two-stroke engines, the presence of a turbine in the exhaust system increases back-pressure. However, a balance must be maintained. If the back-pressure increases too much, scavenging efficiency and delivery ratio will be reduced, resulting in poor engine performance. If the back-pressure is too low, high scavenging efficiency and delivery ratios may result, but the trapping efficiency will be reduced and performance will suffer. The pressure ratio of the exhaust backpressure to the intake pressure will be referred to as the scavenging pressure ratio (SPR) in this thesis. Choosing the turbocharger system to be used, pulse or constant-pressure, therefore needs to be done with performance requirements and system complexity in mind.

Watson and Janota have shown that two-stroke engines can successfully be operated with a pulse turbocharger system [47]. However, careful attention needs to be made to the exhaust manifold design to ensure that positive pressure waves do not arrive at the exhaust ports during the course of the scavenging process. Additionally, effective operation is only accomplished over a limited engine speed range [32]. Often, these engines are operated with auxiliary compressors to aid in scavenging at off-design speeds and for start up. Typically, pulse turbocharging is used with large displacement and uni-flow scavenged engines for marine power generation or locomotives [32]. While, pulse turbocharging can provide substantial pressure energy at the turbine during blow-down, pulse reflections that interfere with the scavenging process are expected to occur in engines with broad engine speed ranges.

A constant-pressure system was used because the engine is expected to operate with a broad engine speed range. Additionally, a constant-pressure system can retain the beneficial tuning characteristics of the exhaust pipe. When a two-stroke engine is turbocharged with a constant-pressure system, the turbine creates a larger back-pressure in the exhaust manifold and an appropriately higher intake pressure is required [32]. During low loads the turbine may not have enough power to sufficiently increase the intake pressure and an auxiliary compressor may be required. For externally-blown uni-flow scavenged engines, the secondary compressor can be a rotary compressor, simple fan, or a reciprocating pump connected either in series or in parallel. For the simple two-stroke engine, the crankcase pump already in series can be used to aid in scavenging. Additionally, Heywood points out that a constant-pressure system is preferred for simple two-stroke engines that uses an under-piston pump [32].

As with any type of scavenging pump, the unsteady flow associated with them may cause surge problems in the centrifugal compressor. To alleviate surge in the compressor, it is suggested that a reasonably large receiver be used between the compressor and the scavenging pump to maintain an adequate margin between the average mass flow rate and the surge limit [47]. The receiver is typically a plenum and/or an intercooler. Based on the available literature, a constant-pressure turbocharger system incorporating an under-piston scavenging pump, intake plenum, and intercooler was used. Figure 45 is a schematic of a constant-pressure turbocharging system with a crankcase scavenging pump and intercooler.
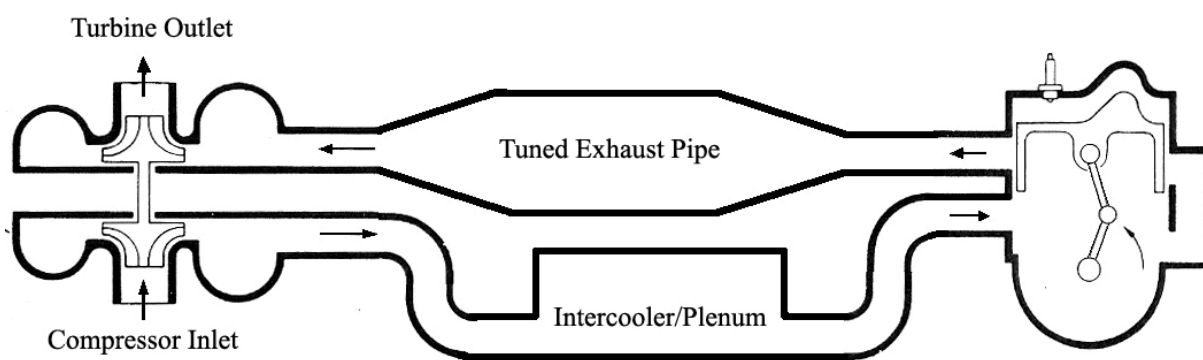
Figure 45: Constant-pressure and crank-case scavenged two-stroke, adapted from [46].

While OEMs have not turbocharged the simple two-stroke engine, it is often done by private parties using aftermarket parts. Typically turbocharged snowmobiles are used for drag racing or deep-powder mountain riding, often referred to as "boon-docking." Most often they are carbureted engines with displacements ranging from 700 cc to 1000 cc, producing between 180 and 315 horsepower. Some examples of turbocharged two-stroke snowmobiles are given in Figure 46. These engines are designed to operate at high engine speeds with no concern for fuel economy or emissions. The result, these engines have extremely high specific power, satisfactory run quality at off-design conditions, high fuel consumption, and poor emissions. The above mentioned negative aspects are why OEMs have not produced turbocharged two-stroke engines. With the advent of successful two-stroke GDI systems, turbochargers can now be utilized to produce clean and fuel efficient two-stroke engines.

Figure 46: *Aftermarket turbochargers installed on two-stroke snowmobile engines.*

4.3   TURBOCHARGER SELECTION

Incorporating a turbocharger into the unsteady flow environment of an internal combustion engine presents significant design challenges. Internal combustion engines are unsteady flow machines that produce strong pulsating flows due to the discrete combustion events. Turbochargers, conversely, are steady flow devic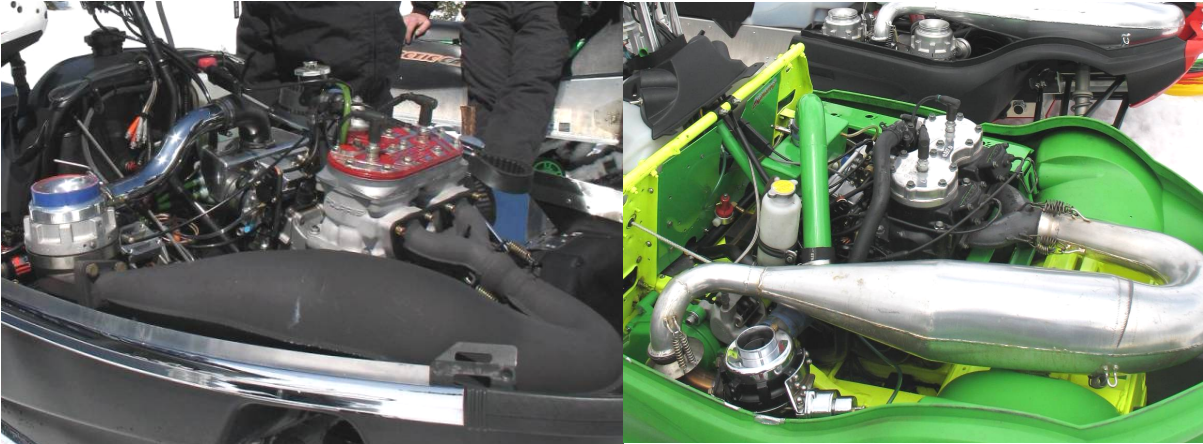es that operate most efficiently at specific operating design points. Operation of the turbocharger away from the design point reduces efficiency and performance. Matching a turbocharger and an engine to maximize turbocharger efficiency while producing the power curve desired requires an understanding of the gas exchange process between the engine and turbocharger.

One of the most significant matching problems is the prediction of on-engine turbine and compressor performance. Currently, most turbochargers are characterized by their off-engine performance assuming quasi-steady operation. The turbocharger performance is represented by maps of the turbine and compressor. Often, turbine maps are not available and turbocharger sizing is accomplished by using compressor maps and trial and error to size the turbine [46].

However, the nozzle area of a turbine can be used to make an initial selection of the turbine for the turbocharger. The nozzle area of a radial-flow turbine with multiple vanes is determined by the cross-sectional area of a single nozzle opening multiplied by the total number of vanes [46]. The larger the nozzle area, the slower a particular turbocharger will operate. The nozzle area for a single-opening or vane-less turbines is defined in a different

manner. They are characterized by the AR number. AR describes the ratio of the turbine inlet area to the distance between the turbine wheel and the center of the turbine inlet area, Figure 47 [46]. Again, the larger the AR number the slower the turbine will operate. Some turbochargers are also described by their "trim." Trim is a relative term used manufacturers to describe the contour of the compressor or turbine wheel profile.
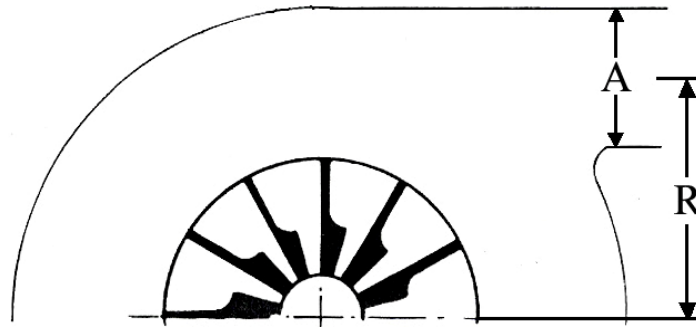
Figure 47: *Single entry vane-less turbine housing adapted from [45].*

Turbocharger sizing begins with sizing the compressor using the compressor maps. The maps consist of constant efficiency contours and speed lines plotted against the compressor pressure ratio (PR) and inlet airflow. The pressure ratio across the inlet and outlet of the compressor housing is defined as:

$$PR = \left(\frac{Pressure_{ambient} + Pressure_{boost}}{Pressure_{ambient}} \right)$$

Equation 4.3.1

Typically, compressor maps show pressure ratio on the ordinate axis and compressor inlet airflow on the abscissa axis, as shown in Figure 48. Compressor inlet airflow is usually represented with units of lb/min or ft^3/min (CFM). Predicting the operating conditions of the turbocharged engine—boost pressure and engine airflow—at specific design points will aid in choosing a compressor that will offer both the correct pressure rise and flow while operating near peak efficiency.
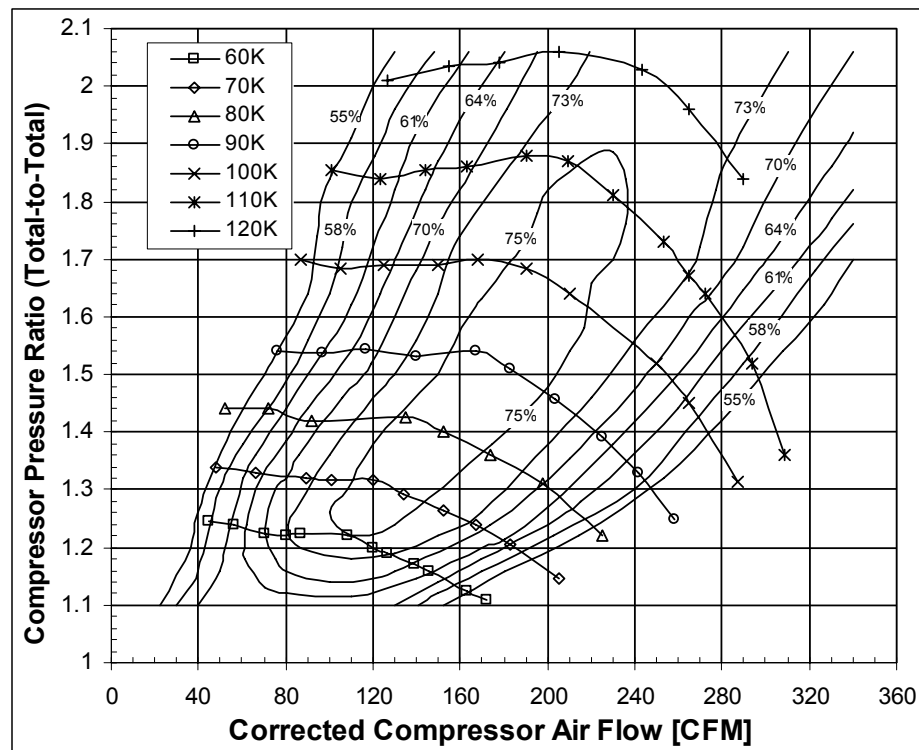
Figure 48: *Typical compressor performance map.*

It is obvious that compressors are more efficient, adding less heat to the air, at particular combinations of PR and inlet airflow. Therefore, the goal should be to find a compressor that has maximum efficiency over what would be considered the most valuable portion of the engine's operating range. Using the five-mode testing procedure as a guide— as it was based on in-field snowmobile data—two-stroke snowmobile engines typically operate between 5000 and 6000 rpm, with short durations at maximum engine speed, 8000 rpm. Therefore, a compressor was needed that would be efficient over those engine speeds.

The first step in selecting a compressor was to determine the desired power increase over the baseline engine. Because this research was aimed to discover the feasibility and potential problems associated with turbocharging a GDI two-stroke engine, conservative goals of 100 hp at 6500 rpm and a peak power output of 160 hp at 8000 rpm were used. Additional operating points were established to produce a smooth desired power curve from 5000 rpm to 8000 rpm. Figure 49 shows both the desired turbocharged power curve and the naturally aspirated baseline engine performance.
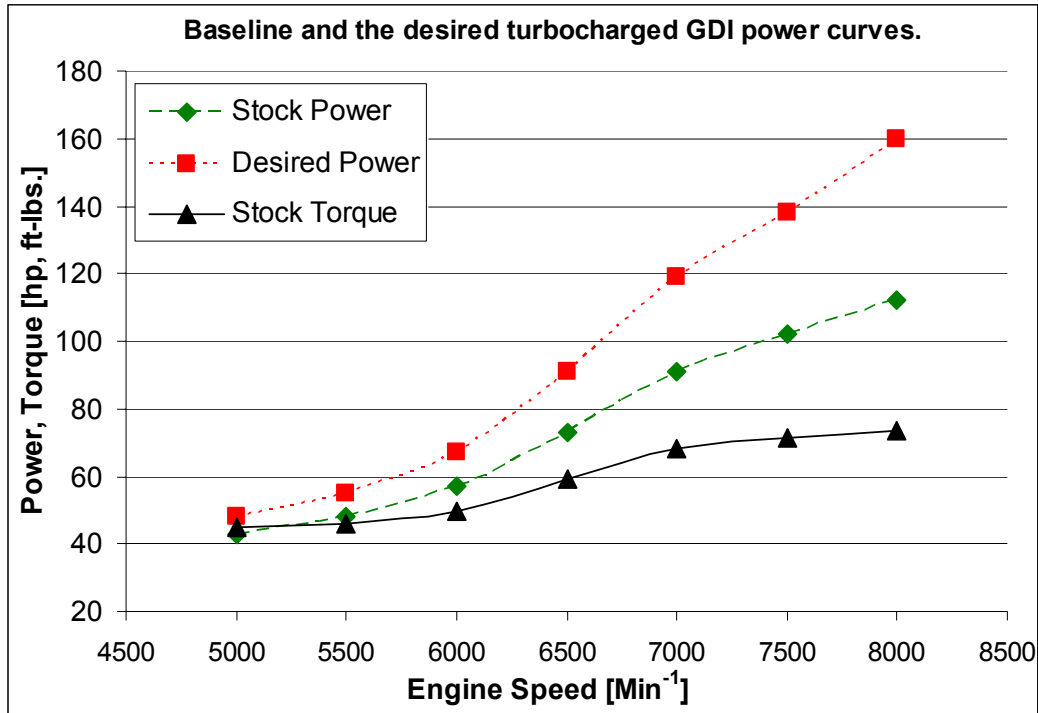
Figure 49: *Baseline and desired turbocharged power output of the UI engine.*

Using the baseline and desired power curves, estimations can be made for the required compressor inlet airflow and pressure ratios for the turbocharged engine. To do this, the baseline engine airflow must be known. Because accurate airflow measurements of simple two-stroke engines cannot be measured directly [17], it must be estimated using the displacement and volumetric efficiency of the engine. Volumetric efficiency is also not easily measurable for two-stroke engines. Therefore, volumetric efficiency was estimated based on the torque of the engine. Several simplifying assumptions were used:

1) The baseline engine peak volumetric efficiency occurred where the maximum torque was produced and was assumed to be 90 percent for this engine.

2) The volumetric efficiency of the other operating points are exactly proportional to the maximum torque output.

3) The turbocharged engine would have the same volumetric efficiency characteristics.

4) All calculations assume steady state.

Given a baseline engine power output, the torque is easily calculated by:

$$Torque = \frac{Power}{2 \cdot \pi \cdot rps}$$

Equation 4.3.2

Using assumption two from above, the maximum volumetric efficiency occurs at peak torque output and the volumetric efficiency of the other design points are related by:

$$Vol_{eff.} = \frac{Torque \cdot Vol_{eff.max}}{Torque_{max}}$$

Equation 4.3.3

Using the displacement, engine speed, and the estimated volumetric efficiencies, the approximate baseline engine intake airflow can be calculated by:

$$CFM_{baseline} = Engine_{displacement} \cdot rpm \cdot Vol_{eff.}$$

Equation 4.3.4

Assuming the trapping characteristics of the baseline engine are mimicked by the turbocharged engine, the calculated baseline engine airflow should be a useful predictor of the turbocharged engine airflow.

The next step is to determine the increase of air that is required for the turbocharged engine. For a given engine, power is directly proportional to the mass of air trapped in the cylinder. The proportional increase in the density of the delivered air, the density ratio (DR_{req}), for the turbocharge engine can be found from the ratio of the desired power to the baseline power by:

$$DR_{req} = \left(\frac{Power_{desired}}{Power_{baseline}} \right)$$

Equation 4.3.5

Using the above assumptions and equations along with the baseline power curve, estimations for the baseline engine volumetric efficiency and air flow were calculated. Those results were used, along with the desired power curve, to calculate the required increase in the density of the delivered air for the turbocharged engine. Table 13 summarizes the results of the calculations for baseline engine airflow and DR_{req} for the turbocharged engine. The necessary increase in mass of air to be delivered to the turbocharged engine, along with the baseline engine airflow, is used to predict compressor performance.

Table 13: Calculated baseline airflow, volumetric efficiency, and DR_req.

Engine Speed RPM	Baseline Power [hp]	Baseline Torque [ft-lbs]	Estimated Volumetric Efficiency [percent]	Calculated Engine Flow [CFM]	Desired Power [hp]	DR_req
5000	43	45	55	59	48	1.12
5500	48	46	56	65	55	1.15
6000	57	50	61	78	67	1.18
6500	73	59	72	99	91	1.25
7000	91	68	84	124	119	1.31
7500	102	71	87	139	138	1.35
8000	112	74	90	153	160	1.43

The next step is to provide best guesses for the required boost that will provide an actual density ratio (DR_del) delivered by the compressor—corrected for compressor efficiency—that will provide the desired power output. Using the initial guess for the boost the PR is known from equation 4.3.1. Assuming an ideal gas and 100 percent compressor efficiency, the temperature of the compressed air will increase according to:

$$T_{2ideal} = T_1 \cdot (PR)^{0.238}$$ **Equation 4.3.6**

The actual compressor outlet temperature will be subject to the compressor efficiency (η_c) at the specific operating conditions. During the first iteration of the calculations for each design point, the compressor efficiency must also be estimated. Typically compressors have efficiencies between 65 and 75 percent when they are sized properly. After choosing the compressor efficiency, the increase in temperature and resulting outlet temperature of the compressor is calculated from:

$$\Delta T_{actual} = \frac{\Delta T_{ideal}}{\eta_c}$$ **Equation 4.3.7**

and,

$$T_{2actual} = T_1 + \Delta T_{actual}$$ **Equation 4.3.8**

Using the actual compressor outlet temperature—at the specified conditions—the actual density ratio, DR_del, supplied by the compressor is:

$$DR_{del} = \frac{T_1}{T_{2actual}} \cdot PR$$ **Equation 4.3.9**

The temperature compensated density ratio gives an estimated power output based on what the compressor is actually capable of supplying at the design conditions:

$$Power_{estimate} = Power_{baseline} \cdot DR_{del}$$ **Equation 4.3.10**

If the estimated power was too low a higher guess was made for the boost. Iterations of changing the boost pressure were used until the estimated power matched the desired power output at each design point. Using the DR_{del} that provided good approximations to the desired power at the design points, the compressor inlet air flow was calculated using:

$$CFM_{turbo} = CFM_{baseline} \cdot DR_{del}$$ **Equation 4.3.11**

The calculated pressure ratio and inlet flow were plotted on the compressor maps to determine the compressor efficiency at those operating conditions. The efficiency was placed back into equation 4.3.7 to determine a more accurate compressor flow. Again, iterations were used for compressor efficiencies until the calculated power converged to the desired power with accurate compressor efficiency.

The compressor sizing process was repeated for three different turbocharger compressor housings: a Garrett GT 15 60 trim with a 0.48 AR, an Aerocharger 53 series VNT with a 143 housing, and an Aerocharger 53 series VNT with a 128 housing. All of the calculations used ambient conditions of 95.8 kPa and 10° C, representative of the University of Idaho engine testing facilities during the winter. The compressor sizing calculations along with the predicted performance plotted on each of the compressor maps are located in Appendix B.

All three of the turbochargers would have offered good performance characteristics at the predicted design conditions. However, the Aerocharger with the 143 housing appeared to be better suited for an engine with more airflow, which is shown by the left-of-center offset of the predicted performance curve on compressor map, Appendix B. The GT-15 and the Aerocharger 128 both had compressor performance that would satisfy the predicted boost and airflow requirements while retaining η_c between 65 and 75 percent, Figures 50 and 51.
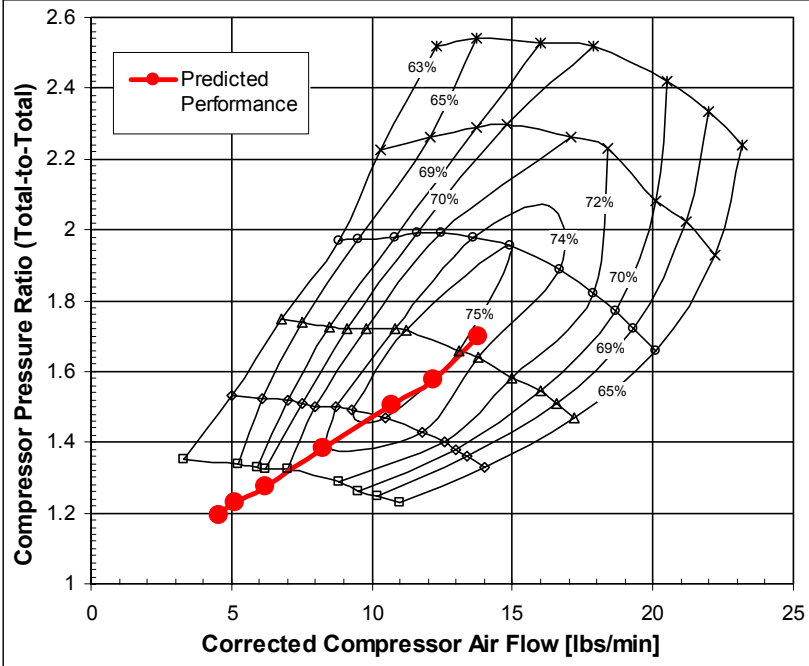
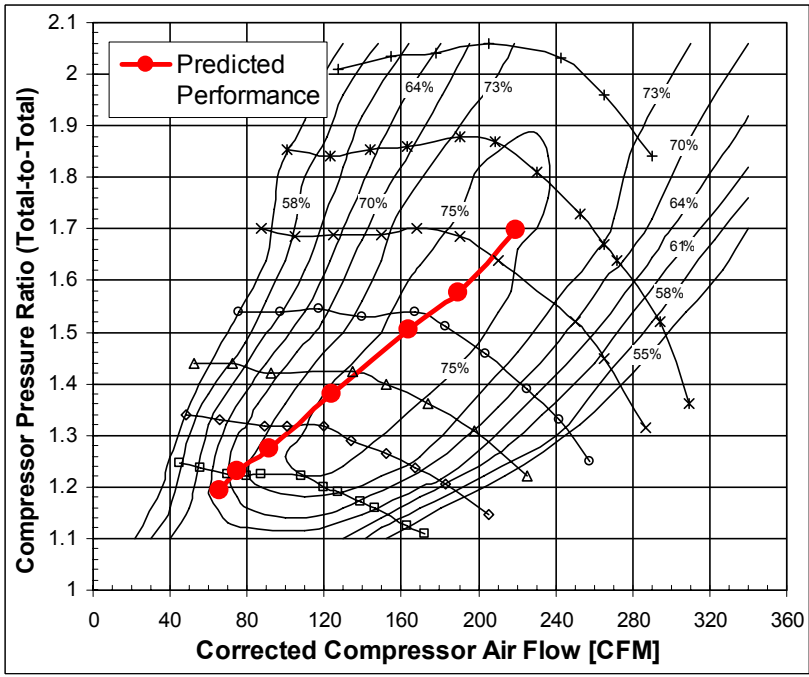*Figure 50: Predicted air flow and PR with the GT-15 turbocharger.*

Figure 51: Predicted air flow and PR for the Aerocharger 53 and with a 128 housing.

The Aerocharger was chosen over the GT-15 for several reasons. The GT-15 was a vane-less turbocharger with an internal waste-gate that required external cooling and oiling

loops, typical of most turbochargers. First, the Aerocharger had a variable turbine housing, which improves turbocharger performance and reduces turbo-lag. Additionally, as discussed earlier, maintaining a proper SPR is extremely important for scavenging and trapping characteristics in two-stroke engines. The variable turbine nozzle would provide additional control of the scavenging pressure ratio. Secondly, the Aerocharger did not require external cooling or oiling loops, which significantly reduces over-all system complexity. Finally, the Aerocharger has worked well as an aftermarket add-on with many snowmobile engines . They are the most successful and the most often used aftermarket turbochargers for snowmobile applications. The predicted compressor and engine performance for the Aerocharger is in Table 14 below.

Table 14: Predicted engine operating conditions for the Aerocharger 128 turbocharger.

Boost [psig]	PR [t/t]	Compressor Efficiency [percent]	Compressor Outlet Temp [C°]	DR_{del}	Desired Power [hp]	Estimated Power [hp]	Estimated Compressor Inlet flow [CFM]
2.70	1.19	64	29	1.12	48	48	66
3.20	1.23	70	30	1.15	55	55	75
3.80	1.27	73	33	1.18	67	67	91
5.30	1.38	75	40	1.25	91	91	124
7.00	1.50	75	48	1.32	119	120	164
8.00	1.58	75	53	1.37	138	139	190
9.70	1.70	75	61	1.44	160	161	220

Aerocharger turbochargers were originally manufactured by Aerodyne of Dallas, Texas. At the time of this work, Aerodyne had sold the manufacturing rights to several smaller companies [48]. There are two turbocharger series designations, 66 and 53. The 66 series are larger than the 53 series and are often used on snowmobile engines with displacements greater than 900 ccs. Each of the series has two turbine housing sizes; the 128 housing of the 53 series is smaller than the 158. The turbocharger used for the UI GDI engine was the smallest and fastest responding Aerocharger available. Side and top views of an Aerocharger are shown in Figure 52 and a cut-away view is provided in Figure 53.
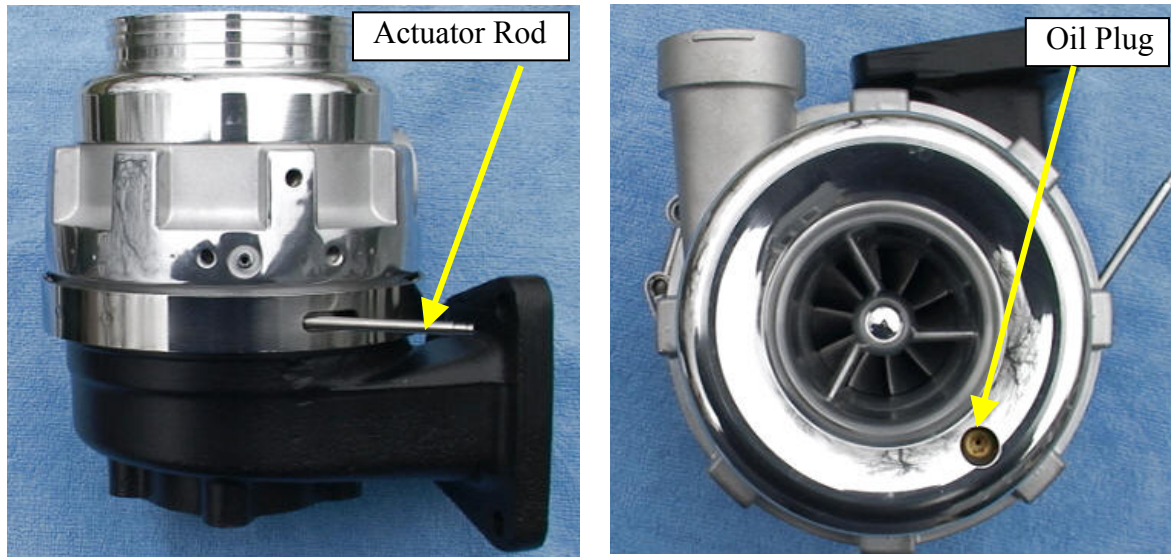
Figure 52: *Two views of an Aerocharger turbocharger.*

The turbine housing has multiple movable vanes similar to the ones described earlier in Figure 44, which are actuated by a steel rod that passes through the turbine housing, shown in Figure 52. The movement of the actuator rod was controlled by a pressure operated bellows with one side open to the atmosphere and the other side connected to the intake pressure at a convenient location. As boost pressure rose, the pressure differential across the bellow would move the actuator rod to open the vanes. The initial vane position could be varied by adjusting a screw located on the vane-actuator housing, allowing precise control of when the turbocharger began to produce boost.

Aerocharger turbochargers are considered one of the most advanced and user-friendly turbochargers available [45]. Installation is very easy because there is no need to develop an oiling or cooling system. They utilize high-precision ball bearings, for quick spool up time, that receive oil from a reservoir in the compressor housing that wicks to the bearings. The oil can be re-filled by removing the brass plug located on the top of the compressor housing. However, without a cooling or oiling system the turbocharger can be overheated. If it is allowed to get too hot the oil will heat up and burn, causing the bearings to seize.
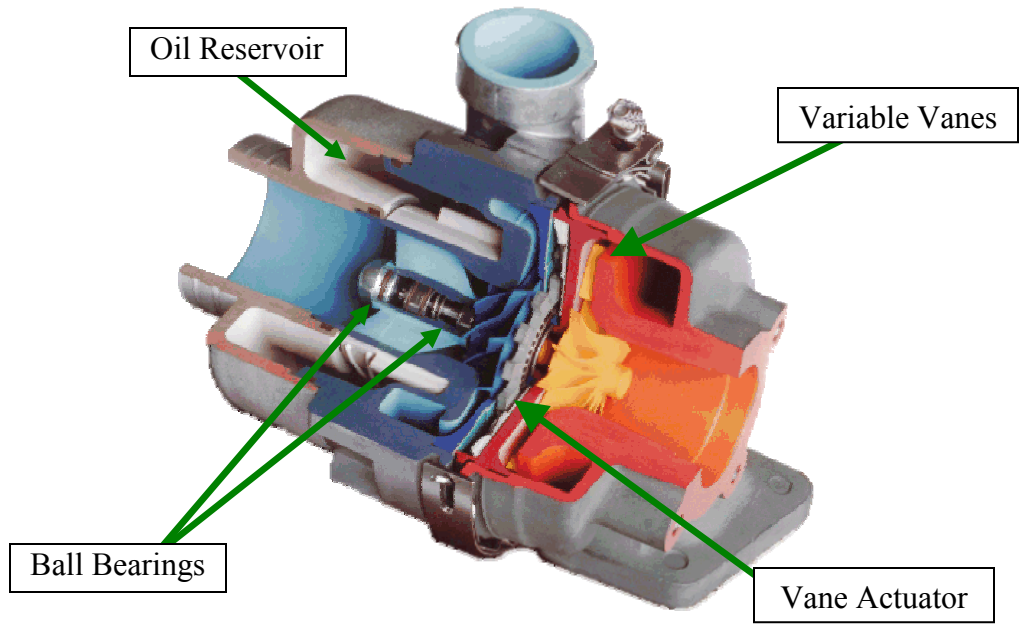
Figure 53: Cut-away view of an Aerocharger turbocharger.

Another feature is that the two housings halves of the turbocharger can be connected in eight different configurations, changing the relative position of the compressor outlet and turbine inlet. This offers a high degree of flexibility to turbocharger placement. However, the turbocharger must be mounted vertically to ensure proper oil distribution to the bearings. The turbine inlet and compressor outlet were clocked 90° to each other for the UI engine, as shown in Figure 54.

Figure 54: UI GDI Aerocharger housing configuration.

As discussed earlier, the UI engine was to utilize a constant-pressure turbocharging system that retained the tuning characteristics of the exhaust pipe. Therefore, the turbocharger would need to be attached to the exhaust stream at the end of the tuned pipe. Snowmobile exhaust systems are generally designed in three pieces consisting of the y-pipe, tuned pipe, and silencer. The turbocharger needed to 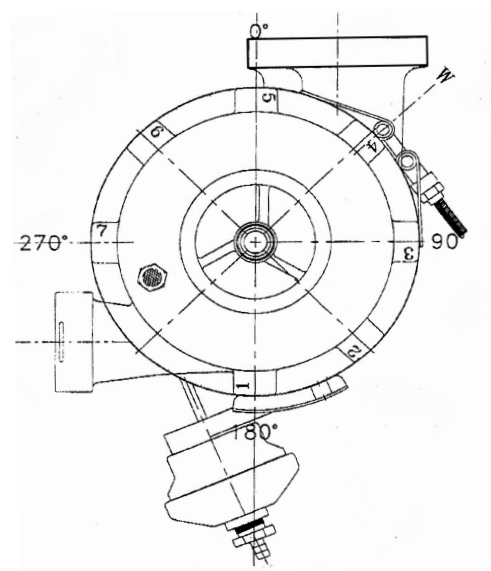be installed where the silencer normally attached to the tuned pipe. The silencer was connected to the tuned pipe by a ball-and-socket joint held together with springs. To connect the turbine inlet flange to the exhaust outlet, the ball end of the tuned pipe was cut off. A flange for the turbocharger to bolt to was machined from mild steel and welded to the end of the tuned pipe. The turbocharged engine outside of the chassis with the turbocharger mounted to the end of the tuned pipe is shown in Figure 55.
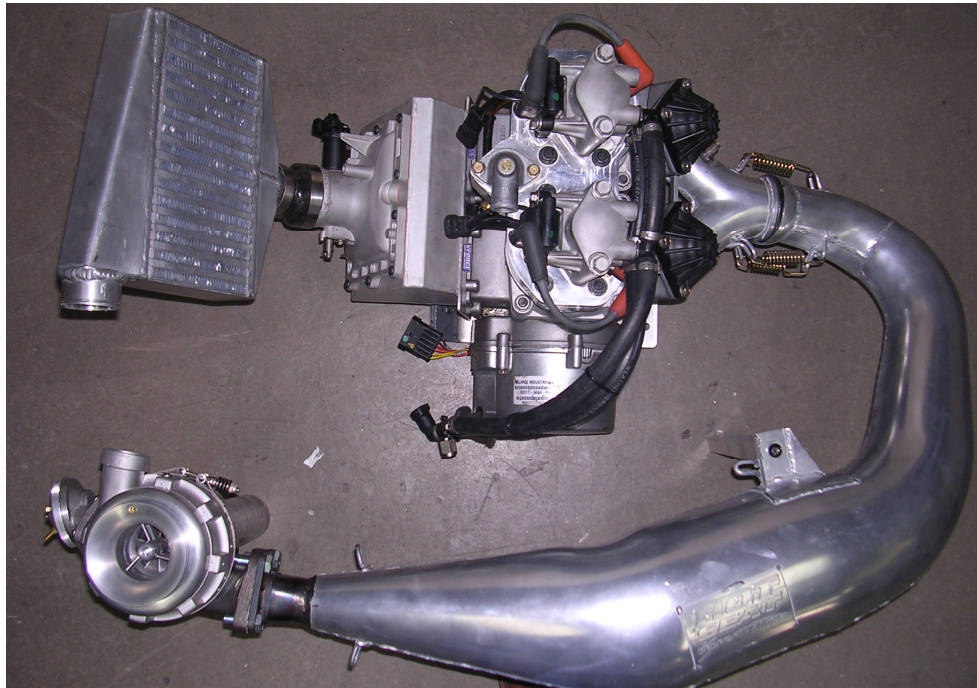

Figure 55: Top view of the UI GDI turbocharged engine.

4.4 TURBOCHARGER SUPPORTING ARCHITECTURE

In addition to the turbocharger, other modifications were made to the naturally aspirated engine. As discussed earlier, combustion events introduce strong pulsations in the exhaust system and can cause the turbocharger to deviate significantly from steady flow

operation. A large volume exhaust manifold was used damp out the pulsations and provide a nearly steady flow in the exhaust stream. A similar unsteady flow can occur in the intake system caused by pulsations created by the piston movement and intake reed valves. Similar to the exhaust, the pulses can be damped out through the use of a large volume intake system.

An intercooler was used to increase intake system volume and to remove heat from the compressed air to increase the density of the delivered air. The intercooler was an air-to-air heat exchanger that relied on airflow through the fins to remove heat from the compressed air. Rather than designing and manufacturing an intercooler one was purchased from a company that specialized in turbochargers. Bell Intercoolers built an intercooler for the engine using the predicted engine airflow and the dimensions of the space the intercooler was to fit in. The intercooler mounted on the engine is shown in Figure 56.
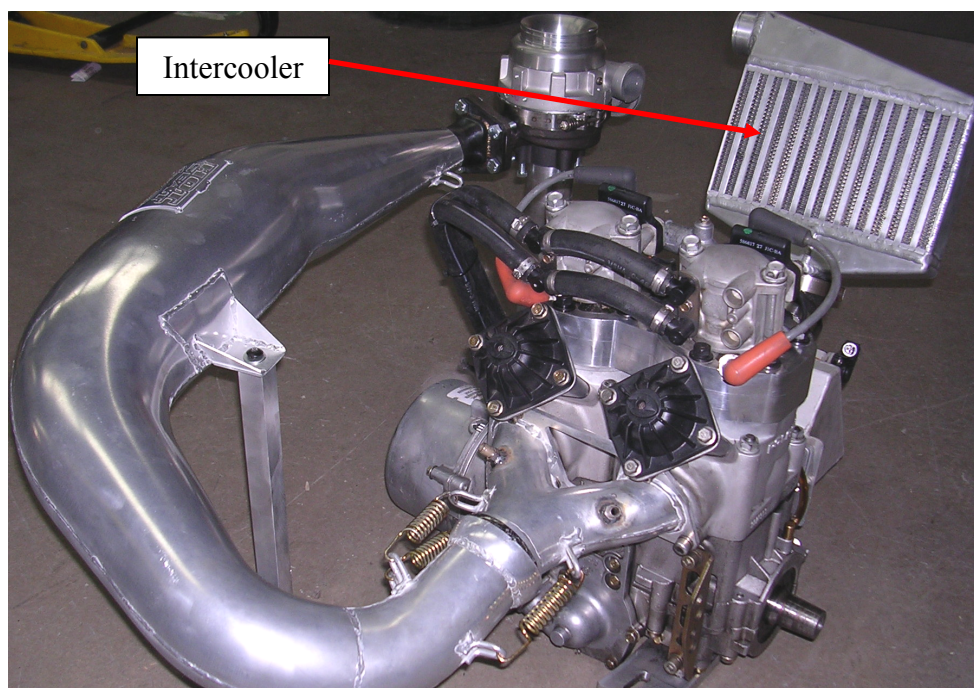
Intercooler

Figure 56: *Intercooler as mounted on the UI GDI engine.*

In addition to the intercooler, an intake plenum was used to help damp out intake pulsations and provide a connection between the intercooler outlet and the engine intake. Two different plenums were designed and used. The first plenum was design to have a volume equal to three times the swept volume of the engine to act as a reservoir of air for the engine to use during quick acceleration. During initial testing when the engine was operating

at low throttle openings and engine speeds between 2000 and 5000 rpm the turbocharger was not providing enough air flow and a vacuum was being created in the plenum. It was determined that the plenum volume was too large and a second one was designed.

The second plenum's volume was reduced to 1.5 times the swept volume. In addition to making the plenum smaller, a reed valve—similar to the engine intake reed valves—was installed in the plenum. The reed valve would ensure the plenum never operated under vacuum. If the plenum were to experience a lower pressure than atmospheric the reed valve would open and let air into the system. The added air would increase the mass flow through the engine, increasing the turbine speed. The turbocharger would then provide more air to the engine. This system proved to work well and the engine performed significantly better with the second plenum in place. A solid model showing the plenum design and the location of the reed valve is shown in Figure 57.
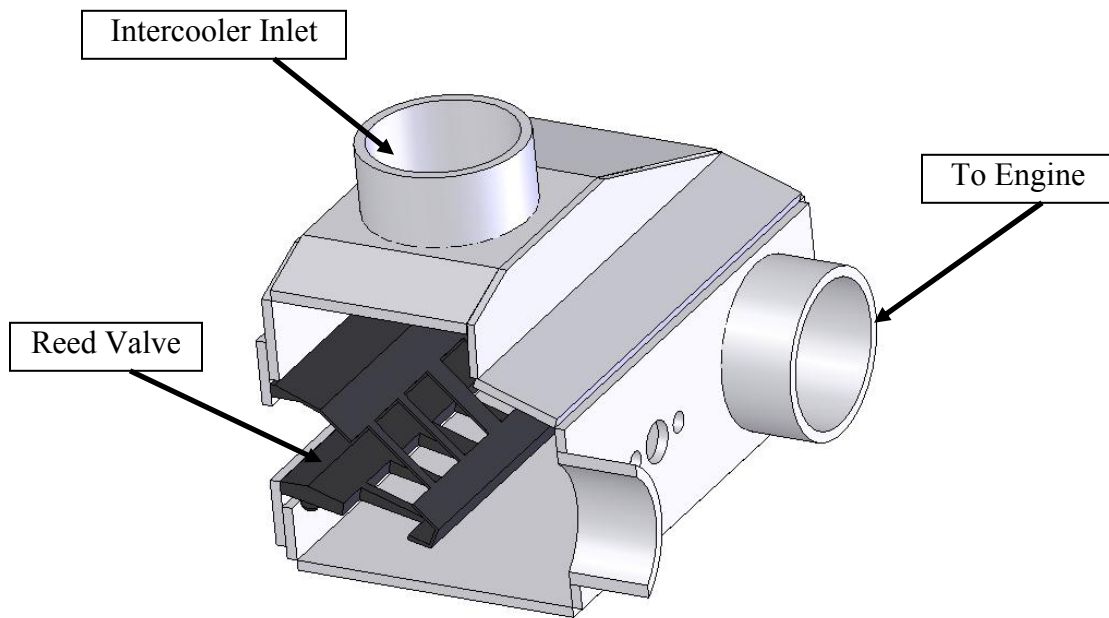
Figure 57: Solid model of the second plenum showing the reed valve.

The last modification made to the naturally aspirated engine for turbocharger operation was to the engine management module (EMM.) The EMM was capable of adjusting fuel and ignition parameters for air density based on ambient conditions using air temperature and pressure sensors. However, the EMM air-pressure sensor had a maximum range of 115 kPa (16.7 psi) absolute, which would only be useful to a boost pressure of 2

psig, Figure 58. The turbocharged engine was expected to operate with at least 10 psig boost pressure. The stock EMM sensor would not be able to compensate the fuel delivery or ignition based on the intake pressure. Without pressure compensation the turbocharged engine would not work. The only solution was to replace the stock pressure sensor with one that could measure to at least 180 kPa (26 psi) absolute, which would allow the engine to operate with boost up to 12 psig. The original pressure sensor was a Motorola sensor with a Freescale part number MPXA4115A. A Motorola sensor with a range up to 250 kPa (36 psi) absolute, part number MPXA250A, was found as a suitable replacement, Figure 59.

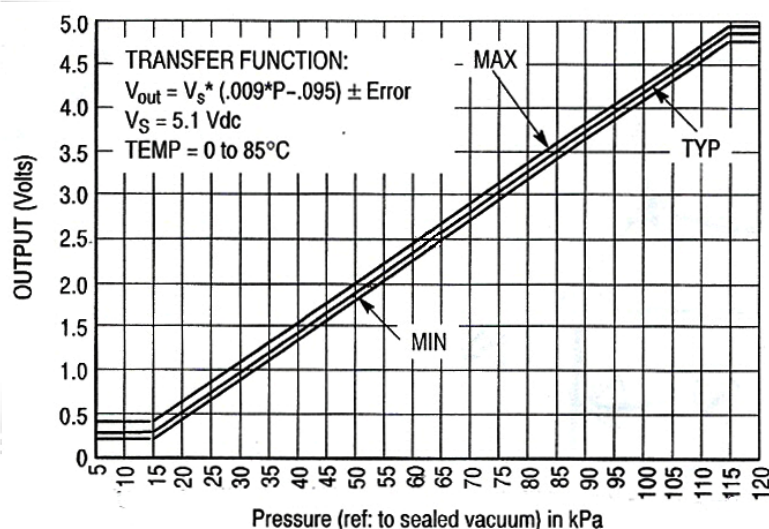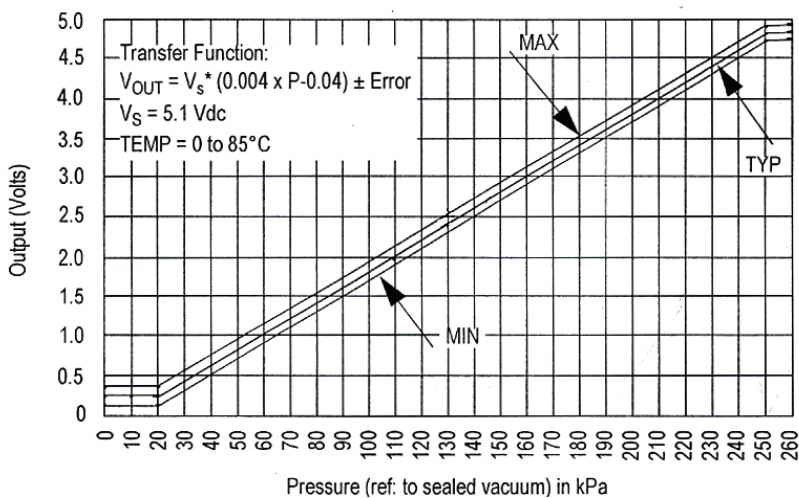*Figure 58: Stock EMM pressure sensor useful range [49].*

Figure 59: Replacement pressure sensor useful range [49].

Unfortunately, there were two problems with this course of action. Unlike most sensors used for engines, the pressure sensor was located inside the EMM, which was a sealed unit. Changing the sensor would require breaking the EMM open and removing electrical components. Additionally, the EMM was programmed with the transfer function for the original sensor, described in Figure 58. While both the replacement and stock sensors used output voltages from 0 to 5.0 volts, the replacement sensor measured pressure from 0 to 250 kPa, rather than the 0 to 115 kPa range used by the original sensor. Simply replacing the sensor would have resulted in the EMM correcting with too low of a pressure compensation from the new sensor. In order to provide the correct pressure compensation the EMM needed to be programmed with a compensation table that would adjust the fuel and spark based on the measured pressure from the new sensor using the transfer function of the original sensor. To accomplish this, the pressure compensation table was programmed similarly to the compensation table in Table 15, below.

Table 15: *The original and new EMM pressure sensor compensation.*

Stock Sensor	EMM Measured Pressure [kPa]	30	40	50	60	70	80	90	100	110
	EMM Fuel Compensation	30%	40%	50%	60%	70%	80%	90%	100%	110%
Replacement Sensor	EMM Perceived Pressure [kPa]	30	40	50	60	70	80	90	100	110
	Actual Pressure [kPa]	54	76	99	121	144	166	189	211	234
	Required Fuel Compensation	54%	76%	99%	121%	144%	166%	189%	211%	234%

5.0   ENGINE TESTING

This section describes the testing equipment, experimental procedures, and the results of testing. One goal of this testing was to determine if stratified combustion would provide enough power to propel the vehicle during light-load cruising. If efficient stratified combustion could be utilized, a significant savings of fuel consumption would result. The other goal was to determine how turbocharging effected engine performance and scavenging in order to determine the direction of future work.

5.1   DESCRIPTION OF TESTING EQUIPMENT

A Land-and-Sea, DYNOmite™ toroid flow nine-inch water-brake dynamometer was used to measure torque and rpm of the engine. The dynamometer is capable of absorbing an engine's power by coupling to the output shaft. The water-brake dynamometer consists of a ribbed rotor encased in a ribbed aluminum housing. The housing has a torque arm with a full-bridge strain gauge attached to it. The dynamometer rotor bolted onto the tapered crankshaft where the primary clutch ordinarily mounts. This allows the rotor to rotate at the same speed as the engine. The torque arm, rigidly attached to the housing, is held in place by the jackshaft where the secondary clutch in normally mounted, see Figure 60.

As the engine rotates, pressurized water enters the rotor near the center of the assembly. The water is accelerated as it travels outward along the rotor until it exits the housing towards the periphery of the housing. The water causes viscous friction between the rotor and the housing. The viscous forces create a torque on the housing about the engine crankshaft. The torque arm prevents the housing from rotating. The torque transmitted into the torque arm is assumed to equal the torque of the rotating shaft. The strain gauge on the torque arm measures the strain on the torque and is used to calculate the applied torque. Engine speed was measured using an inductive pick-up located inside the dynamometer housing. Using the measured engine speed and torque, the power output can be calculated using equation 4.3.2, described earlier. The torque arm was calibrated with a 50 lb (222N) weight supported from an 18-inch (0.45 m) moment arm that was attached to the housing before each set of testing.

In order to measure torque and speed at specific engine operating conditions, the dynamometer controlled the speed of the engine with a load-control valve that regulated the

water flow. The Land-and-Sea supplied computer program, DYNOmax, can be used to electronically control both the load valve and throttle opening for the engine. The load valve and throttle could also be controlled manually. The testing for this research used the software to control the load valve to maintain a constant engine speed while the throttle position was manually controlled to control the load on the engine.
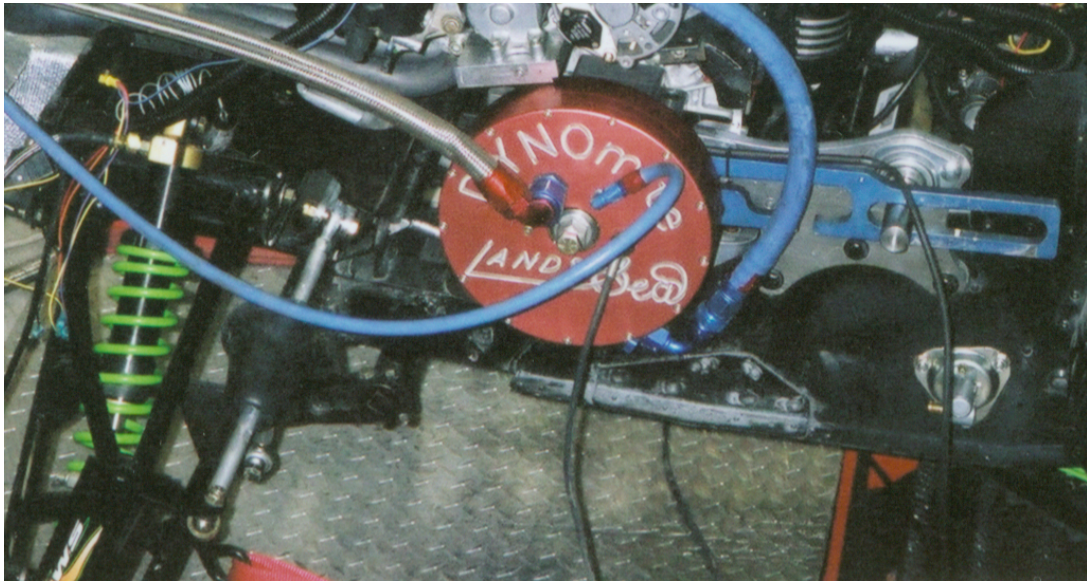

Figure 60: *Water brake dynamometer used for engine testing.*

The water-brake dynamometer proved to be inadequate at controlling the research engine and limited successful engine testing was performed. Water-brake dynamometers are sufficient devices when they are used on engines that are completely tuned. However, they are not useful during engine development when engine mapping is incomplete. The incomplete fuel maps can lead to significant changes in torque output in relatively small rpm or throttle increments. While tuning the engine at a specific operating condition there can be a change in torque that causes a rapid increase in engine speed. The dynamometer attempts to return the engine to the desired hold rpm by supplying more water. If the change in torque, or resulting change in engine speed, is significant, the latency of the hydrodynamic system can cause uncontrollable rpm oscillations. The engine then has to be brought to a slow speed where a low torque output occurs in order to return the dynamometer to a stable condition. Consequently, limited operating conditions were tested. An electric dynamometer

would alleviate these problems and further engine tuning and testing will be possible.

Fuel flow was measured using a MAX Machinery 710 series fuel flow meter.   It measured volumetric fuel flow, but displayed mass flow in units of kg/hr. The meter internally calculated fuel flow mass from the volume flow using user defined fluid densities. A thermocouple measured the fuel temperature for corrections of density changes due to temperature fluctuations. The cart could supply fuel to the engine at either low pressure, for carbureted applications, or at regulated pressures up 100 psig for fuel injected engines. The fuel cart had both a supply and return hose for the engine, as well as a supply and return hose for the fuel source.

The fuel flow meter had a frequency output that varied with fuel flow so it could be used with a data acquisition system (DAQ) to record data. During testing, the frequency output could not be utilized and an alternate method was used to record fuel flow. The fuel cart also had a voltage output that varied linearly with fuel flow. Fuel cart voltage and fuel-flow data was collected using a simple "bucket and stopwatch" method. The results of that test are shown in figure 61. Equation 5.1.1, the best-fit line to the fuel flow and voltage data, was programmed into the DAQ in order to record fuel-flow data.

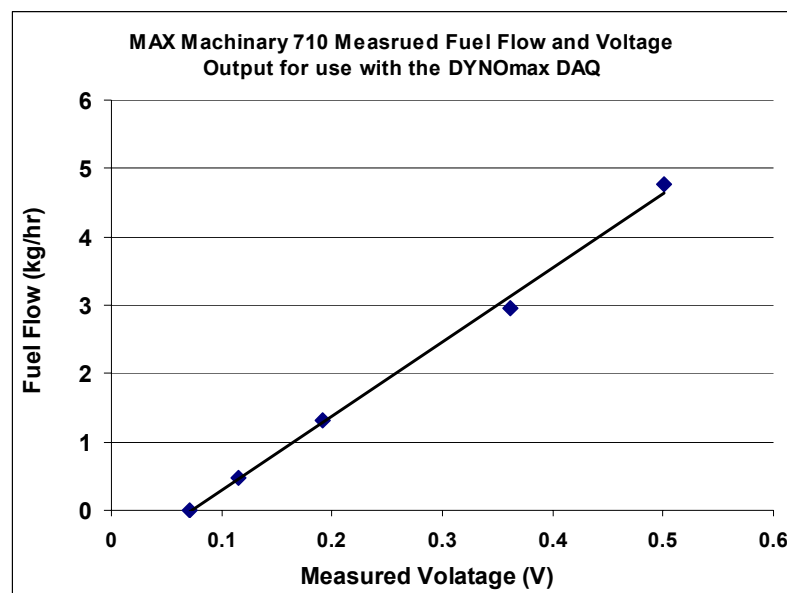$$Fuel_{flow} = 10.863 * V + .792$$

Equation   5.1.1

Figure 61: Fuel cart fuel flow calibration for use with the DYNOmax DAQ.

Initially, an EMS model 5001 five-gas emission analyzer was used to measure exhaust emissions. The EMS measured O_2, CO_2, CO, NO, and UHC (reported as hexane, C_6H_{14}). The gasses were reported as partial pressures with units of either ppm or percent concentration. During testing this analyzer failed and another analyzer was purchased. The second analyzer, a Testo 500 XL, measured NO, NO_2, CO, CO_2, H_2, O_2, and UHC (reported as methane, CH_4). Again, the gasses were reported as partial pressures. Unfortunately, the analyzer was intended to measure low concentrations of CO and UHC typical of a properly tuned engine. If the analyzer sensed too high emissions, UHC greater than 20,000 ppm or CO greater than 5 percent, it would shut down. While these emissions are higher than what was expected for a well tuned GDI two-stroke, during engine development these levels of emissions occurred due to incomplete fuel maps. An emissions analyzer capable of sustained emission levels typical of carbureted two-stroke engines, UHC greater than 60,000 ppm and CO greater than 6 percent, will be required for further engine fuel map development.

Other engine parameters were monitored and recorded for engine tuning and testing using sensors connected to the DYNOmax DAQ. Three ungrounded K-type thermocouples, referred to as EGTs, were used. Two EGTs were placed in the Y-pipe, each placed approximately 1.5 inches downstream from each exhaust port opening. The third EGT was placed at the end of the tuned pipe in the stinger before the entrance to the exhaust muffler. EGTs are an effective tuning aid. Depending on engine load and speed, the exhaust port temperatures should range between 600° and 1300° F. The temperature at the end of the pipe should range between 300° and 1200° F.

The pressures in the intake system and the exhaust system were also measured to aid in engine tuning. Low-pressure sensors, ~30 psig, were placed in the air stream at the compressor outlet, before the throttle plate, after the throttle plate in the plenum, and before the turbine inlet in the exhaust. The difference of the compressor outlet pressure and the pre-throttle plate pressure were used to determine the pressure drop through the intercooler. The two sensors across the throttle plate were used described the pressure drop across the throttle. Finally, the exhaust and plenum pressures were used to calculate the scavenging pressure ratio.

In addition to the low-pressure sensors mentioned above, an attempt was made to use in-cylinder pressure sensors. Combustion pressure sensors are very useful devices for engine

development. The pressure trace can be used to identify cycle-to-cycle variations, peak pressures, identifying detonation, calculating the mass fraction of burned fuel, and calculating the heat release of combustion. All of these parameters can be used to optimize combustion. Placing a sensor in the combustion chamber can be difficult if the head was not designed to accept a sensor. The UI head was designed and manufactured without providing a location for a pressure sensor, making it difficult to place a combustion sensor in the head.

A solution was to use an Optrand optical pressure sensor attached to the sparkplug. The optical pressure sensor uses fiber optics to pass light between the sensor face and circuitry. A steel diaphragm, located at the sensor tip, deflects as cylinder pressure rises. The deflection of the diaphragm is measured by the change in light reflection off of the diaphragm as it is returned to the sensor circuitry. The sensor attached to a modified sparkplug by a welded on attachment. A pressure tap was drilled through the body of the sparkplug to supply the cylinder pressure to the face of the sensor (Figure 62).
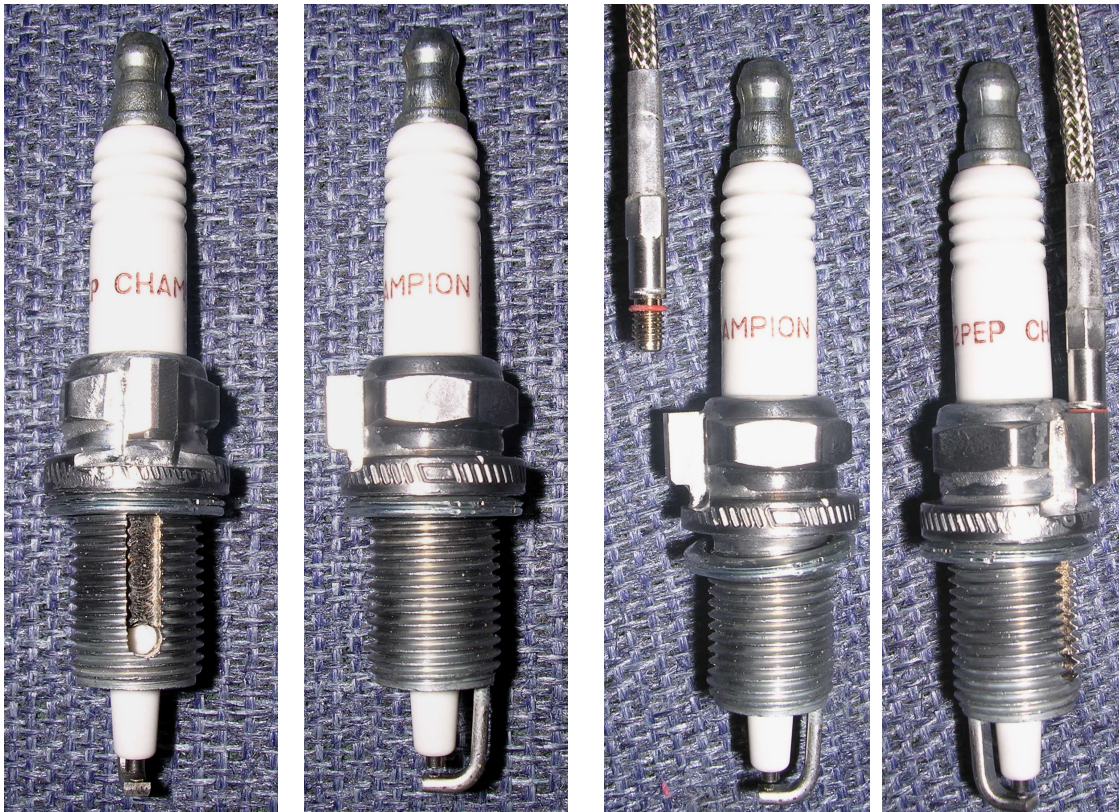

Figure 62: *Modified spark plug to accept the Optrand optical in-cylinder pressure sensor.*

The pressure sensors proved to be very fragile. Because the spark plug holes in the head were at an angle and were not designed to fit the added width of the pressure sensor adapter, the modified spark plugs were difficult to install. Upon tightening the spark plugs, the sensor housing would shear at the interface between the sensor and sensor housing. The sensors are known to have excellent measurement accuracy, limited drift due to temperature changes, and easy user interface to acquire pressure data. Future use of the sensors could be made if the head were redesigned to accept the sensors.

5.2   TESTING METHODOLOGY

There were two experimental goals for this work. The first goal was to investigate stratified operation to determine if it could be used for low load cruising. The second goal was to turbocharge the engine to determine where future research would be required in order to design an efficient turbocharged GDI engine. Without an emissions analyzer engine tuning was based on power output, fuel flow, run quality, piston wash, exhaust pipe EGTs, spark plug color, and exhaust smell.

For stratified tuning and testing the throttle plate was removed. This was done for two reasons. First, removing the restriction on the intake side would result in a higher delivery ratio and would lead to higher trapped charge purity. Providing the best in-cylinder conditions seemed prudent because the goal was to determine the maximum power available during stratified combustion. The second reason the throttle was removed was to ensure power output was a function of delivered fuel quantity rather than throttled air.

Stratified tuning was conducted at 1000 rpm increments starting from 2000 rpm to 5500 rpm with throttle increments ranging from 50 TCs to 300 TCs. The tuning started at the cell in the map that correlated to 2000 rpm and 50 TCs. Tuning continued with increasing TCs until the entire range at 2000 rpm was complete. The engine speed was then increased to 3000 rpm and the throttle returned to 50 TCs. Tuning continued systematically in that manner until all of the cells had been tuned.

During turbocharged testing the engine was operated between 5000 rpm and 8000 rpm, with throttle position ranging from 301 to 1000 TCs. Similar to the stratified testing, tuning started with the slowest engine speed and lowest throttle opening and proceeded with increasing throttle position then engine speed. As stated earlier, the dynamometer response

limited the amount useful engine tuning. This limited turbocharged data collection, as will be discussed in the results section.

5.3   EMISSIONS AND AIR-FUEL RATIO CALCULATIONS

Had a useful emissions analyzer been available, the following calculations would have been used for engine tuning and to determine the EPA emissions number for the research engine. The E score procedure, as touched on earlier in chapter one, weights specific emissions against power output using the SwRI five-mode test. Mode point determination and emissions weighting calculations are based on the five-mode test, while the raw emission calculations are derived from EPA regulations [8]. Specifically, the raw emissions calculations follow the fuel-flow method for calculating mass emissions using raw gas sampling. The EPA used the raw gas method because it was developed for the outboard industry with two-stroke engines in mind [11].
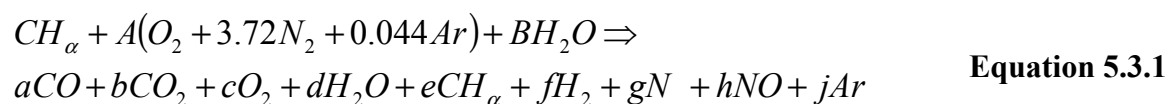
At least five exhaust gasses need to be sampled for the emissions calculations: HC, CO, CO_2, NO_x, and O_2. Along with these gasses the engine torque, speed, and fuel consumption need to be measured. Finally, the hydrogen/carbon ratio of the fuel must also be known. A list of the required measured quantities are given in Table 16. The hydrogen/carbon ratio must be derived from a sample of test fuel to achieve the required accuracy for the EPA regulations. However, for engine development and mapping where fuel sample testing is not a viable option, a ratio of 1.8 can be used for super-unleaded non-oxygenated gasoline [7]. If the fuel is a mixture of ethanol and gasoline, such as E-10, the ratio is typically between 1.8 and 1.9 depending on ethanol content [50].

Table 16: *Measured quantities for emission mass calculations measured during mode i.*

HC_{wet}	Average HC volume concentration in the exhaust, $ppmC_1$
NO_x	Average NOx volume concentration in the exhaust, ppm
[CO]	Average CO percent concentration in the exhaust, dry
$[CO_2]$	Average CO2 percent concentration in the exhaust, dry
$[O_2]$	Average O2 percent concentration in the exhaust, dry
T	Average torque measured at the output shaft, N-m
G_{fuel}	Average fuel mass flow rate, g/hr
RPM	Average measured speed [rpm]
α	Hydrogen/Carbon ratio of the test fuel

To begin the five-mode test the maximum power output at the engines rated speed must be measured. Using the maximum speed and power, the five mode points can be determined using the SwRI mode points table. During testing the engine should be operated for at least 5 minutes at each mode point with emission sampling lasting for at least 1 minute [8]. Emissions should be sampled separately for each mode and calculations carried out to derive the average HC, NO_x, and CO mass emissions during each mode. The average mass emissions are then converted to specific emissions using the average power output at each mode. The average weighted specific emissions can then be calculated using the weighting factors specified for each mode point. Finally, the averaged and weighted emissions for UHC+NO_x and CO can be added together and put into the EPA scoring function to determine the E score. To confirm the test is valid follow the EPA regulations to calculate cycle statistics for the sequence of modes and compare them with the specified values in the regulations. An example calculation for the E score for the 2005 CSC control snowmobile is given in Appendix D.

Air/fuel ratio evaluation is a key factor in determining engine performance and it is a useful tool during engine fuel mapping. Precise measurement of air/fuel ratios in four-stroke engines is a well practiced procedure and is typically determined from oxygen content in the exhaust stream. These techniques are not considered applicable to two-stroke engines and are therefore rarely used [51]. A more obvious method for calculating air/fuel ratio would be to measure the air and fuel flow directly. However, two-stroke engines are strongly influenced by any pressure drop in the inlet or exhaust streams, excluding the addition of an air flow meter [17]. Moreover, evaluation of air/fuel ratios in GDI two-stroke engines is not possible with direct measurement [20]. Several methods have been developed that use the exhaust composition to estimate both the overall and trapped air/fuel ratios as well as the short-circuit ratio [17, 20, 51, 52]. The method proposed by Douglas can be accurate to +/- 0.5percent AFR if the UHC measurements have accuracies similar to those made using FID analyzers [51]. The air/fuel ratio calculations are based on the combustion of a hydrocarbon fuel with air described by the chemical reaction [51]:

$$CH_\alpha + A(O_2 + 3.72N_2 + 0.044Ar) + BH_2O \Rightarrow$$
$$aCO + bCO_2 + cO_2 + dH_2O + eCH_\alpha + fH_2 + gN + hNO + jAr$$

Equation 5.3.1

The principle is that, the air/fuel ratio of the products can be derived by measuring the products of combustion in the exhaust stream [51]. After providing carbon, hydrogen, and oxygen balances, Douglas presents his equation for estimating AFR in a traditional homogeneously charged two-stroke:

$$AFR = K_f \left[\frac{.25[CO]+[CO_2]+[O_2]+.25 \cdot \alpha([CO]+[CO_2])+.5[NO]}{[CO]+[CO_2]+[HC]} \right]$$

Equation 5.3.2

where

$$K_f = \frac{138.18}{12.011+1.008 \cdot \alpha}$$

Equation 5.3.3

$[HC] =$ 12 x NDIR ppm hexane (CH_4) x 10^{-4}

or $[HC] =$ FID ppm methane (CH) x 10^{-4}

$[NO] =$ ppm NO equivalent x 10^{-4}

and all other emissions are in percent by volume [51].

Equation 5.3.2 estimates the global AFR, which is useful for traditional engines. In order to evaluate the trapped air fuel ratio consideration needs to be given to the oxygen and hydrocarbon emissions that represent the unburned air and fuel in the exhaust [51]. This requires the assessment of the air and fuel trapping efficiencies. There are several methods available to calculate the air trapping efficiency; Douglas suggests using full consideration of the combustion equation and derives air trapping efficiency as:

$$TE_{air} = \frac{.5[CO]+[CO_2]+.25 \cdot K_w \cdot \alpha([CO]+[CO_2])+.5[NO]}{.5[CO]+[CO_2]+[O_2]+.5 \cdot K_w \cdot \alpha([CO]+[CO_2])+.25[NO]}$$

Equation 5.3.4

where

$$K_w = \frac{K[CO_2]}{[CO]+K[CO_2]}$$

Equation 5.3.5

and K = water-gas equilibrium constant, 3.25—3.8 [53].

Fuel trapping efficiency is given as:

$$TE_{fuel} = \frac{[CO] + [CO_2]}{[CO] + [CO_2] + [HC]}$$ **Equation 5.3.6**

Using the air and fuel trapping efficiencies Douglas determines the AFR of the combusted mixture using:

$$AFR_{burnzone} = AFR_{overall} \frac{TE_{air}}{TE_{fuel}}$$ **Equation 5.3.7**

Equation 5.3.7 is only valid for rich mixtures for traditional homogeneously charged engines [51]. To determine the burn-zone AFR for engines that use fresh air only for scavenging (GDI) the air trapping efficiencies for a homogeneously rich mixture should always be used. The equation for GDI burn-zone AFR estimation becomes:

$$AFR_{burnzone} = AFR_{overall} \frac{TE_{air(rich)}}{TE_{fuel}}$$ **Equation 5.3.8**

An example of AFR calculations for the 2005 CSC control snowmobile is given Appendix D for reference. Evaluation of the burn-zone AFR will be useful for engine tuning, especially for highly stratified operation when EGT and O_2 measurements do not offer insight into the combustion process. Particularly, burn-zone AFR measurements should allow for better optimization of efficient stratified-charged combustion. As discussed earlier, the air trapping efficiency must be measured from a homogeneously charged engine. A suggestion to determine $TE_{air(rich)}$ for the GDI engine would be to operate the engine using a carburetor to allow calculations for $TE_{air(rich)}$, which can be found from Blair [17].

5.4   TESTING RESULTS

In addition to engine testing using a dynamometer, engine data were collected during in-field operation at the 2006 CSC competition. While at the competition the snowmobile participated in a fuel economy and endurance event that required continuous operation for approximately 100 miles at speeds between 30 and 45 mph. A time history of the engine operating speed was recorded during the endurance run, Figure 63. Based on the data collected, it is clear the engine was typically operating between 4500 and 6500 rpm. Unfortunately, throttle position data could not be recorded and a correlation to engine load

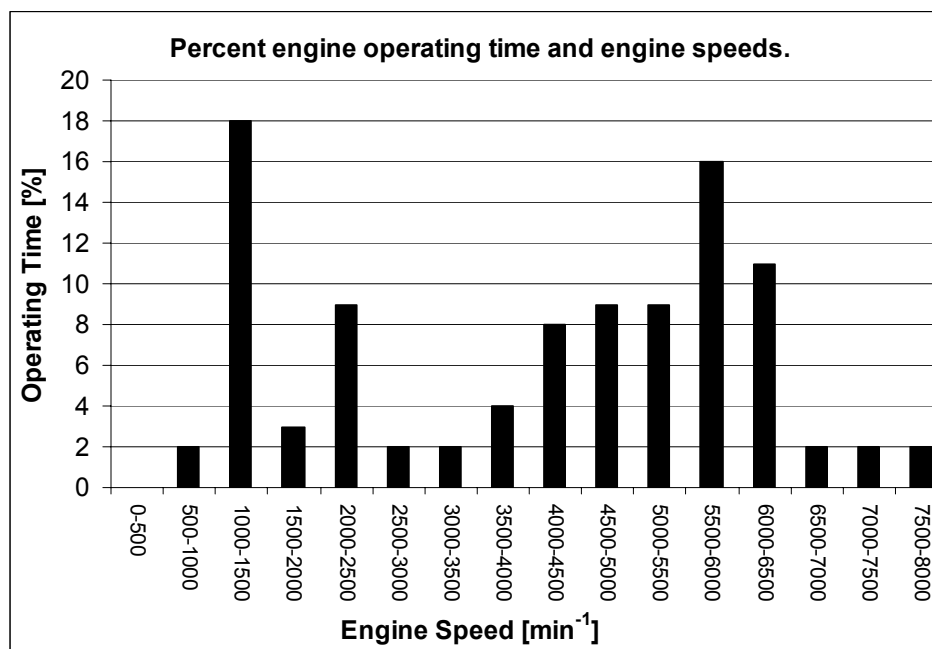could not be made. However, the data do emphasize how important engine efficiency is in that rpm range.

Figure 63: *Time history of engine operating time at specific engine speeds.*

Dynamometer stratified testing also proved to be very insightful. Discussion earlier predicted that the engine would need to be able to produce between 18 and 25 hp to propel the snowmobile at 45 mph. The time-history data of the engine operating speeds showed that during cruising, the engine operated between 4500 and 6500 rpm. Stratified dynamometer testing found the engine was producing between 15 and 23 hp at engine speeds between 4500 and 5500 rpm. The engine operated erratically at speeds greater than approximately 5800 rpm during stratified operation. The dynamometer testing and the 2006 CSC competition data suggest that the engine could be operated with stratified combustion during cruising.

However, this suggestion required further investigation. As discussed earlier, if the stratified combustion is not efficient it will result in a significant *increase* in fuel consumption. The data shown in Figure 64 suggest just that, which shows the stratified dynamometer testing and the mode-four results of the 2005 control snowmobile. The 2005 control snowmobile was used for comparison because the engine had the same displacement and a similar power curve as the UI engine.
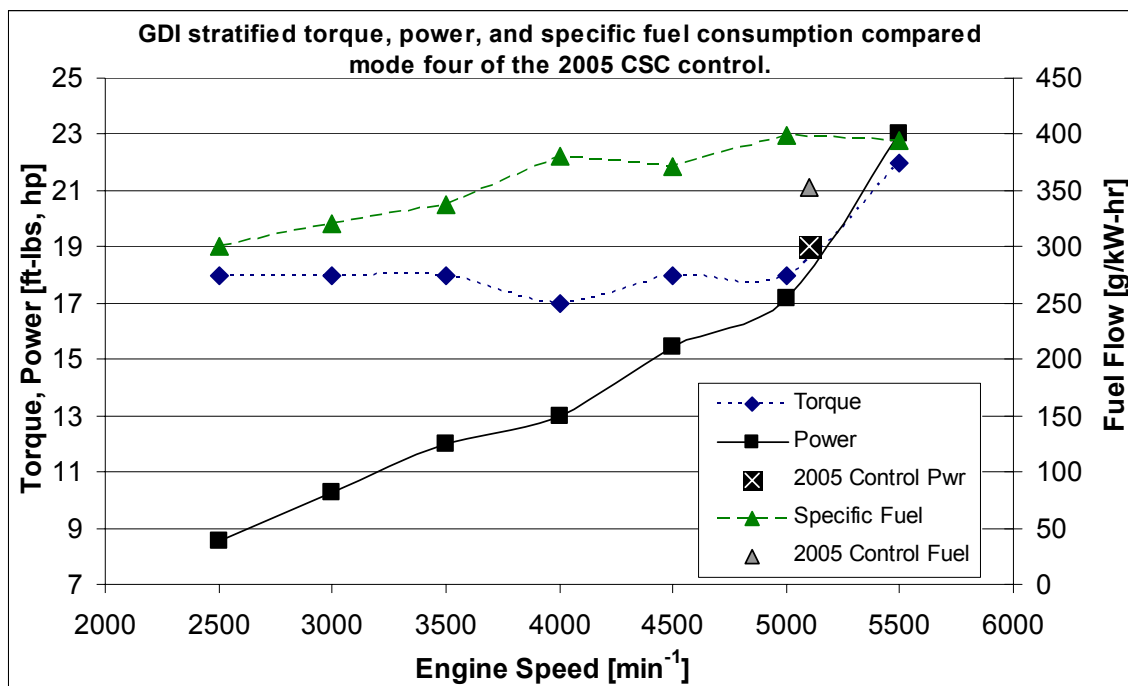
Figure 64: *Stratified GDI torque, power, and fuel consumption.*

Mode four was used because it represented the engine speed and power combination most often encountered during snowmobile operation for a 600 cc two-stroke engines with a power output of approximately 115 hp [11]. The UI GDI engine had a brake-specific fuel consumption of 400 g/kW-hr while producing 17 hp at 5000 rpm and continued to have brake-specific fuel consumption around 400 g/kW-hr up to 5500 rpm with a maximum power of 23 hp. The SDI control engine had a mode-four brake-specific fuel consumption of 353 g/kW-hr while producing 19 hp at 5100 rpm. Clearly the UI engine stratified combustion was not efficient and would be expected to use approximately 12 percent more fuel during light-load operation. It should be reiterated that this engine calibration was created without the use of an emission analyzer as a tuning aid. In order to make the proper decision about using stratified combustion for more than idle, further testing using an emission analyzer and an electric dynamometer should be conducted.

The dynamometer testing results of the turbocharged engine proved to be even more ambiguous. The limited control over the engine with the dynamometer resulted in measurements of only particular operating conditions. Initially, the engine operated well at engine speeds between 3000 and 5500 rpm at all throttle positions but would not operate

above 6000 rpm. As the engine approached 6000 rpm the SPR would begin to approach 1.1 and the engine would become unstable. The conclusion was that the exhaust back-pressure was not high enough and the cylinder would have poor trapping efficiency. The drop in trapped oxygen resulted in a steep drop in torque and engine speed, which would trigger the dynamometer to return the engine to the hold rpm. As the dynamometer lessened its resistance, the engine would have improved trapping and began producing power again. The on-and-off power combined with the latency of the water-brake would cause the engine to oscillate in 2000 rpm swings.

To alleviate this problem the SPR would need to stay above 1.1 to maintain good trapping. An increase in exhaust backpressure was attempted by installing a steel plate with a 1 inch hole placed in-between the exhaust pipe outlet and the turbine inlet. The plate increased the backpressure enough to allow the engine to operate up to 7800 rpm. Although the restriction placed in the exhaust allowed the engine to operate at higher engine speeds by maintaining a SPR above 1.1, it had a negative effect on the engine performance at the lower engine speeds (see Figures 65 and 66). At engine speeds between 5500 and 6500 the SPR was significantly above 1.2. The high exhaust backpressure reduced the mass flow through the engine and reduced the scavenging efficiency, which resulted in less than expected boost and power output at those engine speeds. Between 6500 and 7500 rpm the SPR was typically around 1.25. As the engine speed approached 8000 rpm the pressure ratio began dropping and the engine was unstable beyond 7800 rpm.
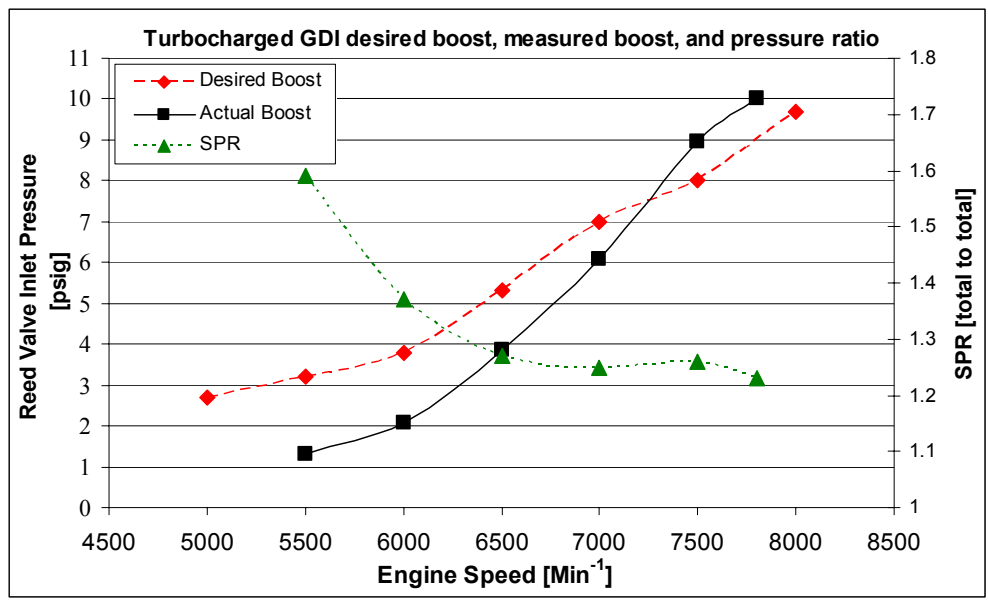
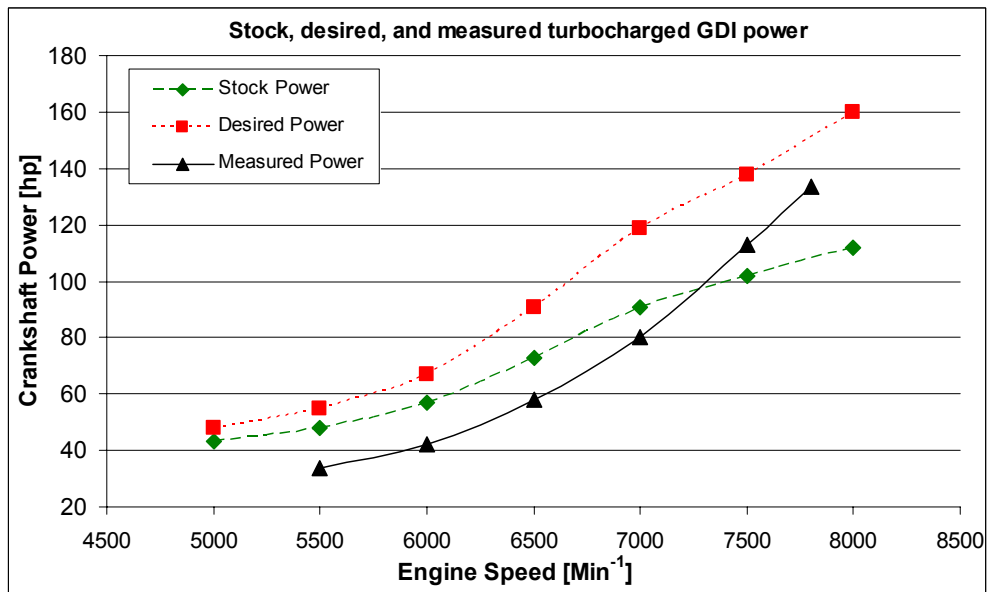**Figure 65:** *Measured intake boost, desired boost, and SPR.*

Figure 66: *Measured turbocharged performance vs. desired performance.*

Using the measured SPR and the estimated volumetric efficiency of the engine, the actual turbocharger compressor performance could be estimated. Figure 67 shows the estimated compressor performance with the measured performance. The Figure clearly shows where the engine was producing less boost than expected. The measured performance follows the predicted performance well. This was partly attributed to the fact that the engine

airflow for both calculations were based on the same engine volumetric efficiencies. A more precise method would have been to attach an airflow meter to the inlet of the compressor even though it was stated earlier that inlet airflow measurements should not be used for two-stroke engines. Airflow measurements for the turbocharged engine should be accurate because the intake system is being boosted and the pressure drop across any measurement device would not effect engine performance.
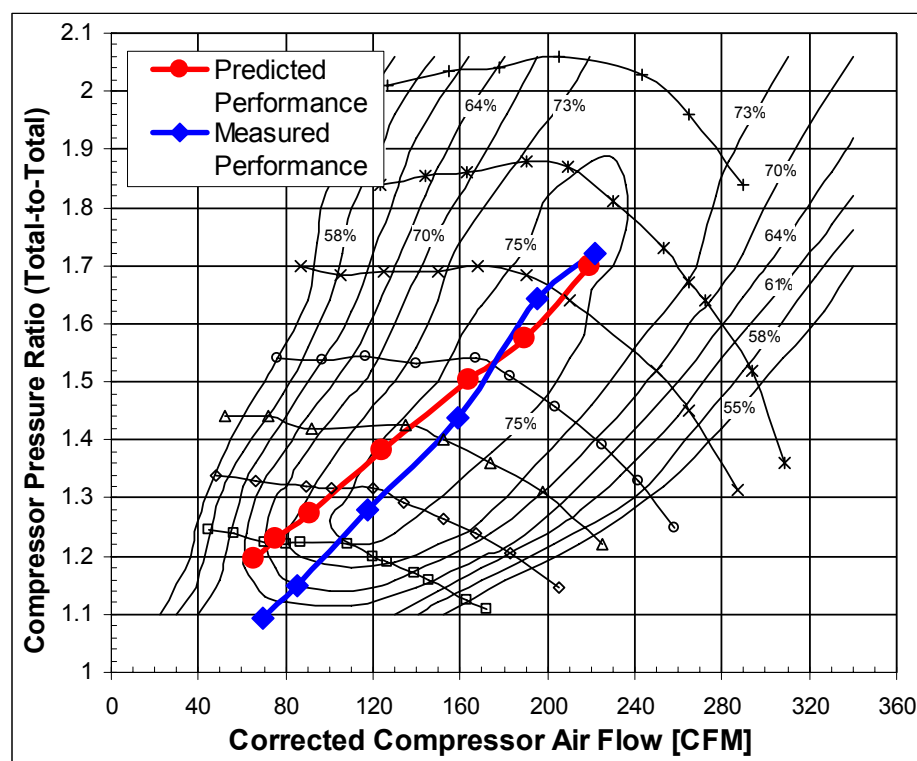

Figure 67: *Actual performance vs. predicted performance.*

The turbocharged engine performance is further described in Figure 68, which compares the stratified and homogeneous operation with data from an Arctic Cat throttle-body fuel injected engine [53]. The GDI stratified data were compared to data corresponding to 30 percent load for the Arctic Cat engine. The stratified data further illustrate that stratified combustion can be used for cruising. The homogeneous data show how the turbocharged engine was making less power than a naturally aspirated engine while the SPR was above 1.3. As soon as the SPR was in the range of 1.3—1.1 the turbocharged engine began producing more power, further reinforcing the SPR effect on engine performance.
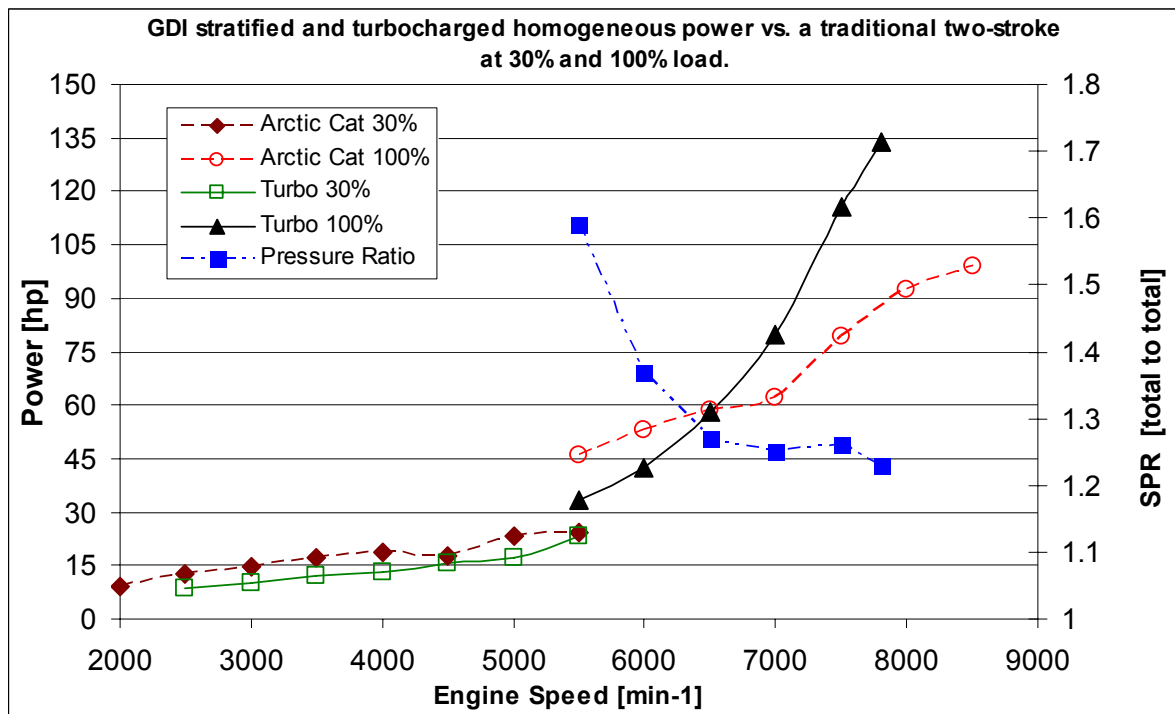
Figure 68: *Measured GDI turbocharged power.*

The last comparison made with the measured turbocharged data is based on specific fuel consumption. Figure 69 compares the turbocharged fuel consumption with the Arctic Cat engine. The Arctic Cat engine has very poor specific fuel consumption, yet it is better than the GDI turbocharged engine at all but the highest engine speeds. This comparison really offers no insight other than to show how poorly the turbocharged engine was tuned.

The data presented clearly show that the stratified combustion strategy and the turbocharged engine both required significantly more research and testing to fully determine their merits for use with snowmobile engines. The compressor performance was near the predicted values and the turbocharger should be continued to be used. Further gains in power and improvements in specific fuel consumption will be found through optimization of the system.
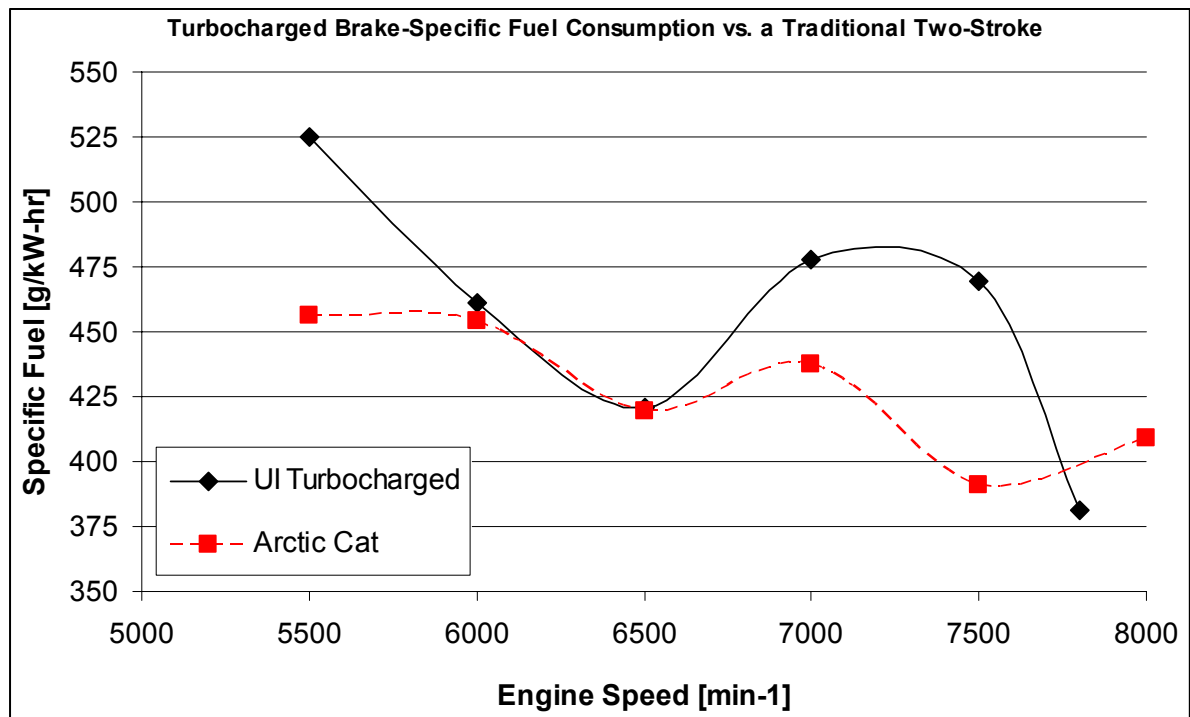
Figure 69: *Measured turbocharged specific fuel consumption.*

6.0   RECOMMENDATIONS AND FUTURE WORK

The current two-stroke engine cannot be matched in terms of its power-to-weight ratio and mechanical simplicity by four-stroke engines in snowmobile applications. Two-stroke snowmobile engines also have fuel economies similar to or better than their four-stoke counterparts. However, the emissions from current two-stroke engines is unacceptable. This work highlighted that GDI two-stroke engines have the potential to maintain their high performance characteristics while having better fuel economy with emission levels that will rival even the cleanest four-stroke engines. Additionally, turbocharging GDI two-stroke engines can provide significant increases in specific power output. This work also showed that a significant amount of work remains before high-performance two-stroke GDI snowmobile engines, naturally aspirated or turbocharged, are ready for use in environmentally sensitive areas. The future work for the naturally aspirated and turbocharged engines are significantly different and should be treated as two separate projects.

There is still a significant amount of design work and testing required for the naturally aspirated GDI engine. To begin, the first E-TEC combustion chamber should be modified to have a trapped compression ratio of 6.5, similar to the stock engine. With the modified head, the engine should be operated using a carburetor that is tuned just rich of stoichiometric. The engine should be fully characterized by measuring engine speed, torque, fuel flow, UHC, CO, NO_x, CO_2, O_2, in-cylinder pressure, and exhaust AFR in increments of 10 percent throttle and 500 rpm over the entire engine speed range. The measured information will provide the necessary information to determine air trapping efficiency, scavenging ratio, volumetric efficiency, heat release, and mass fraction of fuel burned, which will be invaluable for future GDI design and engine tuning. After the testing is completed, fuel mapping could be carried out with accurate measurements of trapped and overall AFRs for the GDI engine.

Because significant gains in fuel economy are possible with efficient stratified combustion, considerable amount of research should be focused in this area. There are many possible solutions that could be researched [17, 20]. One of the most promising is throttle-less operation with homogeneous load control using EGR and/or exhaust throttling. Removing the throttle would allow the engine to better fill the crankcase and consequently

more air would be delivered to the cylinder. During stratified operation the excess air should provide a situation where more fuel could be combusted increasing heat release and stratified efficiency. A throttled exhaust could provide additional control over the scavenging characteristics of the cylinder. As the power requirement increases and the transition is made from stratified to homogeneous combustion, EGR could be routed to the intake stream to reduce the amount of fresh air delivered to the engine, which would limit heat release for medium load operation. During peak power demands the EGR would be eliminated as maximum air utilization would be the goal. This is just one example of a system that could take full advantage of stratified-charged combustion.

In addition to stratified combustion research, in-cylinder data should be measured to determine combustion efficiency and other parameters. The measurements could be used in 1-D engine modeling software, such as Optimum Power's Virtual Two-Stroke, to best determine compression ratio, exhaust pipe design, and intake system geometry. A downfall to the 1-D software is that it will not offer any insight into combustion chamber geometry or port design for the GDI engine. A more powerful 3-D CFD modeling package, such as KIVA, STAR CD, of Fluent, would be required for GDI combustion chamber development. These software packages can model in-cylinder fuel injection and fuel atomization inside the combustion chamber. However, the downfall to these systems is that the entire engine must be modeled and a significant amount of computing power and modeling expertise is required.

Future work on the turbocharged engine would necessarily include the work described above. In addition, research should be directed towards providing the proper SPR across the entire engine speed range. This could be accomplished in any number of ways. One solution might include an external waste-gate in the exhaust pipe and a blow-off valve in the intake system. The valves could be electronically controlled to release pressure based on a logic program that attempted to maintain an optimum SPR. Additionally, the variable turbine vanes could be electronically operated to provide more precise control over the position of the vanes based on actual operating conditions. To improve the low speed power of the engine a smaller volume exhaust pipe could be used to provide more energy to the turbine to increase boost more quickly.

Before any of the above research can be conducted and be expected to have meaningful results, better testing equipment will be needed. The current dynamometer will

not work. A dynamometer with a faster response and better load control will significantly reduce fuel mapping time and increase productivity for experimental testing. Specifically, an electric dynamometer should be purchased. The current fuel-flow meter does not provide the accuracy required for the precise measurements needed for this research, especially during light-load operation. Additionally, the fuel meter does not offer a useful method to record streaming data. A fuel meter that is compensated for fuel temperature and density with an accuracy greater than +/- 2 percent of full scale is necessary to meet the EPA testing standards [8]. Finally, an emission analyzer capable of sustained measurements of UHC and CO concentrations typical of carbureted two-stroke engines and untuned engines is needed. The analyzer should be calibrated to measure UHC as methane with an accuracy similar to FID measurements, which provide better accuracy for emission calculations and specifically trapped AFR [51]. The addition of testing equipment that meet the needs of the specialized testing requirements of GDI two-stroke engines, engine development will occur quicker with better results.

BIBLIOGRAPHY:

1. www.montanadeq.org, 2006.

2. 66 Fed.Reg. 7,260 (Jan. 22, 2001).

3. 68 Fed.Reg. 69,268 (Dec. 11, 2003).

4. The Fund for Animals, *et al.* v. Norton, *et al.*, 294 F.Supp.2d 92 (D.D.C. 2003).

5. Int'l Snowmobile Mfrs. Ass'n, *et al.*, v. Gale Norton, *et al.*, 304 F.Supp.2d 1278 (D.Wyo. 2004).

6. Int'l Snowmobile Mfrs. Ass'n, *et al.*, v. Gale Norton, *et al.*, 340 F.Supp.2d 1249 (D.Wyo. 2004).

7. 69 Fed.Reg. 65,348 (Nov. 10, 2004).

8. 40 C.F.R. §§ 1051, 1065 (2006).

9. Wyo. Lodging & Rest. Ass'n v. U.S. Dep't of the Interior, 398 F.Supp.2d 1197, 1222 (D.Wyo. 2005).

10. Lela C.C., White J.J., "Laboratory Testing of Snowmobile Emissions," Report Number SwRI 08.05486, Southwest Research Institute, San Antonio, July, 2002.

11. Wright, C.W., White J.J., "Development and Validation of a Snowmobile Engine Emission Test Procedure," SAE 982017, Milwaukee, Wisconsin Sept. 1998.

12. www.nps.org, "Winter Use Background Information," National Parks Service, U.S. Department of the Interior, June 2005.

13. Haines, H., Montana Department of Environmental Quality, Personal Correspondence, Feb. 01, 2006.

14. Society of Automotive Engineers, Inc., The SAE Clean Snowmobile Challenge Rules 2005, (www.sae.org/competitions/snow), May 8, 2006.

15. Society of Automotive Engineers, Inc., The SAE Clean Snowmobile Challenge Rules 2006, (www.sae.org/competitions/snow), May 8, 2006.

16. Stone, R., *Introduction to Internal Combustion Engines*. Antony Rowe Ltd. Chippenham, Wiltshire, 1997.

17. Blair G.P. *Design and Simulation of Two-Stroke Engines*. Society of Automotive Engineers, Inc. Warrendale, Pa, 1996.

18. Heywood J.B., *Internal Combustion Engine Fundamentals.* McGraw Hill, Inc. 1988.

19. Bradbury N., French F., DenBraven K., "Improving the University of Idaho Snowmobile," SAE 03-SETC-87, 2003.

20. Nuti, M., *Emissions from Two-Stroke Engines*. SAE International, Warrendale, Pa. 1998.

21. Strauss, S., Zeng, Y., Montgomery, D., "Optimization of the E-TEC™ Combustion System for Direct-Injection Two-Stroke Engines Toward 3-Star Emissions," SAE 2003-32-0007/20034307, 2003.

22. Wasil, J. R., Montgomery, D. T., Strauss, S., "Life Assesment of PM, Gaseous Emissions, and Oil Usage in Modern Marine Outboard Engines," SAE 20044379, SETC Graz, Austria 2004.

23. Society of Automotive Engineers, Inc., The SAE Clean Snowmobile Challenge Results 2003, (www.sae.org/competitions/snow), May 8, 2006.

24. Society of Automotive Engineers, Inc., The SAE Clean Snowmobile Challenge Results 2004, (www.sae.org/competitions/snow), May 8, 2006.

25. Society of Automotive Engineers, Inc., The SAE Clean Snowmobile Challenge Results 2005, (www.sae.org/competitions/snow), May 8, 2006.

26. Information was found at each manufacturers web page, Spring 2006.

27. HowStuffWorks, Inc., "How Car Engines Work," http://www.howstuffworks.com/engine.htm, May 8, 2006.

28. Auth, P., Millhorn, S., Beeler, Z., and Den Braven, K., "Making the Connection: the University of Idaho Clean Snowmobile," SAE 2001-01-3657, Sept. 2001.

29. Auth, P., Chin, M., Hess, P., "Refining the University of Idaho Clean Snowmobile," SAE 2002-01-2756, 2002.

30. Beach, N., et al. "University of Idaho's Clean Snowmobile Design Using a Direct-Injection Two-Stroke with Exhaust After Treatment," Not Published.

31. Bradbury, N., Schiermeier R., Harris, T., "University of Idaho's Clean Snowmobile Design Using a Direct-Injection Two-Stoke," SAE 2005-01-3680, 2005.

32. Heywood, J. B., Sher, E., *The Two-Stroke Cycle Engine, Its Development, Operation, and Design*. SAE Inc., Warrendale, Pa. 1999.

33. Bradbury, N., et al. "University of Idaho's Clean Snowmobile Design Using a Direct-Injection Two-Stroke," SAE   2006, not yet published.

34. National Parks Service, Yellowstone National Park "Snowmobiles Meeting Yellowstone and Grand Teton National Parks' Best Available Technology (BAT) Requirements," February 18, 2005, www.NPS.org

35. Strauss, S., Zeng, Y., "The Effect of Fuel Spray Momentum of Performance and Emissions of Direct-Injected Two-Stroke Engines," SAE 2004-32-0013, 2004.

36. Zhao, F., Harrington, D., Lai, M., *Automotive Gasoline Direct-Injection Engines*. SAE Inc. Warrendale, Pa. 2002.

37. Morikawa K., Takimoto H., Ogi T., "A Study of Direct Fuel Injection Two-Stroke Engine for High Specific Power Output and High Engine Speed," SAE 1999-01-3288 / JSAE 9938043, 1999.

38. Johnson, D., Wong, H., "Electronic Direct Fuel Injection System Applied to an 1100 cc Two-Stroke Personal Watercraft Engine," SAE 980756, 1998.

39. French, M., "Power Generation System for Direct Injected Engines Capable of Starting the Engine without a Battery," SAE 04SETC-76, 2004.

40. Auth P.S., "Determining Hybrid Electric Snowmobile Feasibility Through Simulation," M.S. Thesis, University of Idaho, 2002.

41. Kenewah Research Center, www.mtu.krc.org.

42. Ehrlich, D. "Characterization of Unsteady On-Engine Turbocharger Turbine Performance," Ph.D. Dissertation, Purdue University, December 1998.

43. Xiao, H., "An Advanced Turbocharger Model for the Internal Combustion Engine," Ph.D. Dissertation, Purdue University, August 2000.

44. Ogink, R., "Determination of the On-Engine Performance of an Automotive Turbocharger", Royal Institute of Technology, Internal Combustion Engines Masters of Science Thesis, Stockholm 2000.

45. Bell, A., *Forced Induction Performance Tuning, a Practical Guide to Supercharging and Turbocharging*. Hayes Publishing, Sparkford, UK, 2002.

46. MacInnes, H., *Turbochargers*. HP Books, Berkley Publishing Group, NY. NY, 1984.

47. Watson, N., Janota, M.S., *Turbocharging the Internal Combustion Engine*. Macmillan, New York, 1982.

48. Steve Packer, Manufacturer of Aerocharger Turbochargers, Personal Correspondence, 2005.

49. Freescale Semiconductor, Inc., www.freescale.com/webapp/search/OPSERP.jsp, May 8, 2006.

50. Patzelt, B., Gage Fuels, Personal Correspondence, Nov. 10, 2005.

51. Douglas, R., "AFR and Emissions Calculations for Two-Stroke Cycle Engines," SAE 901599, 1990.

52. Xu, R., "A Convenient Technique for Determining Two-Stroke Emission Measurement Accuracy and A/F Ratio," SAE 961804, 1996.

53. French, F., "Design, Construction, Testing, and Evaluation of a Parallel Hybrid Electric Snowmobile Power Plant," M.S. Thesis, University of Idaho, 2004.

54. Strauss S., Zeng Y., "The Effect of Fuel Spray Momentum on Performance and Emissions of Direct-Injected Two-Stroke Engines," SAE 2004-32-0013 / JSAE 20044300, 2004.

APPENDICES

Appendix A: ENGINE PARAMETERS

Engine geometry and calcualted compresion ratios for the stock, naturally aspirated, and trubocahrged engines (i = 0, 1, 2 respectively).

Geometry of the engines: $i := 0 .. 2$

Number of Cylinders	$n := 2$		
Bore	$d_{bo} := 77.24\,mm$	Chamber Inner Diam	$d_b := 24.77\,mm$
Stroke	$L_{st} := 64\,mm$	Connecting Rod Length	$L_{cr} := 124\,mm$
Exhaust Port Opens	$\theta_{ex} := 102\,deg$	Throw of the Crank	$L_{ct} := .5 \cdot L_{st}$
Intake Port Opens	$\theta_{in} := 120\,deg$		

Clearence Volume $\quad V_{cv} := \begin{pmatrix} 36.22 \\ 32.98 \\ 40.61 \end{pmatrix} cm^3 \qquad$ Squish Volume $\qquad V_{squish} := \begin{pmatrix} 5.24 \\ 7.43 \\ 6.86 \end{pmatrix} cm^3$

Calculations:

Area of the piston $\qquad A_p := \pi \cdot \left(\dfrac{d_{bo}}{2} \right)^2$

Trapped Stroke $\qquad L_{ts} := L_{cr} + L_{ct} \cdot \left(1 - \cos(\theta_{ex}) \right) - \sqrt{L_{cr}^2 - \left(L_{ct} \cdot \sin(\theta_{ex}) \right)^2}$

Total Swept Volume $\qquad V_{sv} := n \cdot \left(\dfrac{\pi}{4} \right) \cdot d_{bo}^2 \cdot L_{st}$

Trapped Swept Volume $\qquad V_{ts} := n \cdot \left(\dfrac{\pi}{4} \right) \cdot d_{bo}^2 \cdot L_{ts}$

Geometric compression ratio $\qquad CR_{g_i} := \dfrac{\left(V_{sv} \cdot \dfrac{1}{n} + V_{cv_i} \right)}{V_{cv_i}}$

Trapped compresion ratio $\qquad CR_{t_i} := \dfrac{\left(V_{ts} \cdot \dfrac{1}{n} + V_{cv_i} \right)}{V_{cv_i}}$

$V_{ts} = 399.866\,cm^3 \qquad V_{sv} = 599.77\,cm^3$

$CR_g = \begin{pmatrix} 9.28 \\ 10.093 \\ 8.385 \end{pmatrix} \qquad CR_t = \begin{pmatrix} 6.52 \\ 7.062 \\ 5.923 \end{pmatrix} \qquad$ Stock compression ratios
Naturally aspirated GDI compression ratios
Turbocharged GDI compression ratios

Appendix B: CALCULATIONS FOR SIZING TURBOCHARGER COMPRESSORS

Procedure for turbocharger compressor sizing and estimating engine performce

$disp := 600cm^3$ — Engine Displacement

$Press_{Amb} := .946atm$ — Ambient atmospheric pressure

$Temp_{Amb} := 283K$ — Ambient air temperature

$R := 0.286 \dfrac{J}{gm \cdot K}$ — Ideal Gas Constant

$i := 0..6$

Stock engine measured and calcualted parameters:

$Pwr_s := 112hp$ $\qquad rpm_s := 8000 \cdot \dfrac{1}{min}$ $\qquad MaxTorque_s := 73.53ft \cdot lbf$

$Torque_s := \dfrac{Pwr_s}{2 \cdot \pi \cdot rpm_s}$

$Max_{eff} := .9$

$Vol_{eff} := \dfrac{Torque_s \cdot Max_{eff}}{MaxTorque_s}$

$CFM_s := rpm_s \cdot disp \cdot Vol_{eff}$

$Vol_{eff} = 0.9$ $\qquad CFM_s = 152.558 \dfrac{ft^3}{min}$

Desired Engine Performance and Turbocharger Flow Calculations:

$Pwr_d := 160hp$ — Choose desired power output at engine operating conditions

$DR_{req} := \dfrac{Pwr_d}{Pwr_s}$ — Calculate density ratio that provides the fraction of increase in the delivered mass of air to meet power increase

$DR_{req} = 1.429$

$Boost := 9.7psi$ — Estimate the boost that will provide the actual density ratio (DR_{del}) similar to the required density ratio. Itterations are required.

$Comp_{eff} := .75$ — Compressor efficiency is found from compressor map at calculated PR (PR) and compressor flows ($Comp_{flow}$). Itterations are required until estimated power matches desired power.

Appendix B: CALCULATIONS FOR SIZING TURBOCHARGER COMPRESSORS

Turbocharger Flow Calculations (continued): $n := 0.238$

$$PR := \frac{Boost + Press_{Amb}}{Press_{Amb}}$$

$PR = 1.698$

Calculated pressure ratio that will occur across the compressor to meet the estimated boost.

$$f := \left(PR^n\right) - 1$$

$f = 0.134$

Factor for calculating the temperature rise from a compressor

$$Temp_{rise} := \frac{f \cdot Temp_{Amb}}{Comp_{eff}}$$

$Temp_{rise} = 50.657 \, K$

Intake temperture rise due to the compression of the intake air

$$Comp_{temp} := Temp_{rise} + Temp_{Amb}$$

$Comp_{temp} = 333.657 \, K$

Calculated compressor discharge temperature

$$DR_{del} := \frac{Temp_{Amb}}{Comp_{temp}} \cdot \frac{Press_{Amb} + Boost}{Press_{Amb}}$$

$DR_{del} = 1.44$

Density ratio that the compressor actually delivers under the given conditions

$$Pwr_{est} := Pwr_s \cdot DR_{del}$$

$$Comp_{flow} := CFM_s \cdot DR_{del}$$

$Pwr_d = 160 \, hp$

$Pwr_{est} = 161.277 \, hp$

Boost and Compressor efficiency inputs should be changed until the estimated power is close to the desired power output.

$$Comp_{flow} = 219.68 \, \frac{ft^3}{min}$$

Once a satisfactory estimated power is calculated, the compressor inlet flow is known. PR, and CFM can be plotted on compressor maps for compressor sizing.

Appendix B: CALCULATIONS FOR SIZING TURBOCHARGER COMPRESSORS

Sample compressor sizing and engine performance calculations used for choosing the Aerocherger 53 series with the 128 housing.

$$disp := 600cm^3 \quad Press_{Amb} := .946atm$$

$$R := 0.286 \frac{J}{gm \cdot K} \quad Temp_{Amb} := 283K$$

Stock engine measured and calcualted parameters: $i := 0..6$

$$rpm_s := \begin{pmatrix} 5000 \\ 5500 \\ 6000 \\ 6500 \\ 7000 \\ 7500 \\ 8000 \end{pmatrix} \cdot \frac{1}{min} \quad Pwr_s := \begin{pmatrix} 43 \\ 48 \\ 57 \\ 73 \\ 91 \\ 102 \\ 112 \end{pmatrix} \cdot hp$$

Stock engine performance

$$Max_{eff} := .9$$

$$Torque_{s_i} := \frac{Pwr_{s_i}}{2 \cdot \pi \cdot rpm_{s_i}}$$

$$Vol_{eff_i} := \frac{Torque_{s_i} \cdot Max_{eff}}{Torque_{s_6}}$$

$$CFM_{s_i} := rpm_{s_i} \cdot disp \cdot Vol_{eff_i}$$

$$Torque_s = \begin{pmatrix} 45.168 \\ 45.837 \\ 49.895 \\ 58.985 \\ 68.277 \\ 71.429 \\ 73.53 \end{pmatrix} ft \cdot lbf \quad Vol_{eff} = \begin{pmatrix} 0.553 \\ 0.561 \\ 0.611 \\ 0.722 \\ 0.836 \\ 0.874 \\ 0.9 \end{pmatrix} \quad CFM_s = \begin{pmatrix} 58.572 \\ 65.383 \\ 77.642 \\ 99.436 \\ 123.954 \\ 138.938 \\ 152.559 \end{pmatrix} \frac{ft^3}{min}$$

Appendix B: CALCULATIONS FOR SIZING TURBOCHARGER COMPRESSORS

Sample compressor sizing and engine performance calculations used for choosing the Aerocherger 53 series with the 128 housing (continued).

$n := 0.238$

Desired Performance:

$$Pwr_d := \begin{pmatrix} 48 \\ 55 \\ 67 \\ 91 \\ 119 \\ 138 \\ 160 \end{pmatrix} hp \qquad Boost_{req} := \begin{pmatrix} 2.7 \\ 3.2 \\ 3.8 \\ 5.3 \\ 7.0 \\ 8.0 \\ 9.7 \end{pmatrix} psi \qquad Comp_{eff} := \begin{pmatrix} .64 \\ .70 \\ .73 \\ .75 \\ .75 \\ .75 \\ .75 \end{pmatrix}$$

$$DR_{req_i} := \frac{Pwr_{d_i}}{Pwr_{s_i}}$$

$$PR_{req_i} := \frac{Boost_{req_i} + Press_{Amb}}{Press_{Amb}}$$

$$\gamma_i := \left(PR_{req}^{\,n}\right)_i - 1$$

$$Temp_{rise_i} := \frac{\gamma_i \cdot Temp_{Amb}}{Comp_{eff_i}}$$

$$Comp_{temp} := Temp_{rise} + Temp_{Amb}$$

$$DR_{del_i} := \frac{Temp_{Amb}}{Comp_{temp_i}} \cdot \frac{Press_{Amb} + Boost_{req_i}}{Press_{Amb}}$$

$$Pwr_{est_i} := Pwr_{s_i} \cdot DR_{del_i} \qquad Comp_{flow_i} := CFM_{s_i} \cdot DR_{del_i}$$

$$Pwr_d = \begin{pmatrix} 48 \\ 55 \\ 67 \\ 91 \\ 119 \\ 138 \\ 160 \end{pmatrix} hp \quad Pwr_{est} = \begin{pmatrix} 48.108 \\ 55.072 \\ 67.136 \\ 91.122 \\ 120.451 \\ 139.452 \\ 161.277 \end{pmatrix} hp \quad PR_{req} = \begin{pmatrix} 1.194 \\ 1.23 \\ 1.273 \\ 1.381 \\ 1.504 \\ 1.575 \\ 1.698 \end{pmatrix} \quad Comp_{flow} = \begin{pmatrix} 65.529 \\ 75.016 \\ 91.448 \\ 124.121 \\ 164.07 \\ 189.953 \\ 219.681 \end{pmatrix} \frac{ft^3}{min}$$

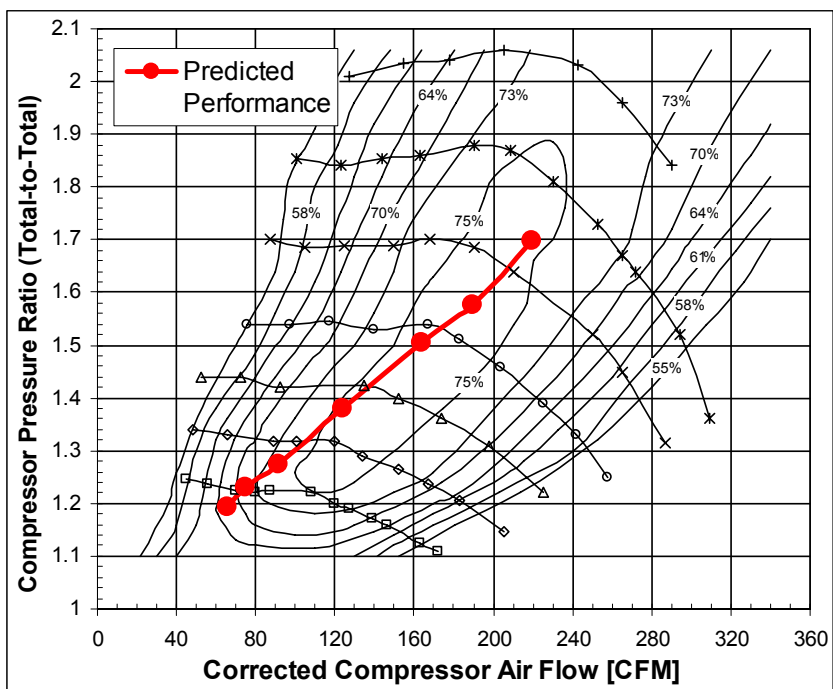**Appendix B: PREDICTED COMPRESSOR PERFORMANCE PLOTS**

Figure X: Compressor map for the 53 series Aerocharger VNT with the 128 housing used for the UI GDI turbocharged engine. Predicted engine performance is plotted.
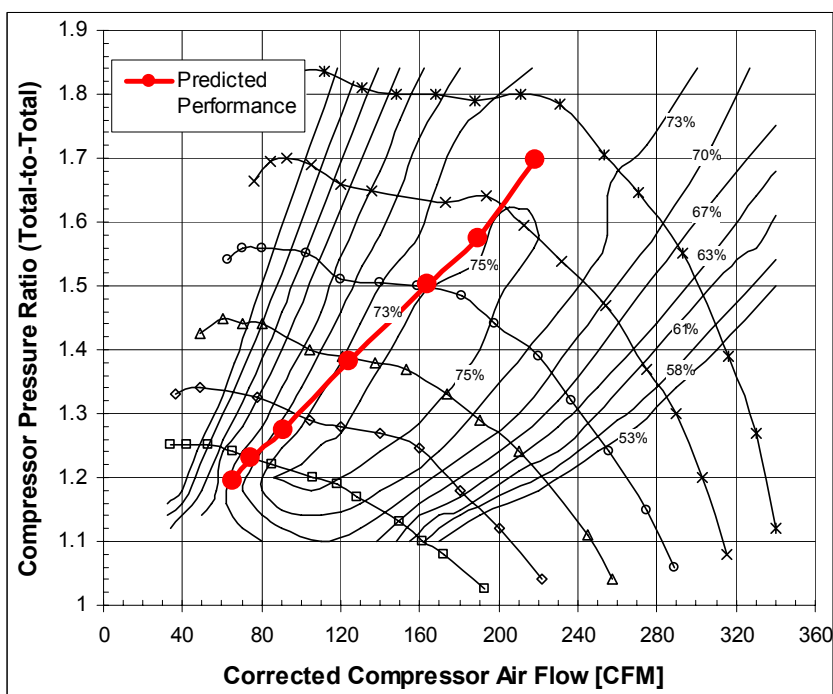

Figure X: Compressor map for a Aerocharger 53 series VNT with the 143 housing used for sizing. Predicted UI GDI turbocharged engine performance is plotted.
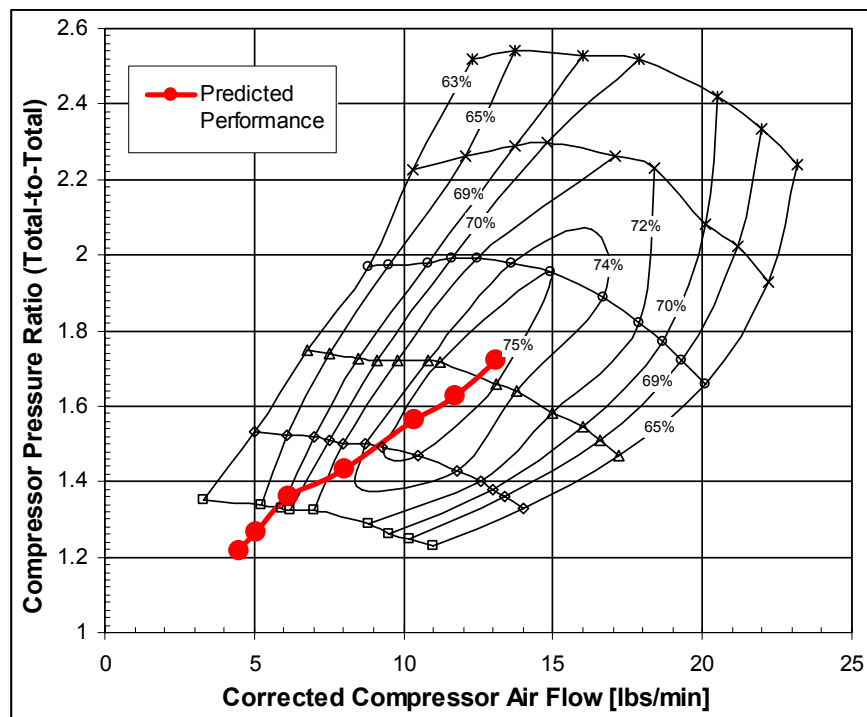
Appendix B: PREDICTED COMPRESSOR PERFORMANCE PLOTS

Figure X: Compressor map for a Garrett GT 15, 60 trim with a 0.43 AR used for sizing. Predicted UI GDI turbocharged engine performance is plotted.
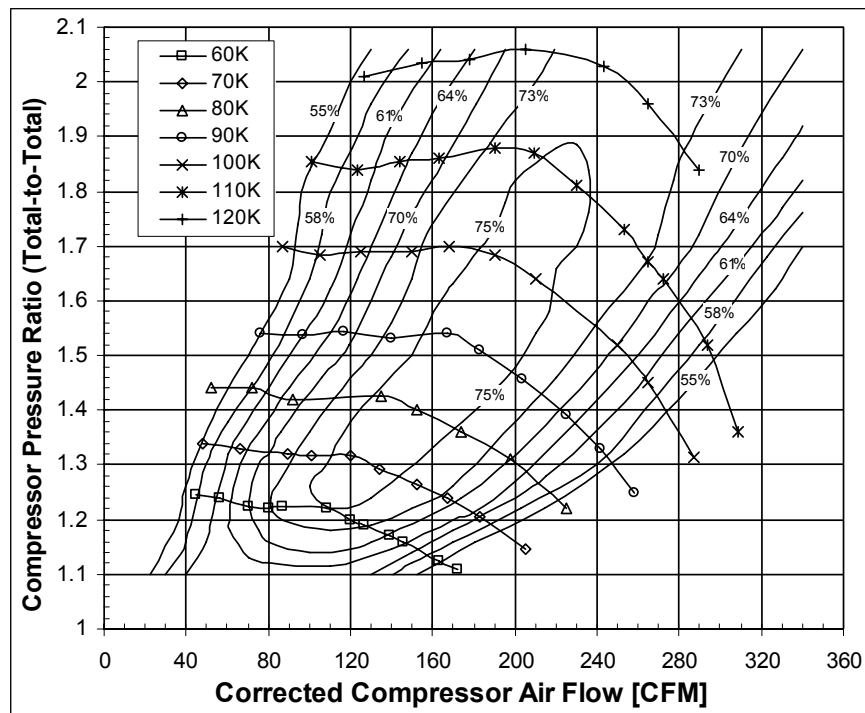
Appendix C: TURBOCHARGER COMPRESSOR MAPS

Figure X: Compressor map for the 53 series Aerocharger with the 128 housing used for the UI GDI turbocharged engine.

Appendix D: FIVE-MODE EMISSIONS AND AFR CALCULATIONS

Raw emissions calculations used for the five-mode emissions testing procedure. Calculations from EPA 40 CFR Sec. 91.419 part (c) fuel flow method for calculating mass emissions. Sample data is from mode 1 of the 2005 SAE CSC control snowmobile.

Measured Parameters: **Where:**

$rpm := 7951 \cdot \dfrac{1}{min}$ rpm = Average measured engine speed during mode i

$Torque := 106.2 N \cdot m$ Torque = Average measured torque during mode i

$G_{fuel} := 37743.49 \dfrac{gm}{hr}$ G_{fuel} = Fuel mass flow rate, [g/hr]

$HC_{wet} := 38868.889$ HC_{wet} = Average volume concentration, ppmC_1 wet (ppm Methane CH_4)

$CO_{dry} := 6.604889$ CO_{dry} = Average percent concentration in exhaust, dry

$CO_{2dry} := 7.6326667$ CO_{2dry} = Average percent concentration in exhaust, dry

$NO_{xwet} := 370.3333$ NO_{xwet} = Average volume concentration in exhaust, ppm wet

$O_{2dry} := 4.297778$ O_2 = Average percent concentration in exhaust, dry

$\alpha := 1.92$ α = Hydrogen/carbon molar ratio of the fuel

Calculated Parameters: **Where:**

$K_H := 1$ K_H = Factor for correcting the effects of humidity on NO_2 formation for four-stroke engines; it should be set to 1 for two-stroke engines.

$M_F := 12.01 + 1.008 \cdot \alpha$ M_F = Molecualr weight of test fuel

$P_{wr} := 2 \cdot \pi \cdot Torque \cdot rpm$ P_{wr} = Average power measured during mode i, [kW]

$H_{2dry} := \dfrac{0.5 \cdot \alpha \cdot CO_{dry} \cdot (CO_{dry} + CO_{2dry})}{CO_{dry} + (3 \cdot CO_{2dry})}$ H_{2dry} = Calculated percent H_2 in exhaust, dry

$K := \dfrac{1}{1 + 0.005 \cdot (CO_{dry} + CO_{2dry}) \cdot \alpha - .01 \cdot H_{2dry}}$ K = Correction factor to convert from dry to wet measurements, wet = dry * K

$CO_{wet} := CO_{dry} \cdot K$

$CO_{2wet} := CO_{2dry} \cdot K$ Dry measured emissions converted to wet using the correction factor "K"

$O_{2wet} := O_{2dry} \cdot K$

$HC_{dry} := \dfrac{HC_{wet}}{K}$ $NO_{xdry} := \dfrac{NO_{xwet}}{K}$ Wet measured emissions converted to dry emissions using the correction factor "K"

$TC := CO_{wet} + CO_{2wet} + \dfrac{HC_{wet}}{10^4}$ TC = Average total wet carbon in exhaust

$M_{CO} := 28.01$ M_{CO} = Molecular weight of CO = 28.01

$M_{NO2} := 46.01$ M_{NO2} = Molecular weight of NO_2 = 46.01

Raw emissions calculations used for the five-mode emissions testing procedure. Calculations from EPA 40 CFR Sec. 91.419 part (c) fuel flow method for calculating mass emissions (Continued).

Calculated Parameters:

Where:

$$W_{HC} := \frac{G_{fuel}}{TC} \cdot \frac{HC_{wet}}{10^4}$$

W_{HC} = Mass rate of HC in exhaust, [gm/hr]

$$W_{CO} := \frac{M_{CO}}{M_F} \cdot \frac{G_{fuel}}{TC} \cdot CO_{wet}$$

W_{CO} = Mass rate of CO in exhaust, [gm/hr]

$$W_{NOx} := \frac{M_{NO2}}{M_F} \cdot \frac{G_{fuel}}{TC} \cdot \frac{NO_{xwet}}{10^4} \cdot K_H$$

W_{NOx} = Mass rate of NO_x in exhaust, [gm/hr]

$$W_{HC} = 8.754 \times 10^3 \frac{gm}{hr}$$

$$W_{CO} = 2.701 \times 10^4 \frac{gm}{hr}$$

$$W_{NOx} = 275.176 \frac{gm}{hr}$$

$$W_{HCspec} := \frac{W_{HC}}{P_{wr}}$$

W_{HCspec} = brake-specific HC emissions, [gm/kW-hr]

$$W_{COspec} := \frac{W_{CO}}{P_{wr}}$$

W_{COspec} = brake-specific CO emissions, [gm/kW-hr]

$$W_{NOxspec} := \frac{W_{NOx}}{P_{wr}}$$

$W_{NOxspec}$ = brake-specific NO_x emissions, [gm/kW-hr]

$$W_{HCspec} = 98.997 \frac{gm}{kW \cdot hr}$$

$$W_{COspec} = 305.479 \frac{gm}{kW \cdot hr}$$

$$W_{NOxspec} = 3.112 \frac{gm}{kW \cdot hr}$$

Accuracy check for emissions measurements. Derived from:

Douglas, R., Queens University Belfast, "AFR and Emissions Calculations for Two-Stroke Cycle Engines," New Developments in Two Stroke Engines and Their Emissions, SAE Paper 901599, 1990.

$$HC_{\%dry} := \frac{HC_{dry}}{10^4}$$

Converting volume concontrations to percentages to simplify the following equations

$$NO_{x\%dry} := \frac{NO_{xdry}}{10^4}$$

$$TC_{dry} := CO_{dry} + CO_{2dry} + HC_{\%dry}$$

TC = Average total dry carbon in exhaust

$$M_t := \frac{100}{TC_{dry}}$$

M_t = Total moles of exhaust gasses

$$a := \frac{CO_{dry}}{TC_{dry}} \qquad b := \frac{CO_{2dry}}{TC_{dry}}$$

$$c := \frac{O_{2dry}}{TC_{dry}} \qquad h := \frac{NO_{x\%dry}}{TC_{dry}}$$

Molar quantities used in balancing the chemical equation for the combustion of a hydrocarbon fuel.

$$A_m := \frac{a}{4} + b + c + \frac{\alpha}{4} \cdot (a + b) + \frac{h}{2}$$

Quantity of "air" used for the combustion of a hydrocarbon fuel.

$$N_{2dry} := 3.727 \cdot A_m \cdot \left(CO_{dry} + CO_{2dry} + HC_{\%dry} \right)$$

Percent dry N_2 in the exhaust

$$Ar_{dry} := .044 \cdot A_m \cdot \left(CO_{dry} + CO_{2dry} + HC_{\%dry} \right)$$

Percent dry Ar in the exhaust

$$Total := CO_{dry} + CO_{2dry} + O_{2dry} + HC_{\%dry} + H_{2dry} + N_{2dry} + NO_{x\%dry} + Ar_{dry}$$

Total exhaust gasses

Total = 103

Percentages of all the constituents in the dried exhaust should add up to 100%. Deviation from 100% indicates errors in emissions measurements.

Calculated Global and Burnzone AFR from raw gas emissions, adapted from:

Douglas, R., Queens University Belfast, "AFR and Emissions Calculations for Two-Stroke Cycle Engines," New Developments in Two Stroke Engines and Their Emissions, SAE Paper 901599, 1990.

Note: Trapping Efficiency (TE) for the fuel and air must be calculated using a carburated (calibrated rich) engine with no after-burn.

$$K_f := \frac{138.18}{12.011 + 1.008 \cdot \alpha}$$ K_f is a constant value given by Douglas

$$AFR_{global} := K_f \cdot \left[\frac{.25 \cdot CO_{dry} + CO_{2dry} + O_{2dry} + .25 \cdot \alpha \cdot (CO_{dry} + CO_{2dry}) + .5 \cdot NO_{x\%dry}}{TC_{dry}} \right]$$

$AFR_{global} = 10.923$ Over-all AFR

$K := 3.5$ K = Water-gas equilibrium constant.
Ranges from 3.25 - 3.8.

$$K_w := \frac{K \cdot CO_{2dry}}{CO_{dry} + K \cdot CO_{2dry}}$$

$$TE_{airrich} := \frac{.5 \cdot CO_{dry} + CO_{2dry} + .25 \cdot K_w \cdot \alpha \cdot (CO_{dry} + CO_{2dry}) + .5 \cdot NO_{x\%dry}}{.5 \cdot CO_{dry} + CO_{2dry} + O_{2dry} + .25 \cdot K_w \cdot \alpha \cdot (CO_{dry} + CO_{2dry}) + .5 \cdot NO_{x\%dry}}$$

$$TE_{fuel} := \frac{CO_{dry} + CO_{2dry}}{TC_{dry}}$$

$TE_{airrich} = 0.793$ Air trapping efficiency

$TE_{fuel} = 0.768$ Fuel trapping efficiency

$$AFR_{burningzone} := AFR_{global} \cdot \frac{TE_{airrich}}{TE_{fuel}}$$

$AFR_{burningzone} = 11.274$

$AFR_{burningzone}$ is the AFR of the trapped charge. Comparing the overal AFR to the burning zone AFR gives an idea of the amount of charge stratification.

Calculating equivalence ratio (ϕ) and relative AFR ratio (λ)

$M_{O2} := 31.999$ $M_{N2} := 28.013$ $M_C := 12.01$ $M_H := 1.008$

$$AFR_{stoich} := \frac{\left(1 + \frac{A_m}{4}\right) \cdot (M_{O2} + 3.72 \cdot M_{N2})}{M_C + \alpha \cdot M_H}$$

AFR_{stoich}: The stoichiometric AFR for perfect combustion from: Blair, G.P., "Design and Simulation of Two-Stroke Engines," Society of Automotive Engineers, Inc. Warrendale, Pa. 1996.

$AFR_{stoich} = 12.459$

$$\lambda := \frac{AFR_{burningzone}}{AFR_{stoich}}$$ $$\phi := \frac{AFR_{burningzone}^{-1}}{AFR_{stoich}^{-1}}$$

$\lambda = 0.905$ $\phi = 1.105$

Example of an EPA 5-mode overall score sheet, accuracy measurements, AFR, and equivelence ratio calculations. Data used in the calculations is from the 2005 SEA CSC control snowmobile, a 2005 Ski-Doo 600cc SDI two-stroke [www.mtukrc.org]. The calculations follow the procedures described above.

Measured Parameters:

$i := 1..5$

$$rpm := \begin{pmatrix} 7951 \\ 6751 \\ 5943 \\ 5153 \\ 1675 \end{pmatrix} \cdot \frac{1}{min} \quad Torque := \begin{pmatrix} 106.2 \\ 55.32 \\ 37.74 \\ 26.67 \\ 0 \end{pmatrix} N \cdot m \quad G_{fuel} := \begin{pmatrix} 37743.49 \\ 12884.39 \\ 7336.516 \\ 5088.168 \\ 1174 \end{pmatrix} \frac{gm}{hr} \quad Weight := \begin{pmatrix} .12 \\ .27 \\ .25 \\ .31 \\ .05 \end{pmatrix}$$

$M_{NO2} := 46.01$

$M_{CO} := 28.01$

$$HC_{wet} := \begin{pmatrix} 38868.889 \\ 17173.333 \\ 15791.803 \\ 28967.241 \\ 57500 \end{pmatrix} \quad CO_{dry} := \begin{pmatrix} 6.604889 \\ 5.695333 \\ 2.379508 \\ 2.967586 \\ 3.147869 \end{pmatrix} \quad CO_{2dry} := \begin{pmatrix} 7.6326667 \\ 9.2536667 \\ 11.186885 \\ 9.8325862 \\ 4.5916393 \end{pmatrix} \quad NO_{xdry} := \begin{pmatrix} 370.333 \\ 451.55 \\ 408.1803 \\ 123.0414 \\ 22.38525 \end{pmatrix} \quad O_{2dry} := \begin{pmatrix} 4.297778 \\ 3.832333 \\ 3.936393 \\ 5.445 \\ 12.04426 \end{pmatrix}$$

Calculated Parameters:

$\alpha := 1.92 \quad K_H := 1 \quad M_F := 12.01 + 1.008 \cdot \alpha$

$P_{wr_i} := Torque_i \cdot rpm_i \cdot 2 \cdot \pi$

$$H_{2dry_i} := \frac{0.5 \cdot \alpha \cdot CO_{dry_i} \cdot \left(CO_{dry_i} + CO_{2dry_i}\right)}{CO_{dry_i} + \left(3 \cdot CO_{2dry_i}\right)} \qquad K_i := \frac{1}{1 + 0.005 \cdot \left(CO_{dry_i} + CO_{2dry_i}\right) \cdot \alpha - .01 \cdot H_{2dry_i}}$$

$CO_{wet_i} := CO_{dry_i} \cdot K_i \qquad\qquad O_{2wet_i} := O_{2dry_i} \cdot K_i$

$CO_{2wet_i} := CO_{2dry_i} \cdot K_i \qquad\qquad NO_{xwet_i} := NO_{xdry_i} \cdot K_i$

$$TC_i := CO_{wet_i} + CO_{2wet_i} + \frac{HC_{wet_i}}{10^4}$$

$$W_{HC_i} := \frac{G_{fuel_i}}{TC_i} \cdot \frac{HC_{wet_i}}{10^4} \qquad W_{CO_i} := \frac{M_{CO}}{M_F} \cdot \frac{G_{fuel_i}}{TC_i} \cdot CO_{wet_i} \qquad W_{NOx_i} := \frac{M_{NO2}}{M_F} \cdot \frac{G_{fuel_i}}{TC_i} \cdot \frac{NO_{xwet_i}}{10^4} \cdot K_H$$

Mass Emissions for each mode

$$W_{HC} = \begin{pmatrix} 8.754 \times 10^3 \\ 1.468 \times 10^3 \\ 847.241 \\ 1.023 \times 10^3 \\ 517.354 \end{pmatrix} \frac{gm}{hr} \quad W_{CO} = \begin{pmatrix} 2.701 \times 10^4 \\ 8.736 \times 10^3 \\ 2.286 \times 10^3 \\ 1.893 \times 10^3 \\ 536.436 \end{pmatrix} \frac{gm}{hr} \quad W_{NOx} = \begin{pmatrix} 248.784 \\ 113.777 \\ 64.418 \\ 12.893 \\ 0.627 \end{pmatrix} \frac{gm}{hr} \quad P_{wr} = \begin{pmatrix} 88.425 \\ 39.109 \\ 23.487 \\ 14.392 \\ 0 \end{pmatrix} kW$$

Weighted Emissions Calculations and EPA Score

$$Pwr_{weight_i} := Weight_i \cdot Pwr_i$$

$$W_{HCweight_i} := Weight_i \cdot W_{HC_i} \qquad W_{NOxweight_i} := Weight_i \cdot W_{NOx_i} \qquad W_{COweight_i} := Weight_i \cdot W_{CO_i}$$

$$Pwr_{weighted\_average} := \sum_{i=1}^{5} Pwr_{weight_i}$$

Weighted average of power for all five modes

$$HC_{weighted\_averaged} := \sum_{i=1}^{5} W_{HCweight_i}$$

Weighted average of HC emissions for all five modes

$$NOx_{weighted\_averaged} := \sum_{i=1}^{5} W_{NOxweight_i}$$

Weighted average of NO_x emissions for all five modes

$$CO_{weighted\_average} := \sum_{i=1}^{5} W_{COweight_i}$$

Weighted average of CO emissions for all five modes

$$HCNOx_{weighted\_average} := HC_{weighted\_averaged} + NOx_{weighted\_averaged}$$

Weighted average of HC+NO_x for all five modes

$$HCNOx_{spec} := \frac{HCNOx_{weighted\_average}}{Pwr_{weighted\_average}}$$

Brake-Specific HC+NO_x weighted average emissions

$$CO_{spec} := \frac{CO_{weighted\_average}}{Pwr_{weighted\_average}}$$

Brake-Specific CO weighted average emissions

$$CO_{std} := CO_{spec} \cdot \frac{kW \cdot hr}{gm}$$

Conversion to unit-less values for EPA scoring function

$$HCNOx_{std} := HCNOx_{spec} \cdot \frac{kW \cdot hr}{gm}$$

$$EPA_{score} := \left[1 - \frac{(HCNOx_{std}) - 15}{150} \right] \cdot 100 + \left(1 - \frac{CO_{std}}{400} \right) \cdot 100$$

$$EPA_{score} = 112.092$$

Calculations to determine accuracy of emissions measurements

$$K_i := \frac{1}{1 + 0.005\left(CO_{dry_i} + CO2_{dry_i}\right)\cdot\alpha - 0.01\cdot H2_{dry_i}}$$

$$HC_{\%dry_i} := \frac{HC_{wet_i}}{K_i\cdot 10^4} \qquad\qquad NO_{x\%dry_i} := \frac{NO_{xdry_i}}{10^4}$$

$$TC_{dry_i} := CO_{dry_i} + CO2_{dry_i} + HC_{\%dry_i}$$

$$a_i := \frac{CO_{dry_i}}{TC_{dry_i}} \qquad b_i := \frac{CO2_{dry_i}}{TC_{dry_i}} \qquad c_i := \frac{O2_{dry_i}}{TC_{dry_i}} \qquad h_i := \frac{NO_{x\%dry_i}}{TC_{dry_i}}$$

$$A_{m_i} := \frac{a_i}{4} + b_i + c_i + \frac{\alpha}{4}\cdot(a_i + b_i) + \frac{h_i}{2}$$

$$N2_{dry_i} := 3.727\cdot A_{m_i}\cdot\left(CO_{dry_i} + CO2_{dry_i} + HC_{\%dry_i}\right)$$

$$Ar_{dry_i} := .044\cdot A_{m_i}\cdot\left(CO_{dry_i} + CO2_{dry_i} + HC_{\%dry_i}\right)$$

$$Total_i := CO_{dry_i} + CO2_{dry_i} + O2_{dry_i} + HC_{\%dry_i} + H2_{dry_i} + N2_{dry_i} + NO_{x\%dry_i} + Ar_{dry_i}$$

$$Total = \begin{pmatrix} 102.989 \\ 105.052 \\ 104.083 \\ 106.203 \\ 106.981 \end{pmatrix}$$

Brake-Specific emissions and fuel consumption for each mode except idle.

$$j := 1..4$$

$$HC_{spec_j} := \frac{W_{HC_j}}{P_{wr_j}} \qquad CO_{spec_j} := \frac{W_{CO_j}}{P_{wr_j}} \qquad NO_{xspec_j} := \frac{W_{NOx_j}}{P_{wr_j}} \qquad Fuel_{spec_j} := \frac{G_{fuel_j}}{P_{wr_j}}$$

$$HC_{spec} = \begin{pmatrix} 98.997 \\ 37.529 \\ 36.072 \\ 71.065 \end{pmatrix}\frac{gm}{kW\cdot hr} \qquad CO_{spec} = \begin{pmatrix} 305.479 \\ 223.383 \\ 97.334 \\ 131.542 \end{pmatrix}\frac{gm}{kW\cdot hr}$$

$$NO_{xspec} = \begin{pmatrix} 2.814 \\ 2.909 \\ 2.743 \\ 0.896 \end{pmatrix}\frac{gm}{kW\cdot hr} \qquad Fuel_{spec} = \begin{pmatrix} 426.842 \\ 329.447 \\ 312.359 \\ 353.549 \end{pmatrix}\frac{gm}{kW\cdot hr}$$

Global and Burningzone Air/Fuel ratio Calculations

$$K_f := \frac{138.18}{12.011 + 1.008 \cdot \alpha} \qquad\qquad K := 3.5$$

$$AFR_{global_i} := K_f \cdot \left[\frac{.25 \cdot CO_{dry_i} + CO_{2dry_i} + O_{2dry_i} + .25 \cdot \alpha \cdot \left(CO_{dry_i} + CO_{2dry_i} \right) + .5 \cdot NO_{x\%dry_i}}{TC_{dry_i}} \right]$$

$$K_{w_i} := \frac{K \cdot CO_{2dry_i}}{CO_{dry_i} + K \cdot CO_{2dry_i}}$$

$$TE_{airrich_i} := \frac{.5 \cdot CO_{dry_i} + CO_{2dry_i} + .25 \cdot K_{w_i} \cdot \alpha \cdot \left(CO_{dry_i} + CO_{2dry_i} \right) + .5 \cdot NO_{x\%dry_i}}{.5 \cdot CO_{dry_i} + CO_{2dry_i} + O_{2dry_i} + .25 \cdot K_{w_i} \cdot \alpha \cdot \left(CO_{dry_i} + CO_{2dry_i} \right) + .5 \cdot NO_{x\%dry_i}}$$

$$TE_{fuel_i} := \frac{CO_{dry_i} + CO_{2dry_i}}{TC_{dry_i}}$$

$$AFR_{burningzone_i} := AFR_{global_i} \cdot \frac{TE_{airrich_i}}{TE_{fuel_i}}$$

$$TE_{airrich} = \begin{pmatrix} 0.793 \\ 0.826 \\ 0.825 \\ 0.757 \\ 0.435 \end{pmatrix} \qquad TE_{fuel} = \begin{pmatrix} 0.768 \\ 0.886 \\ 0.885 \\ 0.799 \\ 0.559 \end{pmatrix}$$

$$AFR_{global} = \begin{pmatrix} 10.922 \\ 12.749 \\ 14.374 \\ 13.711 \\ 15.136 \end{pmatrix} \qquad AFR_{burningzone} = \begin{pmatrix} 11.272 \\ 11.888 \\ 13.404 \\ 12.994 \\ 11.772 \end{pmatrix}$$

Calculating equivalence ratio (ϕ) and relative AFR ratio (λ)

$M_{O2} := 31.999 \qquad M_{N2} := 28.013 \qquad M_C := 12.01 \qquad M_H := 1.008$

$$AFR_{stoich_i} := \frac{\left(1 + \dfrac{A_{m_i}}{4}\right) \cdot \left(M_{O2} + 3.72 \cdot M_{N2}\right)}{M_C + \alpha \cdot M_H}$$

$$\lambda_i := \frac{AFR_{global_i}}{AFR_{stoich_i}} \qquad\qquad \lambda_{burn_i} := \frac{AFR_{burningzone_i}}{AFR_{stoich_i}}$$

$$\phi_i := \frac{\left(AFR_{global}^{-1}\right)_i}{\left(AFR_{stoich}^{-1}\right)_i} \qquad\qquad \phi_{burn_i} := \frac{\left(AFR_{burningzone}^{-1}\right)_i}{\left(AFR_{stoich}^{-1}\right)_i}$$

$$\lambda = \begin{pmatrix} 0.877 \\ 0.988 \\ 1.08 \\ 1.043 \\ 1.121 \end{pmatrix} \qquad \lambda_{burn} = \begin{pmatrix} 0.905 \\ 0.921 \\ 1.007 \\ 0.988 \\ 0.872 \end{pmatrix} \qquad AFR_{stoich} = \begin{pmatrix} 12.459 \\ 12.909 \\ 13.31 \\ 13.146 \\ 13.498 \end{pmatrix}$$

$$\phi = \begin{pmatrix} 1.141 \\ 1.013 \\ 0.926 \\ 0.959 \\ 0.892 \end{pmatrix} \qquad \phi_{burn} = \begin{pmatrix} 1.105 \\ 1.086 \\ 0.993 \\ 1.012 \\ 1.147 \end{pmatrix}$$